ABSTRACT

The choice of appropriate ventilator settings is crucial especially for patients with severely impaired respiratory system to improve the benefit-to-risk ratio of mechanical ventilator by providing adequate gas exchange whilst reducing the risk of ventilator-induced lung injury. However, known bedside measures to guide the clinician in adjusting the ventilator settings are limited in that they tend to give global information regarding the performance of the lungs. Electrical impedance tomography (EIT) is relatively new technique and has been the subject of intensive research since its development in the early 1980s by Barber and Brown. One of the advances in EIT is the development of an absolute EIT system (aEIT) that can estimate absolute values of lung resistivity and lung volumes.

In this thesis, a series of calibration and improvements on the aEIT system conducted by the Sheffield's Group have shown some promising results that allow the system to be the base for the development of a decision support system for guiding respiratory therapy hence enhancing the clinician's expertise with rapid and precise adjustments of ventilator settings. In this research, the intelligent EIT-based decision support system (IEDSS) is developed to provide advice for optimal changes in ventilator settings. The IEDSS is a knowledge-based decision support system which exploits the expert knowledge in deriving the rules for optimal ventilator settings based on blood gases information and the quantitative parameters of the aEIT system. The performance of IEDSS has been validated in a series of simulation scenarios to mimic the real patients' state evolution in the intensive care unit. This simulation has fused the information on blood gasses from the extended version of ventilated patient mathematical model and information on the regional lung behavior from the aEIT related models. The results show that not only the IEDSS can generate good ventilator setting advice but also it is able to minimise the risks of lung injuries in all the simulated patients.

RELATED PUBLICATIONS

1. **Suzani Mohamad Samuri**, George Panoutsos, Mahdi Mahfouf, G. H. Mills, B. H. Brown, 2011, "Towards A Patient-Specific Model of Lung Volume using Absolute Electrical Impedance Tomography (aEIT)", Lecture Notes of Communications in Computer and Information Science (LNCCIS). (In Press)

2. **Suzani Mohamad Samuri**, George Panoutsos, Mahdi Mahfouf, G. H. Mills, B. H. Brown, 2011, "Neural-Fuzzy Modelling of Lung Volume using Absolute Electrical Impedance Tomography", The International Conference on Bio-inspired Systems and Signal Processing (BIOSIGNALS), Rome, Italy. (Published)

3. **S. Mohamad-Samuri**, M. Mahfouf, M. Denaï, J.J. Ross and G.H. Mills, 2010, "Absolute EIT Coupled To a Blood Gas Physiological Model For The Assessment of Lung Ventilation In Critical Care Patients", JOURNAL OF CLINICAL MONITORING AND COMPUTING, 25(1): pp. 27-28. (Published)

4. Denai M. A., Mahfouf M., **Mohamad-Samuri S**., Panoutsos G., Brown B. H. and Mills G. H., 2010, "Absolute electrical impedance tomography (aEIT) guided ventilation therapy in critical care patients: Simulations and future trends", IEEE TRANSACTIONS ON INFORMATION TECHNOLOGY IN BIOMEDICINE 14(3): pp. 641-649. (Published)

5. **S Mohamad-Samuri**, M A Denai, G Panoutsos, M Mahfouf, D A Linkens, T Meekings, G H Mills, B H Brown, 2009, "The Sheffield Mk3.5 Absolute Resistivity aEIT System - Review of Recent Updates and Future Trends", The 10th International Conference on Biomedical Applications of Electrical Impedance Tomography (EIT 2009), Manchester, UK. (Published)

ACKNOWLEDGEMENT

In the name of Allah, the most Gracious, the most Merciful and praise be to Him for His mercy and blessings that have granted me the knowledge and understanding throughout my journey of completing this work.

My greatest and heartfelt gratitude goes to my supervisor, Prof. Mahdi Mahfouf, for his precious guidance, support and encouragement throughout the completion of this research. The significant amount of time, energy, idea, knowledge and patience in guiding me to be the best that I can in this field are very much appreciated.

I also would like to thank Dr. Gary Mills, the consultant anaesthetist, for his invaluable help and support in this work. My special appreciation also goes to Mr. Nathaniel Mills, the senior research charge nurse and Miss. Julie Sorrel, the research sister in the Clinical Research Facility, Sheffield for their help and cooperation during the EIT data collection in the ICU. I gratefully acknowledge Dr. George Panoutsos, Dr. Mouloud Denai, Dr. Ang Wang and Dr. Abdel Hafed for their help and many inspiring discussions during my research.

My thanks to the Ministry of Higher Education and government of Malaysia for sponsoring my study as well as to the Sultan Idris Education University of Malaysia for sponsoring my family to join me during my study.

My heartfelt appreciation also goes to my loving and understanding husband, Harris Hizam for his great patience and support during these four years of my study. Not forgetting my beloved children, Syahmi, Humaira and Syahin who have always been my source of inspiration and keeping my spirit high. Special thanks to my sister in-law, Zahidah Hanis for her great help and sacrifice during the last six months of my study. May Allah reward her with great happiness and ease her in everything that she pursues. Last but not least, my appreciations goes to my parents, Haji Samuri and Hajah Azizah, my mother in-law, Habsah and all my families and friends for their unlimited support and pray.

ABBREVIATION

α_b	oxygen carrying capacity of the blood
β_h	haemoglobin oxygen binding capacity
aEIT	absolute electrical impedance tomography
absR	absolute resistivity
absLV	absolute lung volume
APT	applied potential tomography
AC	alternating current
AgCl	silver chloride
ANN	artificial neural network
AI	artificial intelligent
ALI	acute lung injury
ANFIS	adaptive neural-fuzzy inference system
ARDS	acute respiratory distress syndrome
ASB	assisted spontaneous breathing
AVent	alveolar ventilation
BiPAP	bilevel positive airway pressure ventilation
BO2	oxygen diffusion constant (per litre of blood flowing in pulmonary capillaries)
BP	blood pressure

BTPS	body temperature pressure saturated
C	lung compliance
Cor.	correlation
CaCO2	carbon dioxide content in arterial blood
CaO2	oxygen content in arterial blood
CABG	coronary artery bypass grafting
CT	computerized tomography
C.O.	cardiac output
COPD	chronic obstructive pulmonary disease
CPAP	continuous positive airway pressure
CPPV	continuous positive pressure ventilation
CvO2	venous oxygen content
CxO2	oxygen content of the blood in compartment x
DO2	diffusion capacity of the lung for oxygen
DSS	decision support system
Dept.	department
eSTD	standard deviation of error
EELV	end-expiratory lung volume
EIT	electrical impedance tomography
ELIC	end-expiratory lung impedance change

ET	electrical tomography
ERT	electrical resistance tomography
ECG	electrocardiography
EtCO2	end-tidal carbon dioxide
FiO2	fraction of inspired oxygen
FIS	fuzzy inference system
FRC	functional residual capacity
fEIT	functional electrical impedance tomography
FVC	forced vital capacity
FEV	forced expiratory volume
GDF	gas dissociation function
GV	gas volume
GA	genetic algorithm
GUI	graphical user interface
Hb	haemoglobin concentration
HCO3	bicarbonate
HR	heart rate
I:E	ratio inspiratory to expiratory time ratio
ICU	intensive care unit
II	impedance imaging

IT	impedance tomography
IEDSS	intelligent EIT-based decision support system
I_{MRD}	mean regional density index
I_{LUNG}	lung condition index
JWI	Jabour's weaning index
Kd	relative deadspace (deadspace to tidal volume ratio)
LIP	lower inflection point
LV	lung volume
LLAD	left lung anterior density
LLMD	left lung middle density
LLPD	left lung posterior density
MAD	mean anterior density
MMD	mean middle density
MPD	mean posterior density
MLP	multilayer perceptron
MEEV	mean end-expiratory lung volume
MRD	mean regional density
MRI	magnetic resonance imaging
m.s.e.	mean squared errors
MV	minute volume

MAE	mean absolute error
MVT	mean tidal volume
NHS	national health service
ODC	oxygen dissociation curve
P50	50% saturation normal operating point of the oxygen dissociation curve
PAC	pulmonary artery catheter
PaCO2	arterial partial pressure of carbon dioxide
PAO2	alveolar partial pressure of oxygen
PaO2	arterial partial pressure of oxygen
PB	atmospheric pressure
PCV	packed cell volume
PCO2	partial pressure of carbon dioxide
PDMS	patient data management system
PEEP	positive end-expiratory pressure
Pinsp	inspiratory pressure (above PEEP)
PIP	peak inspiratory pressure
Pmean	mean airway pressure
PO2	partial pressure of oxygen
PpCO2	pulmonary partial pressure of carbon dioxide
PS	pressure support

PSV	pressure support ventilation
PV	pressure volume
Raw	airway resistance
RLAD	right lung anterior density
RLPD	right lung posterior density
RLMD	right lung middle density
RI	respiratory index
ROI	region of interest
RQ	respiratory quotient
RR	respiratory rate (ventilator)
RDS	respiratory distress syndrome
RSBI	rapid shallow breathing index
RV	residual volume
RMSE	root mean square error
S.D.	standard deviation
SO2	oxygen saturation of the blood
SOPAVENT	Simulation of Patient under Artificial Ventilation
SIVA	Sheffield Intelligent Ventilator Advisor
Tinsp	inspiratory time
UIP	upper inflation point

VILI	ventilator induced lung injury
V/Q	ventilation-perfusion ratio
VC	vital capacity
VCO2	carbon dioxide production
VD	physiological deadspace
VO2	oxygen consumption
Vrate	ventilatory rate (the same as respiratory rate (RR))
VT	tidal volume

TABLE OF CONTENTS

ABSTRACT ..... **i**

RELATED PUBLICATIONS ..... **ii**

ACKNOWLEDGEMENT ..... **iii**

ABBREVIATION ..... **iv**

CHAPTER 1 ..... **1**

1 INTRODUCTION **1**

1.1 Research questions and motivation 1

1.1.1 Mechanical ventilation: the act of therapy and injury 1

1.1.2 Mechanical ventilation strategies and their deficiencies 2

1.1.3 Electrical Impedance Tomography (EIT) as lung imaging 3

1.1.4 Physiological modelling of blood gasses for mechanically ventilated patients 4

1.1.5 Intelligent decision support system for intensive care ventilators 5

1.2 Research objectives 6

1.3 Outline of the thesis 7

CHAPTER 2 ..... **10**

2 ELECTRICAL IMPEDANCE TOMOGRAPHY AND DECISION SUPPORT SYSTEMS FOR INTENSIVE CARE VENTILATED PATIENTS – A LITERATURE REVIEW **10**

2.1 Electrical Impedance Tomography (EIT) 10

2.1.1 Introduction 10

2.1.2 A brief historical development of EIT 11

2.1.3 General principle of EIT 12
2.1.4 Relative, multi-frequency and absolute EIT system 15
2.1.5 An overview of the Sheffield Mk 3.5 absolute EIT (aEIT) system 18
2.1.6 EIT application for pulmonary measurement 21
2.1.7 EIT research trends 28
2.2 Decision support systems (DSSs) for intensive care ventilators 30
2.2.1 Introduction 30
2.2.2 Knowledge-based systems 31
2.2.3 Model-based systems 36
2.2.4 Hybrid-knowledge-and model-based systems 39
2.2.5 Current status and research trends 42
CHAPTER 3 45
3 EIT STUDY ON HEALTHY VOLUNTEER SUBJECTS 45
3.1 Introduction 45
3.2 Equipments/tools used with aEIT system 46
3.3 Study protocol and data collection methods 47
3.3.1 Spirometry and aEIT measurements 48
3.3.2 Body plethysmography (Body box) 49
3.3.3 MRI scans 49
3.4 Results and discussions 50
3.4.1 Absolute resistivity-lung volume relationship in aEIT system 50

3.4.2 Comparison between spirometry lung volumes and the aEIT lung volumes in sitting and supine position.....51

3.4.3 Comparison between body box lung volumes and aEIT lung volumes .58

3.5 Summary 62

CHAPTER 4.....63

4 CALIBRATION AND IMPROVEMENTS OF THE SHEFFIELD MK 3.5 aEIT SYSTEM.....63

4.1 Introduction.....63

4.2 A review of amendments of the aEIT software.....64

4.2.1 aEIT lung volume system calibration.....64

4.2.2 Lung weight estimation 66

4.3 The new region of interest (ROI) 67

4.3.1 Step by step process of creating the new region of interest.....68

4.3.2 Multiple regions of interest (ROIs).....70

4.4 Improved results and discussions.....74

4.4.1 Comparison between spirometry lung volumes and the aEIT lung volumes in sitting and supine position.....74

4.4.2 Comparison between body box lung volumes and the aEIT lung volumes 80

4.5 Summary 84

CHAPTER 5.....85

5 EIT CLINICAL TRIALS ON ICU PATIENTS 85

5.1 Introduction.....85

5.2 Study protocol and data collection methods 87

5.2.1 Identifying Participants 87

5.2.2 Data collection methods 88

5.3 Results and discussions 90

5.3.1 PEEP, MEEV and MVT 90

5.3.2 Mean regional densities 92

5.3.3 PEEP induced changes in aEIT quantitative parameters 93

5.3.4 Relationship between MEEV, MAD, MMD and MPD with blood gasses parameters 98

5.3.5 Tidal volume from ventilator versus tidal volume from aEIT 104

5.4 Summary 105

CHAPTER 6 106

6 MODELLING OF aEIT-BASED QUANTITATIVE PARAMETERS USING A NEURAL FUZZY SYSTEM 106

6.1 Introduction 106

6.2 Modelling method 107

6.3 Patient's data 109

6.4 Development of MEEV model 110

6.4.1 Model's inputs selection 110

6.4.2 MEEV model training and testing results 111

6.5 Development of MAD, MMD and MPD models 114

6.5.1 Models' inputs selection 114

6.5.2 MAD, MMD and MPD models training and testing results 115

6.6 Summary 120

CHAPTER 7 121

7 AN INTELLIGENT EIT-BASED DECISION SUPPORT SYSTEM FOR CRITICALLY-ILL VENTILATED PATIENTS IN INTENSIVE CARE UNIT 121

7.1 Introduction 121

7.2 The intelligent EIT-based decision support system (IEDSS) design method 122

7.3 Development of FiO2/PEEP sub-unit 123

7.3.1 Fuzzy partitions for the inputs and outputs 123

7.3.2 Parameters for fuzzy input membership functions 126

7.3.3 FiO2/PEEP fuzzy rule-base derivation 129

7.4 Development of Pinsp/RR sub-unit 135

7.4.1 Fuzzy partitions for the inputs and outputs 135

7.4.2 Parameters for the fuzzy input membership functions 137

7.4.3 Pinsp/RR fuzzy rule-base derivation 138

7.5 Closed-loop validation of the decision support system via simulations of the hybrid aEIT-SOPAVent models 144

7.5.1 Overview of SOPAVent model 145

7.5.2 Validation method 147

7.5.3 Validation results and discussions 149

7.6 Summary 158

CHAPTER 8 159

8 CONCLUSIONS AND FUTURE WORK 159

8.1 Project achievements 159

8.1.1 Comparative study on healthy volunteers leads to calibration and improvement of aEIT system 159

8.1.2 aEIT clinical trials on critically-ill ventilated patients in the ICU 162

8.1.3 Quantitative models for aEIT 163

8.1.4 Development and assessment of the intelligent EIT-based decision support system (IEDSS) 164

8.2 Recommendations for future work 164

REFERENCES 167

APPENDIX A 176

APPENDIX B 179

CHAPTER 1

INTRODUCTION

1.1 Research questions and motivation

1.1.1 Mechanical ventilation: the act of therapy and injury

Mechanical ventilation is synonyms with Intensive Care environment. Patients with respiratory failure for example, are not able to breath by themselves due to various clinical conditions; for example, heart failure, pneumonia, Acute Respiratory Distress Syndrome (ARDS) and Acute Lung Injury (ALI). These conditions may cause the patients to experience air hunger and a build-up of excessive carbon dioxide which usually lead to blood acidosis and as a result impair the patients' body. The treatment for failure to oxygenate rests with the restoration and the maintenance of lung volumes provided by mechanical ventilation with the aim of ensuring that there is enough oxygen in the blood to support the metabolism and increase the patients' comfort. The action to ensure that patients receive enough oxygen is a challenging task.

Although, mechanical ventilation is seen as a life-saving intervention for many patients in the intensive care unit (ICU), it has been associated with adverse effects. One of which that has been the main concern in the ICU relates to the lung tissue damage. Late complications often seen in ARDS patients and directly related to mechanical ventilation include barotraumas (repetitive closing and reopening of injured alveoli) caused by high airway pressures and/or volutrauma (alveolar over-distension when the lung units are physically stretched beyond their normal, maximum inflation point and/or alveolar disruption) caused by high tidal ventilation. In both cases, patients tend to have imbalances in the regional lung ventilation, with gravity-dependent collapse and over distension of nondependent zones. These effects are better known in intensive care therapy as ventilator-induced lung injury (VILI). (Tremblay and Slutsky, 2006; Frank and Matthay, 2003; Moloney and Griffiths, 2004).

1.1.2 Mechanical ventilation strategies and their deficiencies

The essentials in safe ventilatory therapy in patients with severe respiratory failure include lung volume maintenance while avoiding alveolar overdistension. Adequate lung volume is traditionally maintained by varying the tidal volume (VT), inspiratory time (Tinsp) and positive end-expiratory pressure (PEEP) levels. Arterial blood gases (arterial partial pressure of oxygen (PaO_2), arterial oxygen saturation (SaO_2), arterial partial pressure of carbon dioxide ($PaCO_2$)) analysis and airway pressure-volume graphical waveforms have long been considered to be the gold standard clinical practice for assessing the acid-base balance, lung function and as a result guiding the titration of mechanical ventilation for critically-ill patients. These are combined with measurements derived from pressure, flow and volume, which provide information about the mechanical properties of the lungs and chest wall (Lu *et al.*, 2000). However, these methods only provide an indication on the overall lung function and fail to provide full information about the regional lung behaviour (Harris *et al.*, 2005).

Hitherto, lung imaging has relied on bedside X-ray radiography and the gold standard Computed Tomography (CT) which provides comprehensive images of the morphologic structures of the lungs and displays the ventilation distribution with a high spatial resolution. However, during these procedures, the patient is exposed to a substantial dose of radiation and in the case of CT, the patient needs to be transported to the Radiology Department, which is a high risk process in the unstable critically ill (Hinz *et al*., 2006). At present, CT is considered to be an 'occasional' investigation which is only repeated every few days at most. It is costly and both time and labour intensive. These limitations and problems associates with the Intensive Care environment need for an alternative solution which may enhance the quality of current management of ventilated patients.

1.1.3 Electrical Impedance Tomography (EIT) as lung imaging

The development of Electrical Impedance Tomography (EIT) has given a new perspective in Intensive Care environment. Electrical Impedance Tomography (EIT) is a non-invasive, radiation-free monitoring technique which aims to reconstruct a cross-sectional image of the internal spatial distribution of the electrical measurements made by injecting small alternating currents via an array of equally-spaced electrodes attached to the surface of the thorax at about 4-5 cm above the xyphoid process (Denai *et al*., 2010).

1.1.3.1 Absolute EIT (aEIT) as a potential bedside monitoring tool

In this research, the Sheffield Mk 3.5 absolute EIT (aEIT) system has been used. Absolute EIT (aEIT) allows quantification of specific tissue resistivity at a given point

in time, when a lung volume can be derived as compared to just having a difference in impedance over a period of time. In recent years, the Sheffield's Research Group has carried-out a series of calibrations and improvements to enhance the accuracy and consistency of the calculated absolute lung volume and resistivity in the aEIT system. Although the aEIT system is not yet established as a routine clinical tool, it has shown some promising development which has the potential to contribute to significant advances in lung monitoring technique, especially in tracking changes in the lung during mechanical ventilation. In this thesis, the mean end expiratory lung volume (MEEV), the right lung anterior density (RLAD), the right lung middle density (RLMD), the right lung posterior density (RLPD), the left lung anterior density (LLAD), the left lung middle density (LLMD) and the left lung posterior density (LLPD) are the identified quantitative parameters extracted from the aEIT system that have the ability to provide information on the localise patient's lung behaviour. Therefore, a fusion of information from the aEIT system with patient's blood gases parameters is reckoned to be able to assist the clinician to gain a more detailed information about a patient's global and regional lung function information and therefore to lead to an overall optimal ventilator management strategy in the Intensive Care Unit (ICU).

1.1.4 Physiological modelling of blood gasses for mechanically ventilated patients

Simulation and modelling in respiratory physiology offer opportunities for the better understanding of the mechanisms of gas exchange and the pathophysiology of respiratory disorders. SOPAVent (Simulation of Patient under Artificial Ventilation) is a ventilated patient model which was originally developed to validate a fuzzy knowledge-based ventilator management decision support system (Goode, 2001). The model is designed to provide steady-state blood gasses predictions for totally ventilated patients. This early version of SOPAVent has included some disadvantages where some of its physiological parameters need invasive monitoring and excessive

computational time for delivering ‘optimal’ therapeutic decisions. The model was subsequently improved in order to design a model-based decision support system. A mean population method was used to derive these parameters non-invasively (Kwok, 2003). Recently, further improvements have been made to the model with respect to parameters estimations which resulted in the emergence of a continuously updated ventilated patient model (Wang, 2008). The model has shown that by continuously updating the patient’s key parameters based on continuous measurement from ICU, the model can represent the patient state accurately and lead to good blood gases prediction with the patient state evolution.

1.1.5 Intelligent decision support system for intensive care ventilators

A vast amount of data/information that is available in current ICU call for an intelligent system that can fuse and interpret them accurately to provide a more objective and efficient ventilatory therapy. A significant amount of research has been carried-out to develop intelligent decision support systems for ventilator management system. In most of current studies, the intelligent decision support systems are designed to optimise the ventilator settings based on the patient’s blood gases information and measured set of ventilator parameters. In this thesis, the development of an intelligent decision support system that integrates the patient’s blood gases information from a totally non-invasive and continuously updated blood gas model of ventilated patients (SOPAVent), set ventilator parameters and quantitative parameters from aEIT system is investigated. The enhanced version of this intelligent decision support system is developed with the objectives to provide advice for precise adjustment of ventilator settings and minimising the known adverse effects of mechanical ventilation. A knowledge-based approach will be investigated for this purpose.

1.2 Research objectives

The main objectives of this research are to further improve the existing Sheffield Mk 3.5 aEIT system, to model the relationship between the ventilator settings and aEIT quantitative parameters and to develop an intelligent EIT-knowledge-based decision support system for optimal ventilator management in the ICU. In order to achieve this, several sub-objectives have been identified as follows:

1. To conduct a series of investigations on healthy volunteer subjects to further assess the accuracy and consistency of the aEIT system.

2. To further improve the region of interest (ROI) used in the Sheffield Mk 3.5 aEIT system and validate the improved aEIT system.

3. To implement the improved aEIT system using real ICU patients to reflect the ventilator settings-induced changes on the lung absolute volume.

4. To model the relationship between ventilator settings and aEIT quantitative parameters and validate them accordingly.

5. To show how to derive ‘optimal’ advice on ventilator settings via a combination of the expert knowledge with a fuzzy inference system and to evaluate the decision support system via a series of simulated patients’ scenarios.

Indeed, the management of mechanically ventilated patients in the ICU is very complex and challenging. Therefore, to achieve the above mentioned objectives, the work in this thesis has been limited to the management of patients who are fully ventilated with no or very little spontaneous ventilation of their own. Only patients with pressure-control mode will be considered in all the studies with the ventilator settings including the fractional inspired oxygen (FiO2), positive end-expiratory

pressure (PEEP), inspiratory pressure (Pinsp), respiratory rate (RR) and peak inspiratory presuure (PIP).

1.3 Outline of the thesis

This thesis consists of 8 chapters and they are summarised as follows:

CHAPTER 2: LITERATURE REVIEW

This Chapter has been divided into two major sections; i) A number of important research studies and pioneering works related to the EIT application in pulmonary has been reviewed extensively, ii) Major research results and current state-of-the-art related to the various design of decision support systems for ventilators in ICUs are reviewed. In both sections, the current status, research trends and challenges are also discussed at the end of each section.

CHAPTER 3: EIT STUDY ON HEALTHY VOLUNTEERS

In this Chapter, investigations on aEIT measurements involving a group of healthy volunteer subjects are conducted by comparing with results from spirometry and body plethysmography (body box).

CHAPTER 4: CALIBRATION AND IMPROVEMENT OF THE SHEFFILED MK 3.5 aEIT SYSTEM

Efforts to improve the Sheffield Mk 3.5 aEIT software via a series of calibrations and improvements are reviewed first. The latest work of improvement, on redefining new

regions of interest (ROIs) for the lungs and the new sub-ROIs are then presented. Results from the improved aEIT system are also presented and discussed.

CHAPTER 5: EIT CLINICAL TRIALS ON ICU PATIENTS

In this Chapter, the improved aEIT system with the new ROIs is implemented to reflect the PEEP settings-induced changes on the lung absolute volume in the real ICU patients. Relationships between the quantitative parameters extracted from EIT data, ventilator and blood gas parameters are also studied.

CHAPTER 6: MODELLING OF aEIT QUANTITATIVE PARAMETERS USING ANFIS

In this Chapter, the development of mean end expiratory lung volume (MEEV) and mean regional densities (MRD) models using ANFIS are presented. The validation results are then analysed and discussed.

CHAPTER 7: INTELLIGENT EIT-BASED DECISION SUPPORT SYSTEM FOR CRITICALLY-ILL VENTILATED PATIENTS IN INTENSIVE CARE UNITS

Based on the data/information from the aEIT models and a totally non-invasive and continuously updated blood gas model of ventilated patients (SOPAVent) in ICU, an intelligent EIT-based decision support system is designed using the expert knowledge and fuzzy inference system. The decision support is then evaluated via a series of simulated patients' scenarios.

CHAPTER 8: CONCLUSIONS AND FUTURE WORK

This Chapter reviews and summarises the achievements of this project. The achievements and limitations are presented with an indication of a future research platform.

CHAPTER 2

ELECTRICAL IMPEDANCE TOMOGRAPHY AND DECISION SUPPORT SYSTEMS FOR INTENSIVE CARE VENTILATED PATIENTS – A LITERATURE REVIEW

2.1 Electrical Impedance Tomography (EIT)

2.1.1 Introduction

Electrical Impedance Tomography (EIT) is a relatively new version to tomographic imaging techniques and it has been the subject of intensive research since its development in the early 1980s by Barber and Brown at the Department of Medical Physics and Clinical Engineering, Hallamshire Hospital in Sheffield (UK). Since then, EIT is seen to have a superior potential especially in the medical application. In Section (2.1), a brief history of EIT development will be reviewed. The general principle of EIT and different types of the system which exist in the literature will then be presented, followed by an overview of Sheffield Mk 3.5 absolute EIT (aEIT) system. The existing research on EIT application in healthcare will also be reviewed.

This review on research will focus on EIT applications in pulmonary measurement, which will establish the rationale behind the research work in this thesis. Finally, the trends related to the research in EIT will be discussed.

2.1.2 A brief historical development of EIT

The history of research in the electrical properties of biological tissues dated back in the early 1900's. Human tissues have a specific conductance (conductivity), varying from 15.4 mS/cm for cerebrospinal fluid, to 0.06 mS/cm for bone, (Barber, 1995). They consist of cells with conducting contents surrounded by insulating membranes embedded in a conducting medium. These tissues can act as resistive, conductive and also as capacitive. Various tissues have different frequency dependant electrical properties. Nevertheless, in all tissues, the conductivity increases while resistivity decreases from the low frequency values to the high frequency limits. Table 2.1 includes typical values of some tissue resistivity obtained at a frequency of 10 kHz (Brown, 2003).

Table 2.1: Typical values of tissue resistivity at a frequency of 10 kHz [Brown, 2003].

Tissue	**Approximate Resistivity at 10 kHz**
Muscle	2-4 Ω m
Fat	20 Ω m
Lungs	7-20 Ω m (varies with respiration)
Blood	1.6 Ω m
Bone	> 40 Ω m

Due to significant differences observed in the resistivity of different tissues, it should be possible to produce images showing the resistivity distribution. The first publication of an impedance image was that of Henderson and Webster in 1978 (Henderson and Webster, 1978). They used 100 electrodes arranged in a rectangular array on one side of the chest, with a single electrode on the other side, and produced an image of the intervening tissue conductivity. In the past literature, several titles have been adopted to describe impedance imaging system, which include electrical tomography (ET), impedance imaging (II), resistance imaging (RI), electrical resistance tomography (ERT), impedance tomography (IT) and applied potential tomography (APT). Lately, the term which has been widely used to describe this imaging technique becomes the electrical impedance tomography (EIT). According to Brown, this term has an advantage in that it may include resistive, capacitive and inductive tomographies (Brown, 2003).

The first clinical impedance tomography system was developed in the Department of Medical Physics in Sheffield by Barber and Brown in the 1980's. The Sheffield Mark 1 Applied Potential Tomography (APT) system became commercially available, and was used in many different clinical centres across a range of studies (Brown and Barber, 1987). In the early 1980's, the Sheffield Group originally published tomographic images of the arm, showing areas of increased impedance corresponding to bone and fat. The first review of potential clinical applications of EIT was published in 1985 (Barber and Brown, 1985). The paper includes the original tomographic image of an arm, and also the first tomographic images taken of the lungs.

2.1.3 General principle of EIT

In general, all proposed impedance imaging shared the same objective: to produce cross-sectional images of the distribution of conductivity, or alternatively specific

resistance (resistivity) of the internal structure of an object using different current injection patterns and voltage measurement sequences. In EIT, current patterns are injected into the body via surface electrodes and boundary voltages are measured to reconstruct a cross-sectional image of internal distribution of the conductivity or resistivity. An illustration of a typical EIT system that uses a set of equally spaced electrodes attached to the surface of the chest at about 4-5 cm above the xyphoid process is depicted in Figure 2.1. Most EIT equipments use alternating currents (AC) with amplitude and frequency varying from 1-10 mA and 1 kHz-1 MHz for medical applications.

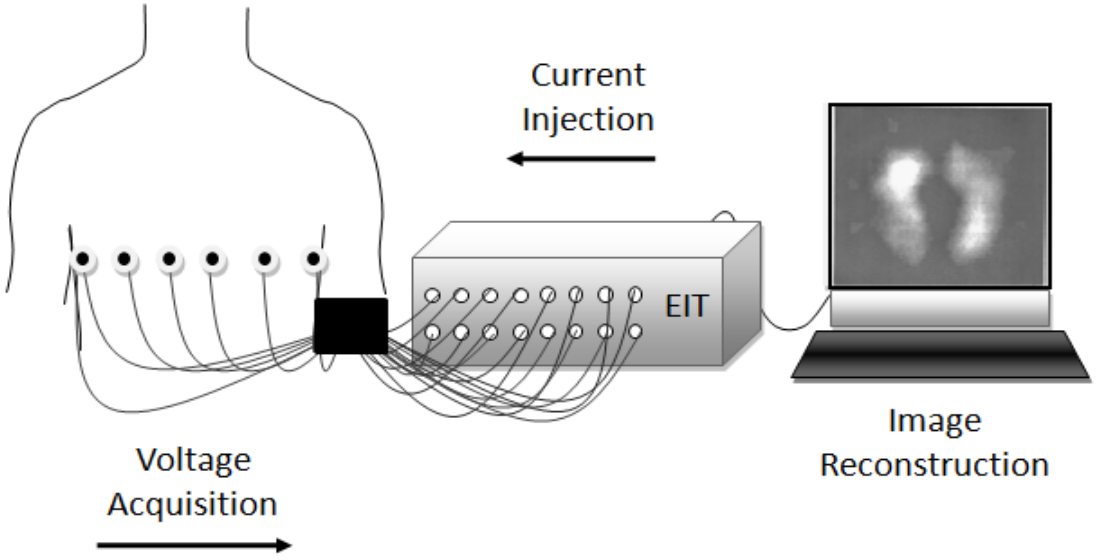

Figure 2.1: A typical EIT system with 16 electrodes for current injection and voltage acquisition [Denai *et al*., 2010].

There are two basic stages to produce an impedance image; 1) The collection of a set of independent transfer impedance and 2) The solution of an inverse problem to produce an image from the set of the independent transfer impedances. Currently, there are three ways used in different EIT system for the collection of transfer impedance; 1) Polar, 2) Dipole/Adjacent and 3) Trigonometeric configuration (Korzhenevskii, 1997; Barber, 1984; Gisser, 1988). The most popular data collection

strategy is the dipole/adjacent configuration. In a 16-electrode system, where adjacent configuration is used, current is applied to an adjacent pair of electrodes and the resulting voltages between the remaining 13 pairs of electrodes are measured. For example, current is injected through electrode pair (1,2) and the resulting boundary voltages differences are measured from electrode pairs (3,4), (4,5), ..., (14,15), (15,16) as shown in Figure 2.2.

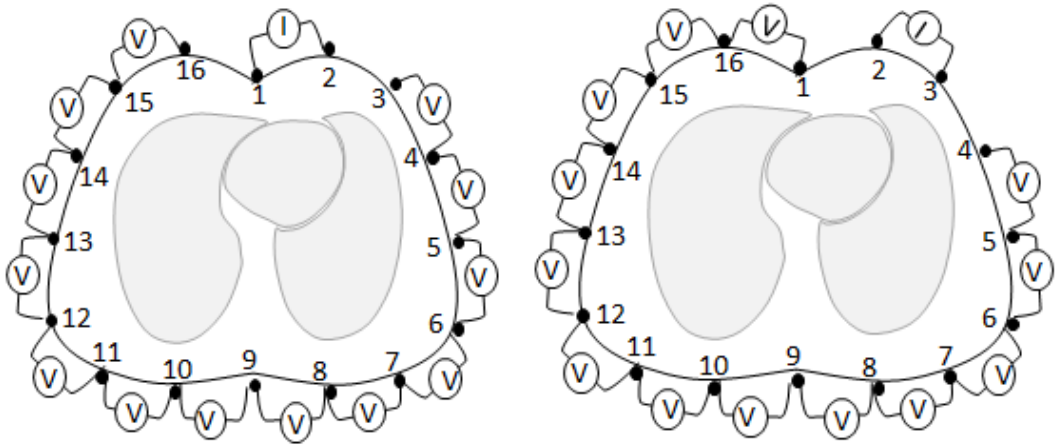

Figure 2.2: Adjacent measurement configuration with 16 equally spaced electrodes [Denai *et al.*, 2010].

This procedure is repeated 16 times with current injected between successive pairs of adjacent electrodes until all 16 possible pairs of adjacent electrodes have been used to apply the known current. By applying a current trough all the adjacent electrode pairs, in turn $N(N\text{-}3)$ measurements will be obtained (whereby N is corresponds to number of electrodes used). However, according to the reciprocity principle, only $N(N\text{-}3)/2$ measurements are independent and can be used to reconstruct the resistivity distribution. For example, in Figure 2.2 (left), the voltage measured between electrode 7 and 8 will be the same as that measured between 1 and 2 (if current I is injected between 7 and 8) (Geselowitz, 1971; Lehr, 1972). Therefore, in a 16-electrode system, (16 x (16-3))/2 = 104 independent transfer impedance measurements can be made.

The process of recovering the conductivity distribution within the body from the applied currents and measured boundary potentials is known as the *inverse problem* in EIT. This is a nonlinear and severely ill-posed problem. There are two approaches for solving the image reconstruction problem in EIT. *Static* reconstruction produces an image of the absolute conductivity distribution of the medium based on one set of measurements. *Dynamic* or *difference* imaging attempts to recover the change in resistivity based on measurements made at two different time periods.

2.1.4 Relative, multi-frequency and absolute EIT system

2.1.4.1 Relative/functional EIT

There are three types of impedance measurement systems which have been reported in the literature namely the relative, multi-frequency and absolute (Brown *et al*., 2002; Brown, 2003). For most of the recent EIT studies, the focus has been on the changes in impedance with time (relative/functional EIT). To produce this 'relative' value of resistivity, a series of measured surface voltages are collected from the subject over time. A single set of the measured surface voltages, from a point in time, are then set as a reference point and the rest of the measured series are compared relative to the reference set, this is called 'projecting back'. By comparing two data sets, the associated change in resistivity that produces the change in surface voltage measurements can be calculated, and the distribution of relative resistivity variation can be plotted. Further description about this process is well described by Barber and Brown in their paper (Barber *et al*., 1989).

2.1.4.2 Multi-frequency EIT

The multi-frequency EIT as demonstrated by Brown *et al*. (1994), could be used to record the change in tissue resistivity with frequency, as opposed to the relative change in resistivity with time. In multi-frequency EIT the image is reconstructed using a slightly modified version of the back projection algorithm, whereby a reference data set is generated from a single frequency and the variation in resistivity of a single pixel can be measured over a range of frequencies (Brown *et al*., 1994; Brown *et al*., 1995).

2.1.4.3 Absolute EIT

The new absolute impedance tomography takes this a step further, by not only looking at the changes in impedance, but also producing absolute (as opposed to relative) values of impedance that can be compared to normal or reference values. The research in absolute EIT has hitherto centred on healthcare application or to be specific in the application of pulmonary measurement and imaging. In this case, the method of determination of lung absolute resistivity (Brown *et al.*, 2002) is based on a 3D finite difference model of the thorax developed from computerised tomography (CT) cross sections of a normal subject (Zubal *et al*., 1994) (Figure 2.3) and scaled to take into account the geometry of the chest (circumference and ellipse ratio) of a particular subject.

The elements in the model were assigned fixed resistivity values in the range 1-80 Ω-m depending on their anatomical location (fat, muscle, bone, blood or lung) in the CT images. The modeled data are then compared with the real measurements over a pre-determined region of interest for values of the lung resitivities between 3 and 80 Ω-m. The value of lung resistivity, which minimises the mean difference between these data sets, is returned as the value of the absolute lung resistivity, an EIT image is

reconstructed by filtered back projection (Barber and Seagar, 1987). Figure 2.4 illustrates the process of acquiring the absolute resistivity in the absolute EIT system.

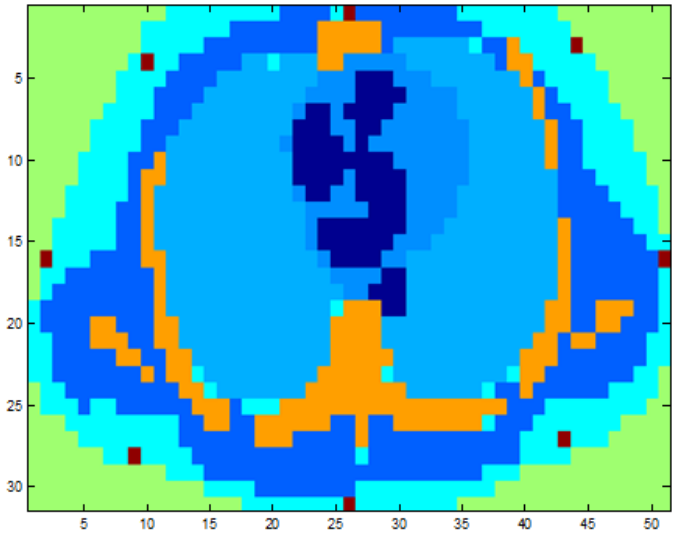

Figure 2.3: One plane from the adult finite difference model based on segmented CT images provided by George Zubal – Yale (1994).

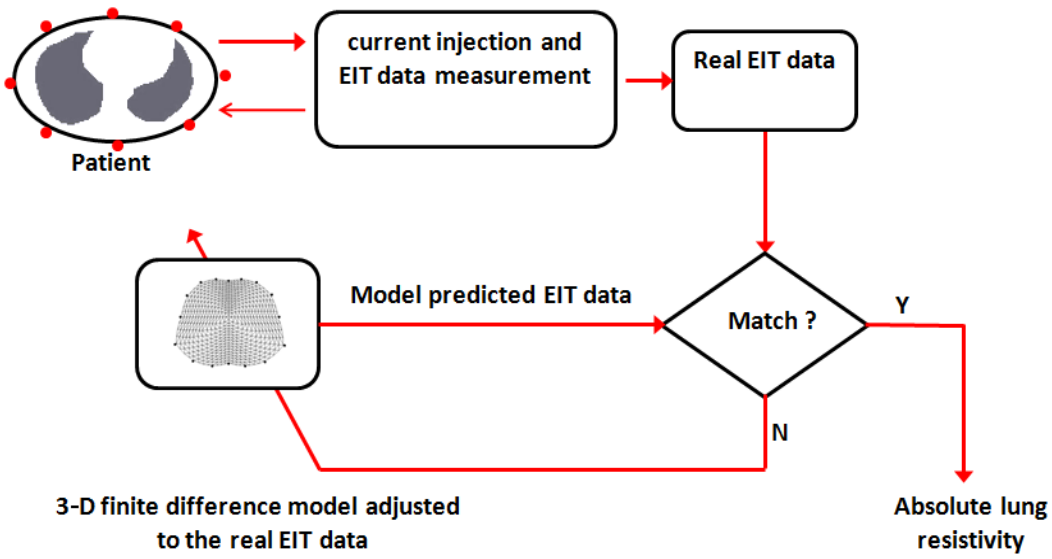

Figure 2.4: Flow chart that illustrates the process of acquiring the absolute lung resistivity in the absolute EIT system.

Another attractive aspect in absolute EIT that has instigated the interest of those involved in healthcare domain is its ability to produce or calculate the absolute lung volume. As lung resistivity is a function of the frequency of the applied current, at high frequency, when the cell membranes (which act as the capacitive reactance) are reduced virtually to zero, the lungs can be visualised as two equivalent electrical components; air with almost infinite resistivity and lung tissue with an almost homogeneous resistivity determined by that of the intra-cellular and extra-cellular fluids (Barber and Borsic, 2005). If these resistivities are known, then it will be possible to calculate both lung density and air volume using a Cole equation and Nopp model (Brown and Mills, 2006).

2.1.5 An overview of the Sheffield Mk 3.5 absolute EIT (aEIT) system

The Sheffield group has developed the Mk 3.5 (Wilson *et al*., 2001), an EIT system which uses a multi-frequency system to calculate the absolute resistivity of the lungs; this is the latest of a number of systems developed in Sheffield (Table 2.2). The previous version of this Mk 3, called the Mk 3, uses 16 interleaved drive and receive electrodes (Brown *et al*., 1994). One major use of the Mk 3 system was in modelling adult and neonatal lung tissue with the objective of monitoring both regional lung ventilation and thoracic fluid changes (Nopp *et al*., 1997; Smallwood *et al*., 1999; Noble *et al.,* 2000). Several drawbacks on the system were identified; 1) The use of interleaved drive and receive electrodes produce problems in image reconstruction, 2) Difficulties happened during placing this 16 electrodes around the thorax of neonates, 3) Mk 3 system did not use programmable devices, hence any changes to the data acquisition protocol required significant changes to the electronic devices which lead to version control and support problem (Wilson *et al*., 2001). Therefore, due to these problems, the Mk 3.5 aEIT system was developed.

The Mk 3.5 aEIT (Figure 2.5) uses eight AgCl ECG type electrodes to inject small alternating currents at 30 frequencies between 2 kHz and 1.6 MHz, collecting data and providing real-time imaging at 25 frames per second. The data is measured using adjacent drive and receive combinations of electrodes, connected to the data acquisition unit via tri-axial cables. A detailed description of the system hardware components is described by Wilson *et al*. (2001). Unlike the Mk 3 system, which used analogue demodulation, the Mk 3.5 aEIT system uses digital signal processing for both the generation of the current drive frequencies and demodulation of the measured signals. The current digital technology employed in Mk 3.5 aEIT system allows the system to have a direct digital link with a computer in order to change data acquisition protocol through a simple user interface (Wilson *et al*., 2001). The computer user interface to control the Mk 3.5 system is written in MATLAB, and is able to display real-time images. Figure 2.6 shows the Mk 3.5 data acquisition graphical user interface.

Table 2.2: Table showing details of previous EIT systems developed in Sheffield.

System	No. of Electrodes	Drive Pattern	Frequency	Technology	Date
Mk 1	16	Adjacent	50 kHz	Analogue	1987
Space/Portable	16	Adjacent	50 kHz	Analogue	1989
Mk 2	16	Adjacent	20 kHz	Digital	1990
Mk 3	16	Interlaced	8: 9.6 kHz – 1.2 MHz	Analogue	1993
Mk 3.5	***8***	***Adjacent***	***30: 2 kHz – 1.6 MHz***	***Digital***	***2000***

Figure 2.5: The Sheffield Mk 3.5 aEIT system.

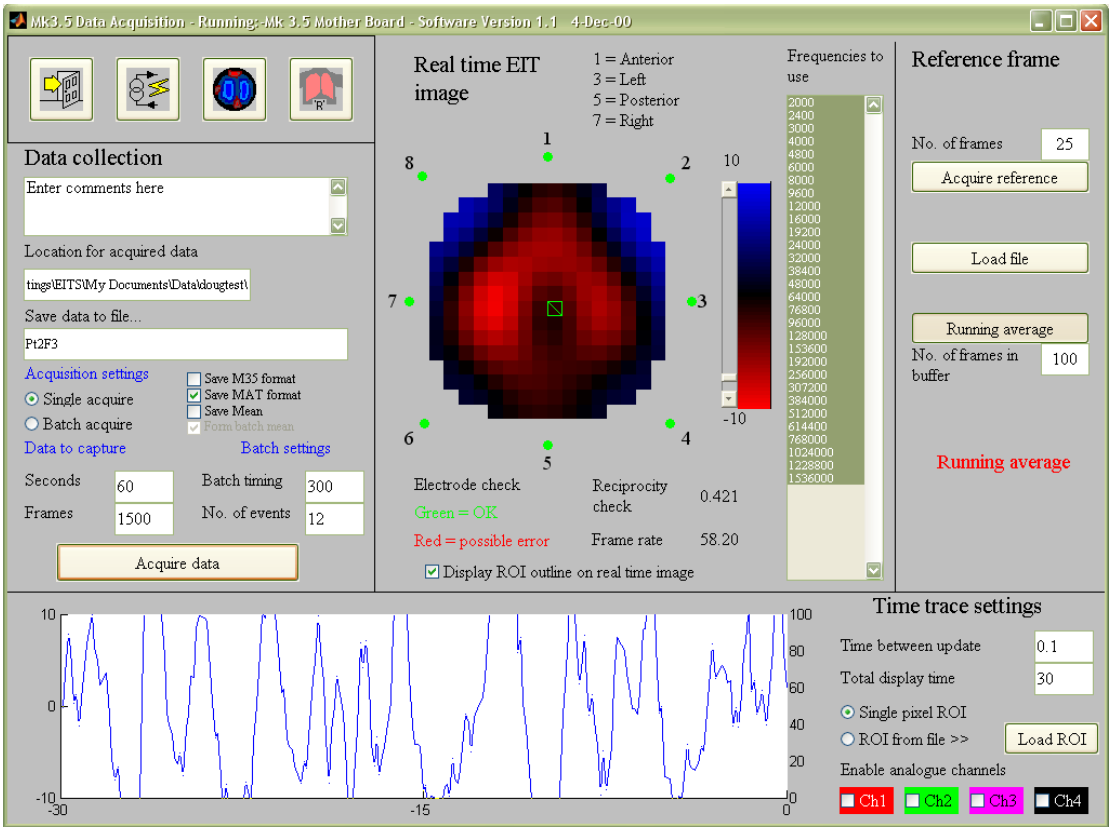

Figure 2.6: Screen shot taken from the Sheffield Mk 3.5 EIT data acquisition screen.

2.1.6 EIT application for pulmonary measurement

Among the clinical applications of EIT being investigated include monitoring internal bleeding, studying emptying of stomach, etc., but the monitoring of the pulmonary function has always been regarded as the most promising application which can benefit the most from the development of EIT. According to Brown, lung tissue has a resistivity which is about five times greater than most of other soft tissues in the thorax (Brown, 2003). This resistivity of lung changes was due to inspiration and expiration activity. During inspiration, alveoli are expected to swell ensuing in a longer path for the electric current to travel around them and hence increase the resistivity. These changes have made it possible for EIT to monitor the pulmonary function.

2.1.6.1 EIT images of pulmonary function

The first images of the pulmonary function used a simple back-projection algorithm to reconstruct cross-section images of the thorax. The equipment used 16 electrodes and produced an image resolution of 104 pixels. The functional image showed an increase in resistivity during spontaneous inspiration of the subject (Brown *et al*., 1985). In 1987, Brown and Barber have produced EIT images of the human thorax (Brown and Barber, 1987) and from both studies, EIT has shown the ability to measure functional changes but with limitation to its image resolution.

It was obvious that the technique would benefit the on-line pulmonary monitoring and therefore an initial investigation was performed on EIT as a real-time imaging technique. Brown and Barber (Brown ad Barber, 1988) showed that real-time image reconstruction is feasible and it offers a better monitoring tool as compared to off-line processing of averaged data. Additionally, the limitation of EIT to produce dynamic but not static images was also discussed. In 1995, a real-time EIT system and its

operation were presented by Smith *et al*. (1995). The possibility to improve image resolution was noted by increasing the number of electrodes but the potential design difficulties of increasing the number of electrodes such as data acquisition time, frame rate as well as signal to noise ratio performance was also discussed. Griffiths *et al*. (1992) was attempted the complex impedance imaging of the thorax. It was reported that changes in the complex impedance measured can be related to true changes in the thorax tissues, but the source related to the complex impedance change was not identified.

Brown *et al*. (1994) had investigated the use of multi-frequency EIT for producing EIT images. The results showed that it was possible to identify tissues on the basis of their impedance spectrum and the spectrum of the changes in impedance during breathing. In the following year, Brown and his Group had used the multi-frequency EIT system with frequencies between 9.6kHz-1.2MHz to record the images of the lungs from 12 normal subjects during various breathing manoeuvres. The impedance changes with frequency were modelled based on the Cole equation (Cole and Cole, 1941). The results demonstrated that identification of the lungs was possible using multi-frequency EIT images and parametric modelling based on the Cole equation (Brown e*t al*., 1995).

In 2002, Brown *et al.* had completed a study on 142 normal neonates to determine whether the absolute lung resistivity can be determined non-invasively. The results have shown that calculations of the absolute impedance of the neonatal lungs could be achieved by including simple measurements of body shape and size in multi-frequency EIT (Brown *et al.*, 2002). The method presented in this study is considered to be the first successful attempt at measuring absolute values for lung resistivity *in vivo*.

2.1.6.2 EIT for ventilation imaging

In the summary of the possible clinical applications of EIT, Brown *et al*. had previously suggested the use of EIT in lung imaging and ventilation monitoring (Brown *et al*., 1985). Therefore in this Section, various experimental and clinical studies done by EIT researches to validate the capability of EIT to correctly determine changes in regional air content will be reviewed, in which established medical techniques such as computed tomography (CT), single photon emission computed tomography (SPECT), ventilation scintigraphy, spirometry and body plethysmography have been applied as reference techniques. The performance of EIT has been tested under different conditions of spontaneous, different breathing manoeuvres and artificial ventilation.

Coulombe *et al*. (2005) had elicited a parametric model of the relationship between EIT and total lung volume with the aim at facilitating inter-individual comparisons of EIT images by providing volumetric scale in place of the usual arbitrary units scale. The lung volume changes predicted by the model were compared to the volume changes measured by Spirometry. The model was able to predict the lung volume changes with 9.3% to 12.4% accuracy. These studies confirmed the fact that there exists a significant correlation between the variable derived by EIT and lung volume changes measured with spirometer and it is possible to model associated relationship. Panoutsos *et al*. (2007) conducted a study on 8 healthy male subjects with the aim to initially compare the lung volume estimates from a spirometer and body plethysmography (body box) against lung volume derived from the Sheffield Mk 3.5 absolute EIT (aEIT) system. In this initial investigation, they have found out that the absolute resistivity measurements were reasonable but the performance of the subsequent lung volume calculations was erratic. The error pattern revealed a consistent logarithmic relationship between the measured (spirometer and body box) values and the values obtained from the aEIT. Therefore, a full assessment of the ability of the aEIT system to perform measurements of the lung function was

conducted. An investigation into the calculations of the Nopp adult lung model (Nopp., *et al*., 1997) used in the aEIT software to estimate the lung resistivity has been done. Instead of modifying the Nopp model, a new calibration function was introduced to filter the output of the model hence allows the correction of the model. The results of the improved aEIT system show an increased accuracy on the absolute lung volume estimation and the removal of the logarithmic bias from the measurements but the need for a larger study that includes more subjects towards the development of multiple region of interests (ROIs) based on anatomical groups was also highlighted (Panoutsos *et al*., 2008). Detail reviews on the results from these studies are presented in Section 4.2 of this thesis.

EIT research has not only focused on EIT as a global lung ventilation imaging, but also as a potential regional lung ventilation imaging which is foreseen to be an interesting monitoring technique for use in the intensive care setting. In 2003, Hinz *et al.* have validated the functional EIT (fEIT) for measuring regional ventilation distribution by comparing it with single photon emission computerised tomography (SPECT) scanning in 12 anesthetised and mechanically ventilated pigs. They found a linear correlation between fEIT and SPECT scanning, whether breathing was spontaneous or mechanically delivered did not affect the correlation. A slight overestimation of ventilation in well-ventilated areas and a slight underestimation in poorly ventilated areas were seen but the difference was <10% of ventilation measured by SPECT scanning (Hinz *et al*., 2003). Victorino *et al*. (2004) have conducted a study on 10 mechanically ventilated patients to validate EIT measurements of ventilation distribution, by comparison with dynamic computerised tomography (CT) in a heterogeneous population of critically ill patients. EIT images from patients under controlled mechanical ventilation were found to be reproducible and presented good agreement to dynamic CT scanning. Depending on electrode positioning, EIT slightly overestimated ventilation imbalances but can reliably assess ventilation distribution during mechanical ventilation. Hahn *et al*. (2006) had also completed some useful work comparing aEIT, fEIT and CT scans on 4 intensive care patients. In this study, the absolute resistivity distribution was quantified by a

modified simultaneous iterative reconstruction technique (SIRT) scaled in Ωm. Such studies revealed that the fEIT images give reliable information on the relative chages in lung resistivity distribution but they require a reference measurement before the changes. The aEIT has an advantage in that it can provide information on the underlying cause. For example, in the case of an overdistension of lung tissue, a high air content will show a high resistivity and a fluid accumulation which also reduce ventilation show a low resistivity in aEIT. Tunney *et al*. (2007) and Pulletz *et al*. (2008) reported that the EIT is able to detect the changes in single lung ventilation of the patients, by showing a good separation of ventilated and non-ventilated sides of the lung. In 2010, Nebuya *et al*. compared the regional lung density estimated by aEIT with chest X-ray and CT images in 11 patients undergoing mechanical ventilation. The patients were grouped into 4 categories: normal lung, pneumonia, atelactasis and pleural effusion and the lung densities were estimated for 4 lung regions defined as right anterior, left anterior, right posterior and left posterior. The overall results show that it is feasible to obtain a quantitative value for regional lung density using aEIT with significant differences were found in regional densities between the normal lung and diseased lungs (Nebuya *et al*., 2010).

2.1.6.3 Optimisation of ventilator therapy using EIT

Optimisation of lung recruitment and the maintenance of open airways are very important in determining the outcomes of ventilated patients in the Intensive Care, while lung over-distension (volutrauma) and pressure damage (barotraumas) must be avoided. In most recent researches in the optimisation of ventilator therapy, EIT is found to have the potential to qualitatively and quantitatively assess different conditions of the lung during mechanical ventilation in critically ill patients and experimental animals. The regional ventilation and aeration distributions can also be assessed by EIT consecutively during a sequence of multiple changes in ventilator settings, e.g. during an incremental and decremental PEEP trial. Hinz *et al*. (2003) have used an open circuit nitrogen washout technique to measure the end-expiratory

lung volume (EELV) and compare with the end-expiratory lung impedance change (ELIC) measured by fEIT in 10 mechanically ventilated patients. In order to induce changes in the end-expiratory lung volume (EELV), PEEP levels were increased from 0 mbar to 5 mbar, 10 mbar and 15 mbar. The results showed that by increasing PEEP stepwise from 0 mbar to 15 mbar resulted in a linear increase of EELV and ELIC. However, the EELV and ELIC only represent the global parameters of the whole lung and expected that regional heterogeneity of the pulmonary compliance may cause slightly different results depending on the transverse slice monitored by EIT.

Pressure-Volume (PV) graphical waveforms have long represented the gold standard clinical practices for assessing the lung function and guiding the titration of mechanical ventilation in critically-ill patients. In 2006, Hinz *et al*. have proved that the lower and upper inflection points obtained from conventional global PV curves are not representative of all regions of the lungs. They have compared the lower inflection point (LIP) and the upper inflection point (UIP) obtained from Spirometry, EIT global and EIT regional PV curves respectively in up to 912 regions of interest (ROI) from 9 ventilated patients with acute respiratory failure (ARF) (Hinz *et al*., 2006). They have found a broad intra-individual heterogeneity of LIP and UIP regarding the pressure and numbers of regions in the regional measurements. The findings in this study are similar with the study conducted by Kunts *et al*. who found a significant higher LIP in the dorsal part compared with anterior part of the lung (Kunts *et al*., 2000). Another interesting work has been accomplished by Erlandsson *et al*. in the same year. They have evaluated the EIT in optimising PEEP to maintain a normal FRC and oxygenation, with minimal pulmonary and circulatory side-effects, before and after the abdominal surgery in morbidly obese patients which have an increased risk for peri-operative lung complications and develop a decrease in FRC. PEEP was titrated according to the baseline of the EIT tracing, where an upward slope of the baseline indicates recruitment and a downward slope indicates derecruitment and horizontal baseline indicates a stable end-expiratory lung volume. They have concluded that EIT enables rapid assessment of lung volume changes in morbidly obese patients and optimisation of PEEP.

Frerich *et al*. (2007) have found an excellent reproducibility of regional lung ventilation distribution determined by EIT in 10 ventilated supine pigs with repeated changed in PEEP settings. The study confirmed that highly significant shifts in regional lung ventilation distribution from ventral to dorsal regions in both lungs after PEEP increase. However, this study was performed under controlled experimental conditions in animals without lung pathology. Therefore the authors suggests that further studies on patients under multiple ventilator conditions are needed to support that EIT could be applied for bedside monitoring of mechanically ventilated patients with respiratory failure in the future.

Meier *et al*. (2008) have studied about the global, regional lung recruitment and lung collapse in experimental acute lung injury (ALI) on 6 anaesthetised and mechanically ventilated pigs by comparing results from EIT and CT images during incremental and decremental PEEP trial. A significant correlation was found between relative impedance and CT gas volume (GV) at the end of inspiration ($r=0.75$, $p<0.01$) and expiration ($r=0.78$, $p<0.01$) in all animals. They also observed that during the decremental trial, derecruitment first occurred in dependent lung areas, which indicated by lowered regional tidal volumes measured in this area and by a decrease of PaO2/FiO2. These observations are possible with EIT, hence they concluded that the ability of EIT in assessing the regional changes is considered to be superior to global ventilation parameters provided by established method in assessing the beginning of alveolar recruitment and lung collapse.

Bikker *et al*. (2010) discovered that the optimal PEEP should be titrated individually and cannot be generalised for a group of patients. In their investigation, a significant difference was found in response to a stepwise decrease in PEEP between patients with and without lung disorders, indicating a different PEEP dependency between these 2 groups. EIT measurements performed clearly visualise improvement and loss of ventilation in dependent and non-dependent parts, at the bedside in the individual patient. Differences in response to decremental PEEP steps were found not only

between patient groups, but also within groups (Bikker *et al*., 2010). In the same year, Denai *et al*. have produced a comprehensive physiological model to demonstrate the potential usage and ability of EIT to assess regional ventilation distribution in the lungs. This combines a model of respiratory mechanics, a model of lung absolute resistivity as a function of air content and a 2D-finite element model of the thorax with 16 electrodes to simulate EIT current injection and voltage measurements. The resulting physiological model can simulate different scenarios of acute respiratory distress (ARDS) lungs and reproduce consistent images of lung ventilation distribution in response to different PEEP levels. This simulation model illustrated the behaviour of EIT when detecting collapse or fluid shifts in damaged lungs and its potential to guide the titration of applied pressures during ventilator therapy hence allowing the clinicians to achieve the best compromise when adjusting airway pressures to reduce over-inflation of non-dependent lung units and to re-inflate collapsed airways (Denai *et al*., 2010).

2.1.7 EIT research trends

A number of important studies and ground-breaking research especially related to EIT application in pulmonary measurement have been reviewed extensively in this section. Despite the attractions of a safe, relatively inexpensive, non-ionising and non-invasive technique for measurement and imaging of the lung, EIT is still not widely used for routine clinical settings due to problems with electrodes error and reliability of measurements that have yet to be resolved. EIT also leads to low image resolutions and is unlikely to compete with chest X-ray, CT scans, or MRI scans in production of images for anatomical information. Instead, in recent years EIT research emphasise has been moving towards trying to obtain information such as the work of local lung ventilation, regional tidal volume, functional residual capacity, fluid accumulation and redistribution of lung recruitment.

Most of the studies on EIT as a lung imaging tool have so far focused on the changes in impedance with time (relative/functional EIT), instead of the absolute values. Functional imaging avoids the problem of having to take into account the shape of the body, but has the disadvantage of only detecting changes of the impedance distribution. Instead, the new absolute EIT takes this a step further, by not only looking at the changes in impedance during the respiratory cycles, but also producing absolute (as opposed to relative) values of impedance that can be compared to normal or reference values. Absolute EIT allows quantification of specific tissue resistivity, where absolute lung volume can be derived. It is envisaged that the absolute EIT is one of the main research areas that will receive the most attention within the next few years especially in the application of lung imaging. Although absolute EIT has shown some encouraging developments, it still faces some problems relating to the model used to produce the absolute resistivity. In order for the absolute EIT to fulfil its ability, hardware and software used to process the data must be continuously assessed and improved to minimise the errors and provide good reproducibility. Once this is accomplished, the ability to compare values with normal ranges to enable therapies where correction towards normal is helpful, such as the application of PEEP during mechanical ventilation would be the main advance.

Since EIT imaging offers online and long-term assessment of the lung's regional ventilation distribution in critically-ill patients, decision support systems can therefore be evolved to support clinical decision-making for optimising lung ventilation and ventilator manoeuvres such as lung recruitment. With this information available at the bedside, along with other relevant patient's physiological parameters routinely monitored in ICUs such as blood gases, a complete clinical picture of ventilated patients is available to support clinical decision-making and guide ventilator therapy. In the next section of this Chapter, recent research advances relating to the three major types of clinical decision support systems (knowledge-based, model-based and hybrid-knowledge-and model-based) will be reviewed and discussed.

2.2 Decision support systems (DSSs) for intensive care ventilators

2.2.1 Introduction

Large amounts of information generated by biomedical technologies often lead to considerable challenges, especially in intensive care units (ICUs) where many life-threatening events occurred and entail for immediate attention and implementation of corrective action. Mechanical ventilation is one of the crucial ICU tools which requires processing a large number of data to become information which then can be interpret by the clinician/expert to becomes knowledge for diagnostic and/or therapeutic purposes. Over the years, research has focused on helping clinicians in this field with their information processing needs and improves the clinical outcomes by development of advisory or decision support systems (DSSs). Various definitions have been given to describe these DSSs. Sim *et al*. (2001) had described the DSSs as software that designed to be a direct aid to clinical decision-making, in which the characteristics of an individual patient are matched to a computerised clinical knowledge base and patient-specific assessments or recommendations are then presented to the clinician for a decision. Osheroff *et al*. (2004) defined DSSs as the clinical knowledge and patient-related information, intelligently filtered or presented at appropriate times to enhance patient care. Regardless of definitions given to these systems, the main goal remaining that they are designed to help the clinicians integrate the huge amount of available data and make the best choice for the patients.

In the past few decades, many decision support systems (DSSs) have been developed for ventilator management in the ICUs. The systems' structure described in the literature can be classified into knowledge-based, model-based and hybrid-knowledge-and-model-based. With respect to planning and control, most of the DSSs developed are open-loop systems. Open-loop systems do not take direct therapeutic

actions; instead series of advices are proposed to the clinicians who are responsible for the comfort of patients and it is always up to them whether to execute or disregard this advice. An alternative to these systems is to control the ventilator directly and automatically by the DSSs, which is called the closed-loop system. Another system found in the literature is called the critiquing system, where the computer system does not offer treatment advice, instead, it criticises treatment decisions made by the clinicians based on its knowledge of the problem domain. Therefore, in this second section of the Chapter, recent work relating to these common structures of DSSs for intensive care ventilators will be reviewed and the current status and research trends in this field will also be discussed.

2.2.2 Knowledge-based systems

A knowledge-based system is the most common structure used in the development of DSSs. It is also known as an expert system, which contains clinical knowledge, usually about a very specifically defined task and are able to reason with data from individual patients to come up with sensible conclusions. Although there are many variations, the knowledge within an expert system is dominantly represented in the form of a set of rules.

The earlier knowledge-based DSSs for ventilator therapy were developed in 1980s where they were open-loop and designed with fixed rules based on clinical guidelines. One of the earliest systems developed was the VQ-ATTENDING, which used to critique the physician's settings rather than provide treatment options and suggest alternative plans (Miller, 1985). Another rule-based advisory system was introduced in 1986 which was designed to treat neonates with respiratory distress syndrome (RDS) (Carlo *et al*., 1986). The system made recommendations on whether to increase or decrease FiO2, PEEP, I:E, RR and PIP on the basis of set clinical guidelines. COMPAS stands for computerised patient advice system was introduced

and evaluated in 1989 by using several patients suffering from acute respiratory distress syndrome (ARDS) (Sittig *et al*., 1989). This system used expert treatment protocols in 5 ventilatory modes. It used a blackboard data base structure and a computerised clinical information system called HELP, which provided patient data to the system; data that was input by respiratory therapists, nurses and other medical personnel. The recommendations of this system were provided to obtain and maintain acceptable blood gas values for patients. The system's recommendations are reported to have a good agreement with those of clinicians most of the time but encountered problems in terms of error propagation caused by incorrect data entry in the system which caused a series of inappropriate treatment suggestions by the system.

The VentEx stands for Ventilator Expert (Shahsavar *et al*., 1994) system is an open-loop knowledge-based system used in the care of patients with respiratory failure. The knowledge is quantitatively and qualitatively represented by both rules and objects (hybrid representation) using the Nexpert object knowledge representation scheme. VentEx decision-support is in the form of recommendations during different phases in therapy including initiation, treatment and weaning phase. In the initiation phase, the system recommends initial settings for ventilator mode, minute volume (MV), respiratory rate (RR), inspiratory time (Tinsp), PEEP and inspired fraction of oxygen (FiO2). During the treatment phase, changes in ventilator settings are recommended. The suggested settings for MV, RR, PEEP and FiO2 are quantitatively presented together with previous settings. During the weaning phase, indications and contraindications for weaning are presented. In the following year, results of the system's validation were presented (Shahsavar *et al*., 1995). They have validated the results for initiation phase by comparing the advice produced by the system with the real clinical outcomes and found 78% agreement between the system and real clinical outcomes for indications and contraindications for ventilator therapy. For the treatment and weaning phase, real data from 12 patients with 6 different diagnoses were included. In this validation, VentEx achieved 77.8-95.5% acceptable advice which was considered encouraging but not satisfactory.

One of the systems that has successfully marked the early demonstration of closed-loop ventilator management on humans was NeoGanesh (Dojat *et al*., 1997). The system was devoted to closed-loop control of pressure support ventilation (PSV) and decision for extubation. In NeoGanesh, the knowledge was acquired from knowledge of ventilation management of the clinical staff of the ICU. It has several advantages which include a 24-h a day adaptation of respiratory assistance to the needs of the patients, reduced need for monitoring, better weaning outcomes and a reduction of the duration of mechanical ventilation. The architectural design of NeoGanesh was based on three fundamental tasks in medical reasoning: i) Monitoring, ii) Diagnosis and iii) Therapy planning. The system was evaluated in two steps. The first step was to evaluate the capability of NeoGanesh to maintain the patient in a zone of respiratory comfort defined as: 12<RR<28 cycles/min, tidal volume> 300ml and end-tidal CO2 pressure < 55mmHg. 19 patients were divided into 2 groups according to their results from a number of tests. In the second step, 5 patients were ventilated randomly for 24 h with and without NeoGanesh. Results show that NeoGanesh maintained the patients within a comfortable zone of ventilation during 91±8% of the total duration of ventilation compared to 71±18% without it and patients spent 4±7% of the total duration in severe situations compared to 18±15% without use of the system. This preliminary validation shows that patients show less signs of respiratory discomfort with automatic control of the ventilation than without it. The diagnosis proposed by the system concerning the capability of the patient to breathe without external assistance is more efficient than by the usual manual procedure.

Since the early 1990's, there has been an increasing interest in the use of fuzzy logic in biomedicine. It is a method of handling data that allows ambiguity and as a result, it is particularly suited to medical applications. Fuzzy logic systems have been found to be easy to configure and tune, unlike Artificial Neural Networks (ANN), the logical constructs used in these systems are easy to describe and closely approximate the thinking processes used in clinical decision making (Hanson *et al*., 2001). Fuzzy

control processes have been used for the administration of anaesthetics in the operating room (Mason *et al*., 1996; Zbinden *et al*., 1995; Ross *et al*., 1997) and also for control of mechanical ventilation (Schaublin *et al*., 1996; Nemoto *et al*., 1999).

Sun *et al*. (1994) have implemented a fuzzy logic-based controller in a microcomputer based system for adjustment of inspired oxygen concentration (FiO2) in ventilated newborns. The goal of this control system is to maintain patient oxygenation (measured by oxygen saturation using pulse oximetry) at a target level set by the physician. In this system, the fuzzy logic controller was utilised based on "rules" generated by neonatologists who routinely provide care for ventilated infants. It is an open-loop system which did not control the ventilator directly; instead, the system operates by displaying suggested FiO2 changes to the physician, who then decides whether to execute the recommended change to ensure medical safety until the system is fully tested for clinical efficacy. The fuzzy controller showed promise in the preliminary trials to control patient oxygen saturation levels and was able to maintain target SaO2 better than routine manual control. However, further clinical trials and additional patients' data were emphasised to test the actual clinical efficacy of the controller and allow fine tuning of the control parameters.

Nemoto *et al*. (1999) reported a system which used fuzzy logic for automatic control of pressure support mechanical ventilation. The membership functions for this controller were designed heuristically. The outputs were based on the fuzzy membership levels of the patient's condition and its trend. The controller was evaluated by comparing its output with the actual changes made by the clinicians. They have validated the system using retrospective clinical data from 13 COPD patients and found that in 72-78% of cases, the agreement between the fuzzy controller and the changes actually made clinically was within ±2 cmH2O.

In 2003, Kwok *et al*. presented a work on modelling the clinicians' advice for decision-making. They had derived the rules for changing the inspired oxygen (FiO2) using adaptive neuro-fuzzy inference system (ANFIS) instead of acquiring the knowledge from the expert which is time consuming. In this development, PaO2 from arterial blood-gas measurement was chosen as the control parameter and it was set to be 15 kPa. Since PaO2 is not taken regularly; therefore the system developed was an event-driven control system. The change of the inspired fraction of oxygen (FiO2) advised by 8 clinical experts responding to 71 clinical scenarios was recorded. ANFIS and multilayer perceptron (MLP) were then used to model the relationship between the inputs (current PaO2 level, current FiO2 and PEEP level) and the output (change in FiO2). The controllers were then validated using the simulation results by clinicians. Both ANFIS and MLP were found to correlate with the clinicians' decision better (correlation coefficient=0.694 and 0.701 respectively) than the previous fuzzy advisor (FAVEM). In this work, the use of ANFIS has shown the ability to facilitate the modelling of the clinicians' knowledge in the development of intelligent advisors for intensive care ventilators. Although both ANFIS and MLP were capable of modelling the clinicians' decision-making accurately, but ANFIS is more interpretable than MLP.

The latest work on DSSs that uses fuzzy logic was presented by Kilic *et al*. (2010). They have designed a fuzzy logic inference system for decision making in weaning from mechanical ventilation and tested and compared its efficiency with those of rapid shallow breathing index (RSBI), pressure time index (PTI) and Jabour's weaning index (JWI), in predicting expert opinion over randomly generated clinical scenarios. In this fuzzy logic inference system, they have used 9 variables and 5 rule blocks within 2 layers which have been designed to evaluate the appropriateness of systematic perfusion, ventilation, acid-base balance and mechanical endurance of respiratory muscle for weaning. For the system validation, a surgeon involved in treatment of critically ill patients and who was unaware of the study objectives has been asked to make predictions on 100 computer generated clinical scenarios and the efficiency of calculated predictors have been evaluated to predict expert opinion. The

validation results had shown that the RSBI has failed to predict expert opinion in 52% of scenarios, while the fuzzy logic inference system has shown the best discriminative power in predicting expert opinion.

2.2.3 Model-based systems

In contrast with the knowledge-based, model-based systems are available in which the treatment methods are optimised by simulating a physiological model of the patient. In 2001, Goode had presented a model-based fuzzy logic advisory system for intensive care ventilators called the FAVEM (Goode, 2001). The system was based on an improved Dickinson's MacPuf model: the SOPAVent (Simulation of Patient under Artificial Ventilation). FAVEM gave advice on five ventilator settings: FiO2, PEEP, minute ventilation, tidal volume and inspiratory time. The initial fuzzy rules were handcrafted based on an extensive literature survey and consultations with a clinical expert. These initial fuzzy rules were then modified heuristically using simulation results on the SOPAVent. The system was validated using retrospective clinical data from 11 patients. In 23.5% of the cases, the advisor was judged to give poor matching to the clinician's decision. The level of decision matching was therefore considered disappointing and the authors emphasised several reasons which includes an inability of the system to reject measurement errors, the need for other measurement or information to be included and the need for larger range of acceptable blood gas levels.

Recently, Rees *et al*. (2006) have developed a DSS for optimising mechanical ventilation in patients residing in the intensive care unit. The system includes physiological models and utility functions in a decision theoretic approach to optimise ventilation. Physiological models are used to simulate the effects of changes in ventilator settings on pressures and volumes in the lung and the oxygenation and acid-base status of the blood. The DSS includes physiological models of O2 and CO2

transport, storage and lung mechanics. The system also includes penalty functions describing the goals and side effects of mechanical ventilation. The total penalty is obtained as an addition of the individual penalties for insufficient oxygenation, acidosis and alkalosis, risk of oxygen toxicity and absorption atelectasis and barotraumas. The system can be used to estimate patient specific parameters providing a clinical picture of the patient's state describing all measurements, to answer "what if" questions, simulating the effects of different ventilator strategies and to find the optimal ventilator strategy; a process which occurs automatically in the DSS using repeated simulations to find the ventilator strategy which gives the minimum total penalty.

Allerod *et al*. (2008) had validated the feasibility of the DSS proposed by Rees *et al*. (2006). The system was assessed by estimating patient specific parameter values, evaluating the fit of the physiological models and comparing the DSS suggested values of tidal volume, respiratory frequency and FiO2 with those selected by the clinician. They have used retrospective clinical data from 20 patients following uncomplicated coronary artery bypass grafting (CABG) with cardiopulmonary bypass. The models fit well to measured data with the exception of some of the variables describing oxygenation (SaO2, PaO2 and SvO2). On average, it was possible to select ventilator settings which reduced the penalty associated with oxygen toxicity, with a substantially smaller increase in penalty associated with oxygenation. In general, the penalty functions included in the DSS provides a good balance between competing goals in this patient group. Despite these encouraging findings, no prospective evaluation of the advice of the DSS was performed. The simulations performed by the models were not evaluated and some consideration as to the accuracy of these simulations was still required. Values of model parameters are assumed to be constant which is clearly invalid for large changes in ventilation which may have an effect on both respiratory and circulatory parameters.

The latest model-based DSS for ventilated intensive care patients found in the literature was developed by Wang *et al*. (2010). The design approach used is based on a goal-directed multi-objective optimisation strategy to determine the optimal ventilator settings that effectively restore gas exchange and promote improved patient's clinical conditions. Previously developed simulation of patient under artificial ventilation (SOPAVent) model was used to predict continuously and non-invasively the patient's respiratory response for different ventilator settings. Figure 2.7 depicts the architectural design of this DSS. The DSS provides advice on FiO2, Pinsp and Vrate settings only because of the unproven SOPAVent's performance to predict PEEP and Tinsp. The advisor was divided into 2 subsystems; i) FiO2 which mainly affects the patient's oxygenation and ii) Pinsp/Vrate which mainly influence the minute volume ventilation of the patient.

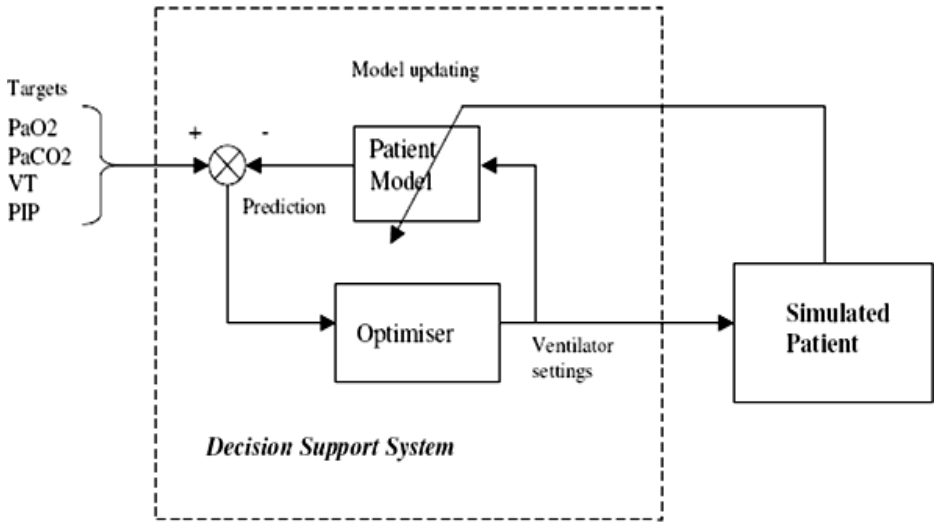

Figure 2.7: The architectural design of adaptive ventilator management decision support system [Wang *et al*., 2010].

The main control parameters are PaO2, PaCO2, peak inspiratory pressure (PIP) and tidal volume (VT), which the target values were suggested by senior ICU clinicians. For Pinsp/Vrate subsystem, the main goals were to maintain the patient's PaCO2 within the assigned normal range while avoiding excessive airway pressure (PIP) and

tidal volume (VT). The objective function for the Pinsp/Vrate subsystem was formulated using the aggregated multi-objective function and the selection of the weighting parameters was crucial as it decides on the relative importance of the individual goals and whether the optimal compromise among the competing therapeutic goals is achievable or not. Genetic algorithm (GA) optimisation technique has been used in this study. For the FiO2 subsystem, the main goal was to maintain PaO2 within the normal range. The same method developed by Kwok *et al*. (2004) was applied to search for FiO2 that meet the PaO2 target. A closed-loop validation was performed to assess the system's ability to deal with different simulated patients' scenarios designed to produce lung pathophysiological conditions similar to those observed in real clinical environment and evaluate whether this DSS can produce clinically meaningful advice and consistent performance under various competing therapeutic goals. In all simulation scenario, considered, the system was able to generate satisfactory ventilator settings under competing therapeutic goals. However, the authors did emphasised that the system needs to be evaluated for its relevance, performance, efficiency and impact in real clinical settings. One of the main limitations of the system is the unavailability of PEEP advice. The current DSS was also designed with fixed ventilator targets, which in real clinical settings is not realistic, since these often vary depending on the patient's condition. Hence, more flexible target-setting component should be included in future work.

2.2.4 Hybrid-knowledge-and model-based systems

An exclusively knowledge-based approach may have the tendency of biases in the expert's knowledge and a purely model-based system is difficult in that a complex yet accurate and effective model is barely available. Therefore, researchers in this field have investigated an alternative structure that combined the knowledge and model-based to complement the weaknesses of each system's structure. In general, rules for the knowledge component of the system are based on combination of the patient's physiological model as well as the clinical guidelines.

Kwok *et al*. (2004) developed the Sheffield Intelligent Ventilator Advisor (SIVA) that combined knowledge and model-based decision support system for intensive care ventilator management that offers more objectivity than conventional knowledge-based system and eliminates the need for an extensive and complicated mathemathical model. The system provides settings for inspired oxygen (FiO2), positive end expiratory pressure (PEEP), respiratory rate (RR) and inspiratory pressure (Pinsp) for ventilated ICU patients. The system was divided into two main modules: i) The top-level module is a qualitative (knowledge-based) component to provide advice on direction of change of each ventilator setting and set the target for the lower level module, ii) The lower-level module is a quantitative (model-based) component which designed to define the amount of changes for the relevant ventilator parameters (Figure 2.8).

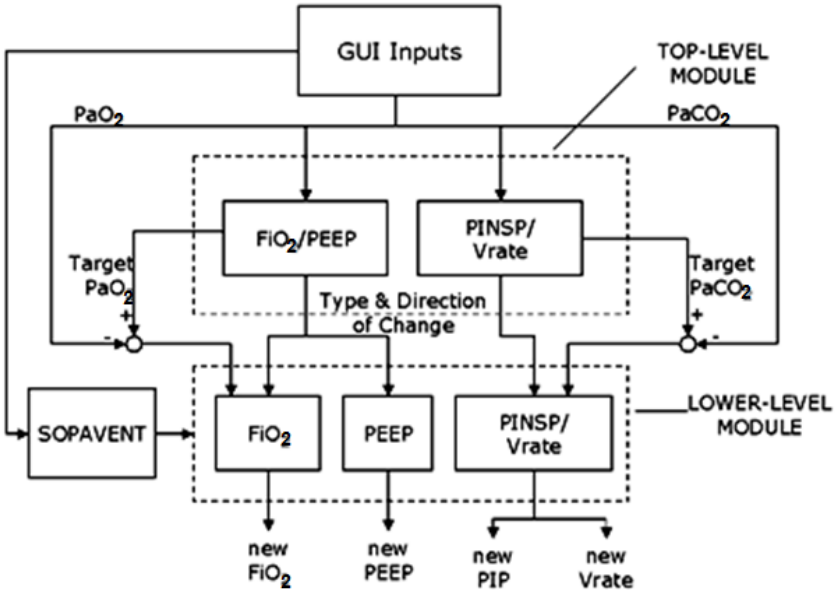

Figure 2.8: The architecture of SIVA [Kwok *et al*., 2004].

Each module was divided into FiO2/PEEP subunit which controls the oxygenation related settings and Pinsp/Ventilatory rate subunit which controls the settings relating to the minute ventilation. Each subunit generates advice for 2 ventilator settings and is

implemented in 2 fuzzy rule bases, one for each ventilator setting. The primary inputs for FiO2/PEEP were PaO2, previous PaO2, FiO2, previous FiO2 and PEEP. While primary inputs for Pinsp/Vrate were PaCO2, previous PaCO2, pH, Pinsp and Vrate. The advice given by the top-level have been validated against retrospective real patient data and compared with intensivists expertise and performance under simulation conditions. Since the lower-level generated the quantitative component of the advice, it received inputs from the top-level module, which include the target blood gas levels and the type and direction of the change required for each ventilator setting. Then the amount of change required was calculated in each ventilator setting based on mathematical model of the respiratory system (SOPAVent) which predicted the blood gases of the simulated patient under artificial ventilation. However, due to the limitation of the model, the change in PEEP was not derived using a model-based method. Closed-loop simulations were performed to validate the system's performance assuming various clinical scenarios including sudden changes in the patients' parameters such as shunt or deadspace with noise and disturbances. The results showed that the advice given by the system was appropriate and the blood gases resulting from the closed-loop decision support were acceptable. However, the authors did emphasise on more work needed to be carried-out to model the effects of PEEP while prospective clinical studies should be undertaken.

FLEX, a new computerised system for mechanical ventilation that can be used both as an open-loop advisory tool and also as automatic controller for weaning has been developed by Tehrani *et al*. (2008). Unlike most previous system that only concentrate on one mode of ventilation, this system was designed for use in a wide range of ventilator mode. It used knowledge-based as well as model-based rules to determine optimal settings of the ventilator, however, it did not simulate the oxygen and carbon dioxide transport models of the patients. Instead, many of its rules were considered adaptive and derived based on physiological models and hypotheses. The system utilises the ventilator settings and measured ventilator data which can be provided directly from the ventilator. The monitored patient data can be input directly to the system or keyed in manually, depending on how the data was obtained. The

system can be used in volume control/assist or pressure control/assist modes as well as pressure-support (PS) mode for weaning. The open-loop advisory system has been tested by comparing the system recommendations with clinical data. The sample results demonstrated that FLEX recommendations were in line with clinical determinations. In closed-loop mode, one of the potential advantages of FLEX is to automate the weaning process and allow for more frequent weaning evaluations. FLEX showed much clinical potential, where it was able to predict failure of weaning in 2 patients via recommendation not to wean in these patients. However, the authors also highlighted that more detailed clinical evaluations of the open-loop as well as the closed-loop weaning version of FLEX are needed to fully assess the effectiveness of the system in the treatment of mechanically ventilated patients with different underlying illness.

2.2.5 Current status and research trends

Over the last forty years, extensive research has been carried-out on decision support systems for intensive care ventilators both theoretically and practically. The intensive care environment seems to gain the most from decision support systems application due to the greatest challenges in the timely management of vast amount of data/information from the advanced mechanical ventilators and the opportunities to increase efficiency in patient care. There are three categories of decision support systems' structure that have been reviewed; i) Knowledge-based, ii) Model-based and iii) Hybrid-knowledge-and-model-based. Although model-based systems can be informative to clinicians, parameters which required by the physiological models are often uncertain and expect data that are not available in real-time or data whose estimation is difficult or imprecise. The major advantage for knowledge-based is that the rules embedded in the systems are easy to explain and closely approximate the thinking processes used in making clinical decisions. Various types of artificial intelligent (AI) tools also have been used in designing the decision support systems such as fuzzy logic, neuro-fuzzy inference system (ANFIS), neural networks, genetic

algorithms and so on to process clinical signs, symptoms and laboratory test results in relation to the structure used. The availability of these AI tools have been recognised as to perform as intelligent assistants to clinicians providing constantly monitoring electronic data streams for important trends or adjusting the settings of mechanical ventilations.

Despite the increasing trend towards automation, the majority of the up-to-date decision support systems are still mainly open-loop systems whose parameters need to be adequately set by clinicians. If the systems are to be implemented in a closed-loop mode, validation algorithms, data abstraction and smoothing techniques are needed to be incorporated into the system to prevent incorrect data entry. Most of the systems described in the literature are not in clinical use due to lack of continuous evaluation or assessment in the real clinical environment. In most published papers on decision support systems, the evaluation of the system have focused on evaluation by simulation and very few evaluations focused on the impact of the systems on clinical care. One of the reasons for this, as mentioned by East *et al*. (1995), is that these systems are pure engineer-oriented products, not related to common clinical practice and it is not mature enough to support the real clinical situation and hence less acceptance by the clinicians. However, it is undeniable that real-monitoring and control systems are extremely difficult to evaluate due to the fact that it is an interdisciplinary field which requires commitments from the clinical medicine, computer systems and biomedical engineering personnel. Therefore, as an alternative, these systems were mostly evaluated by comparing the compliances between system's suggestions with actual decisions made by the clinicians on recorded patient cases or via simulations of patient's conditions and used some index to represent the success of the ventilator control system.

Future decision support systems are more likely to act as the useful device that can help clinicians in managing information from the advanced mechanical ventilation. From current trend of decision support systems' design methodologies, there is a

potential for electrical impedance tomography (EIT) to be incorporated as one of the system's input to give extra information about the regional lung functions and hence improve patient's outcome. However, according to Tehrani and Roum (2008) for the future decision support to be useful, such systems should be designed to be effective, safe and easy to use at the patient's bedside and these systems are expected to be capable of noise removal, artefact detection and effective validation of data.

In this context, a series of investigations on healthy volunteer subjects to access the accuracy and consistency of the Sheffield Mk 3.5 aEIT system measurements will be presented and the outcome of the investigations will be analysed and discussed in the next Chapter.

CHAPTER 3

EIT STUDY ON HEALTHY VOLUNTEER SUBJECTS

3.1 Introduction

The efforts to investigate the feasibility of Electrical Impedance Tomography (EIT) to assess the lung ventilation have been extensively reviewed in Chapter 2. However, the review showed that most of the EIT lung ventilation related studies currently focuses on relative/functional EIT not absolute EIT. Therefore, in this Chapter, a series of investigations on twelve (12) healthy volunteer subjects were conducted with the aim to assess the accuracy and consistency of the Sheffield Mk 3.5 aEIT system (software of version 1.047) measurements by comparing them with results from spirometry and body plethysmography (body box) data. Spirometry is a simple test to measure static lung volumes such as vital capacity (VC), tidal volume (VT), forced vital capacity (FVC) and forced expiratory volume (FEV) while body box is a more complex procedure which is commonly used to measure the residual volume (RV), total lung capacity (TLC) and functional residual capacity (FRC) of the lungs (Behr and Furst, 2008). This Chapter is organised as follows; first, the equipments used together with aEIT system, study protocol and data collection methods are reviewed; then, the lung volumes calculated from the aEIT system are compared with the one measured from spirometry and body box and the results are analysed and discussed; finally, conclusions are drawn based on the performance of the aEIT system.

3.2 Equipments/tools used with aEIT system

The subjects' chest circumferences were measured using a disposable tape measure. "Mitutoyo Absolute Digmatic" callipers were used to measure the patients' chest; measurements were taken of chest width and depth in order to calculate an ellipse ratio (Figure 3.1).

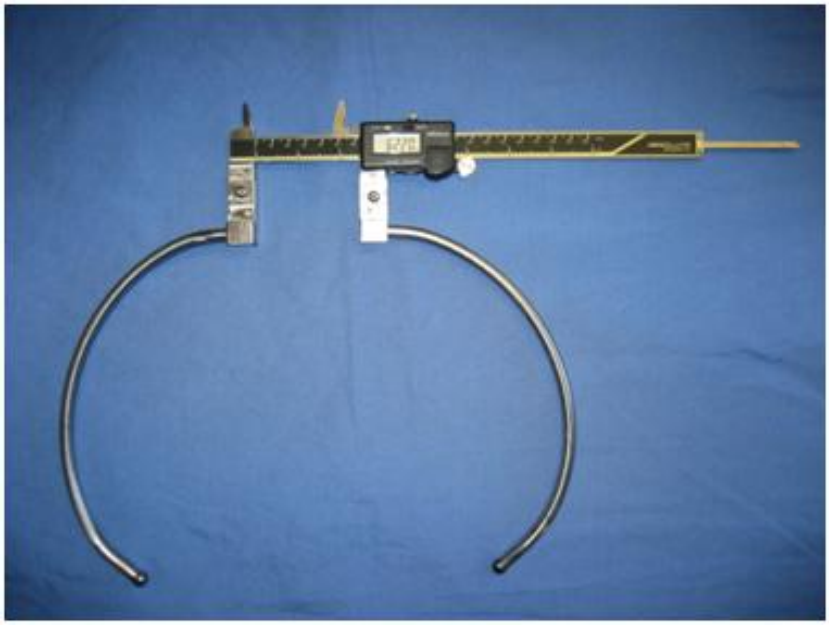

Figure 3.1: Chest callipers.

The Skintact Premier ECG electrodes (Figure 3.2) were used with the aEIT data collection unit.

Figure 3.2: Skin surface electrodes used for aEIT system.

The aEIT data were acquired via the Sheffield Mk3.5 aEIT system which is the latest of a number of EIT systems developed in Sheffield (Wilson *et al*., 2001). Details of this aEIT system hardware and previous EIT system developed in Sheffield can be found in Chapter 2. The Sheffield Mk3.5 aEIT software of version 1.047 (written in MATLAB) that contains the computer user interface and various models was used to control the Mk3.5 system and estimate the absolute lung resistivity and volume.

3.3 Study protocol and data collection methods

The study involved twelve healthy volunteers (8 males and 4 females) with different body sizes and thorax shapes. Demographics information of the subject such as gender, height and chest circumference was recorded. The chest width and depth were also recorded in order to calculate an ellipse ratio. These data are necessary for the aEIT system to estimate the absolute lung resistivity and volume. Table 3.1 shows the demographic information of all the healthy volunteer subjects.

Table 3.1: Demographics information of the healthy volunteer subjects

Subject	Gender	Height (cm)	Chest	
			Ellipse ratio	Circumference (cm)
1	F	163	1.36	82
2	F	171	1.42	89
3	F	147	1.50	88
4	F	150	1.44	86
5	M	172	1.44	94
6	M	181	1.37	113
7	M	175	1.62	94
8	M	178	1.29	97
9	M	185	1.39	110
10	M	170	1.41	100
11	M	185	1.35	107
12	M	170	1.50	91

3.3.1 Spirometry and aEIT measurements

The subjects were connected to the Sheffield Mk3.5 aEIT system via the 8 electrode array and simultaneously breathing through the spirometer tube (SensorMedics). Ideally, the electrodes should be attached in a horizontal plane 5cm above the xyphoid process, and equally spaced around the circumference (Figure 3.3). Data were recorded for 60 sec involving quiet breathing at functional residual capacity (FRC); one litre breathing and maximum inspiration and expiration manoeuvres in sitting at 45^0 (sitting with slightly leaning back) and supine (lying flat) positions respectively. According to the clinician, these positions are the most common positions for the patients in the intensive care unit (ICU). Therefore, it is essential for the subjects to be at these positions when the study commenced so that it can imitate the real situation of how the patient's body were being positioned in the ICU.

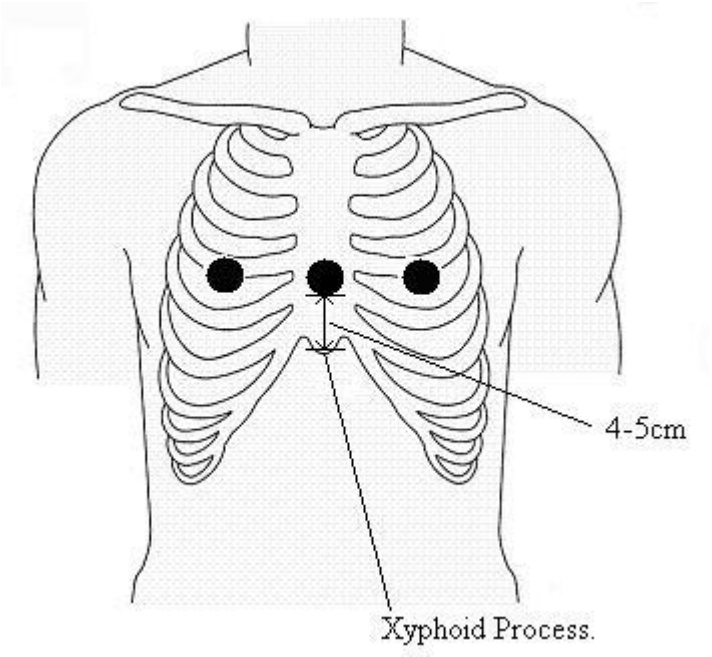

Figure 3.3: The level of the EIT electrodes array in the frontal plane [Tunney, 2007].

3.3.2 Body plethysmography (Body box)

In body plethysmography (body box), the subjects were asked to breathe at FRC, inhale and exhale to the minimum and maximum volumes respectively and perform panting.

3.3.3 MRI scans

These MRI scans were performed to determine the position, shape and size of regions of interest which most consistently contain lung tissue, rather than heart or chest wall. A more accurate regions of interest i.e. the areas of the thorax on aEIT imaging where lung tissue exists in human subjects, will be established. The subjects were asked to breathe at FRC for 2 mins and then the MRI scan was started and lasted for say 20 sec., at which point the subject was asked to take maximal breath in until the lungs are

absolutely full, then exhale until the lungs are as empty as possible. Scanning was continued for 10 sec after the maneuver has ended. This recording was repeated three times. These MRI images are expected to be able to define common areas of lung tissue or regions of interest in all subjects.

3.4 Results and discussions

Before the lung volume calculated from aEIT system were analysed, it is essential to know how this absolute lung volume was being calculated in the current aEIT system. Hence, the relationship between absolute resistivity and lung volume is presented. Then, the lung volumes obtained from the 12 healthy volunteers using aEIT, spirometry, and body box are analysed and compared. The MRI images were studied and analysed later for the work on improvement of regions of interest. The values recorded with the body box are taken as the reference values. Poor data due to significant electrical interference or poor electrode contact have been excluded (these were indicated by '-'). The percentage of mean absolute error (MAE%) and standard deviation of the errors (eSTD) were used as the performance indices for all the analyses.

3.4.1 Absolute resistivity-lung volume relationship in aEIT system

In Sheffield Mk 3.5 aEIT system, the model of lung density ($\rho lung$) as a function of absolute lung resistivity ($absR$) obtained by Nopp et al. (1997) has been employed to calculate the absolute lung volume ($absLV$) as follows:

$$\rho lung = 3.12 - 3.24\,[ln(absR)]^{0.3} + 0.81[ln(absR)]^{0.6} \quad \textbf{(3.1)}$$

In this equation, the *absR* has been calculated using the Zubal model as explained in Section 2.1.4.3 in Chapter 2. According to Nopp model (Nopp et al., 1997), if the lung weight (*Wlung*) is known, then the *absLV* can be calculated as:

$$absLV = \frac{Wlung}{\rho_t}\left(\frac{\rho_t}{\rho lung} - 1\right) \quad \textbf{(3.2)}$$

Where ρ_t denotes the density of the lungs condensed matter, which has been fixed to $1050 Kg.m^{-3}$ (Duck, 1990). In the current aEIT system, the *Wlung* is estimated by models based on information of body height and gender. Details about these models can be found in Section 4.2.2 of Chapter 4.

3.4.2 Comparison between spirometry lung volumes and the aEIT lung volumes in sitting and supine position

From the results related to quiet breathing, 1 litre breathing and maximum breathing recordings of spirometry, tidal volume (VT), 1 litre breaths and vital capacity (VC) were extracted and analysed. While tidal volume (VT), 1 litre braths, functional residual capacity (FRC), vital capacity (VC), total lung capacity (TLC) and residual volume (RV) were the volumes extracted from the aEIT recordings during quiet, 1 litre and maximum breathing. The readings from the spirometry are an average taken of every breath during the manoeuvres. For quiet breathing and 1 litre breathing, these are the mean value of the 16-20 breaths and for the maximal breathing; the VC values are a mean of the 6 (2 sets of 3 big breaths) measurements taken. For the aEIT readings, the VT during quiet breathing and 1 litre breathing are the mean values of all the breaths for the whole 60 seconds of the recording. While the VC, TLC and RV during the maximal breathing, these are the mean of the 3 big breaths taken within 60 seconds of the recording. One typical set of subject results estimated by the aEIT in the sitting and supine position is shown in Figures 3.4 and 3.5.

For each subject, the mean tidal volume (VT), 1 litre breaths and vital capacity (VC) calculated by aEIT were compared with the mean tidal volume (VT), 1 litre breaths and vital capacity (VC), measured from the spirometry. Tables 3.2–3.4 summarise the results for analysis of these lung volumes in sitting position while Tables 3.6-3.8 summarise the analysis results in supine position. The performances of the aEIT in sitting position are compared and shown in Figure 3.6 and Table 3.5, while Figure 3.7 and Table 3.9 show the performances of aEIT in the supine position.

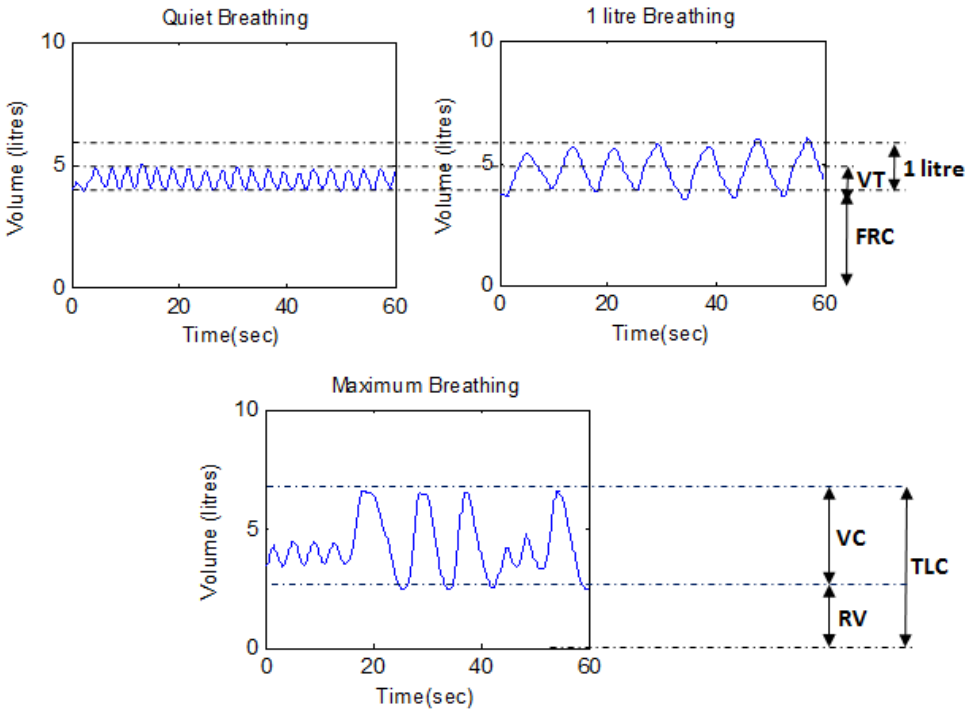

Figure 3.4: aEIT lung volumes during the three manoeuvres in the sitting position.

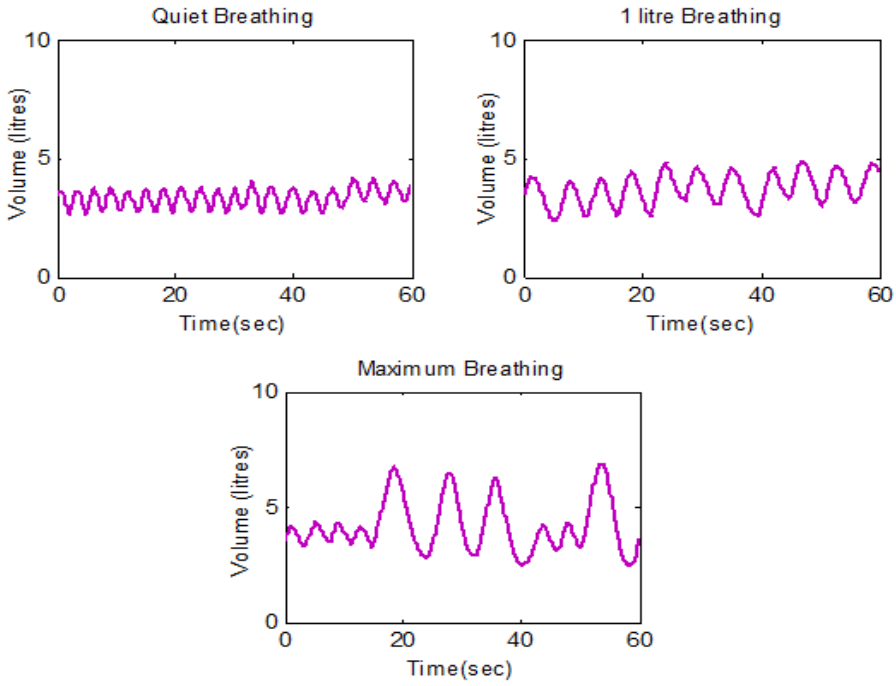

Figure 3.5: **a**EIT lung volumes during the three manoeuvres in the supine position.

3.4.2.1 Results in sitting position

Table 3.2: Comparison between VT from aEIT and the VT from spirometry in the sitting position (-: data missed due to poor recordings).

Subject		**Tidal volume (VT)**		
		Spirometry (litre)	**EIT (litre)**	**Absolute Error**
Females	**1**	0.29	0.81	0.52
	2	0.22	0.68	0.46
	3	0.63	0.62	0.01
	4	0.81	1.38	0.58
Males	**5**	0.36	0.96	0.60
	6	1.01	0.46	0.55
	7	0.60	0.94	0.34
	8	0.21	0.44	0.23
	9	0.80	0.54	0.26
	10	0.33	-	-
	11	1.48	0.76	0.72
	12	0.68	0.51	0.17

Table 3.3: Comparison between 1 litre breaths from aEIT with 1 litre breaths from spirometry in the sitting position.

Subject		1 Litre breaths		
		Spirometry (litre)	**EIT (litre)**	**Absolute Error**
Females	**1**	0.74	1.79	1.05
	2	0.80	1.33	0.53
	3	1.11	0.91	0.20
	4	0.88	1.64	0.76
Males	**5**	0.82	1.32	0.50
	6	1.18	0.71	0.47
	7	1.10	1.01	0.09
	8	0.89	1.03	0.14
	9	0.99	0.54	0.45
	10	0.73	1.16	0.43
	11	1.24	0.69	0.55
	12	0.94	1.39	0.45

Table 3.4: Comparison between VC from aEIT against the VC from spirometry in the sitting position (-: data missed due to poor recordings).

Subject		Vital capacity (VC)		
		Spirometry (litre)	**EIT (litre)**	**Absolute Error**
Females	**1**	3.00	4.21	1.21
	2	4.05	-	-
	3	2.35	3.00	0.66
	4	2.88	5.69	2.81
Males	**5**	3.63	5.31	1.68
	6	5.24	3.36	1.88
	7	4.59	6.73	2.15
	8	4.55	4.60	0.05
	9	5.97	3.72	2.25
	10	2.25	2.73	0.48
	11	5.66	3.16	2.50
	12	3.90	5.38	1.48

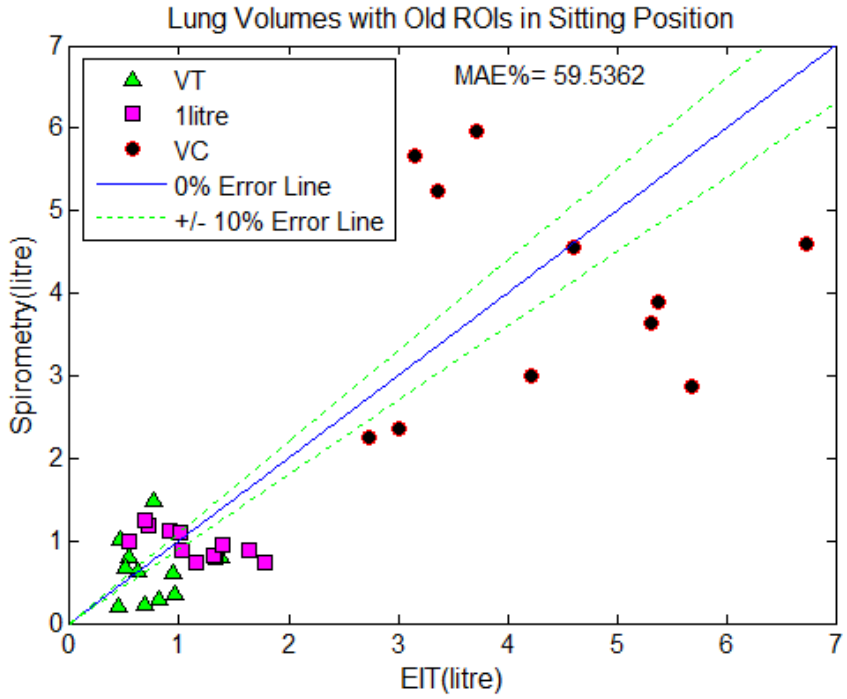

Figure 3.6: Scatter plot shows the VT, 1 litre breaths and VC calculated by the aEIT software against the one measured from the spirometry in the sitting position.

Table 3.5: Summary of the performance indices for aEIT in comparison with spirometry in the sitting position.

	Sitting		
	Tidal volume (VT)	1 litre breaths	Vital capacity (VC)
MAE (%)	86.71	52.75	39.68
eSTD	0.28	0.39	1.29

3.4.2.2 Results in supine position

Table 3.6: VT from aEIT against the VT from spirometry in the supine position.

Subject		Tidal volume (VT)		
		Spirometry (litre)	**EIT (litre)**	**Absolute Error**
Females	**1**	0.44	0.97	0.53
	2	0.18	1.07	0.89
	3	0.53	0.78	0.25
	4	0.78	1.05	0.27
Males	**5**	0.41	0.72	0.31
	6	1.66	0.75	0.91
	7	0.51	0.80	0.30
	8	0.24	0.81	0.57
	9	1.25	1.00	0.25
	10	0.40	0.64	0.24
	11	1.25	0.80	0.45
	12	1.01	0.90	0.11

Table 3.7: 1 litre breaths from aEIT against the 1 litre breaths from spirometry in the supine position.

Subject		1 Litre breaths		
		Spirometry (litre)	**EIT (litre)**	**Absolute Error**
Females	**1**	1.15	1.76	0.61
	2	0.82	1.53	0.71
	3	1.10	1.76	0.66
	4	0.78	1.47	0.69
Males	**5**	1.03	1.6	0.57
	6	1.31	0.91	0.40
	7	1.36	1.24	0.12
	8	0.60	0.98	0.38
	9	1.43	0.81	0.62
	10	0.70	1.18	0.48
	11	1.20	0.92	0.28
	12	1.13	1.41	0.28

Table 3.8: VC from aEIT against the VC from spirometry in the supine position.

Subject		Vital capacity (VC)		
		Spirometry (litre)	**EIT (litre)**	**Absolute Error**
Females	**1**	2.93	4.43	1.50
	2	4.14	6.15	2.01
	3	2.76	5.35	2.59
	4	3.09	7.81	4.72
Males	**5**	3.18	5.76	2.58
	6	5.35	2.91	2.44
	7	4.14	6.89	2.75
	8	4.29	4.6	0.31
	9	5.76	4.33	1.43
	10	1.65	2.46	0.81
	11	5.54	3.64	1.90
	12	3.76	6.13	2.37

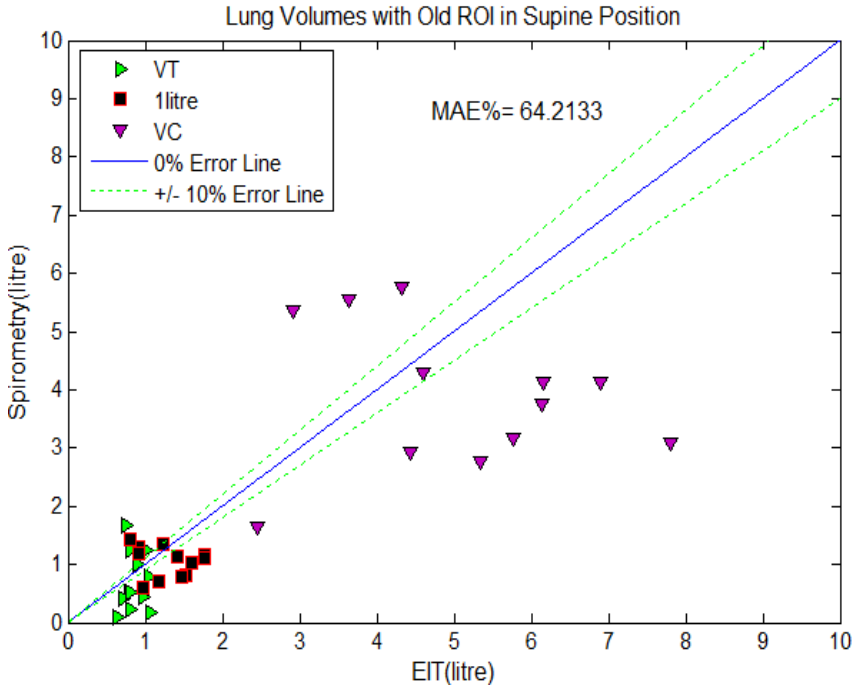

Figure 3.7: Scatter plot shows the VT, 1 litre breaths and VC calculated by the aEIT software against the one measured from the spirometry in the supine position.

Table 3.9: Summary of the performance indices for aEIT in comparison with spirometry in the supine position.

	Supine		
	Tidal volume (VT)	1 litre breaths	Vital capacity (VC)
MAE (%)	77.03	50.35	65.26
eSTD	0.14	0.34	1.61

The overall results of absolute lung volumes calculated by the aEIT show a large deviation from the spirometry measurements in both sitting and supine positions. The average accuracy for aEIT is about 40% in the sitting position and 36% in the supine position. It is obvious that the absolute lung volumes reading in the supine position have contributed to a larger error as compared to the absolute lung volumes in the sitting position. It is also observed that most of the lung volumes from the aEIT readings are overestimated. It is suspected that the use of one fixed region of interest has led to this problem, where this one region of interest is not able to be fix with all subjects due to inter-individual differences in the human thorax anatomy and hence produce significant errors in absolute lung volume calculation.

3.4.3 Comparison between body box lung volumes and aEIT lung volumes

The mean tidal volume (VT), functional residual capacity (FRC), total lung capacity (TLC), residual volume (RV) and vital capacity (VC) calculated by aEIT were recorded for all subjects and compared with the mean tidal volume (VT), functional residual capacity (FRC), total lung capacity (TLC), residual volume (RV) and vital capacity (VC), measured from the body box. Table 3.10-3.14 summarise the results for analysis of these lung volumes and the performances of the aEIT are compared and shown in Figure 3.8 and Table 3.15. The '-' sign indicates that there are no body box measurements done and also poor EIT data recordings for that particular subject.

Table 3.10: VT from aEIT against the VT from the body box (-: data missed due to poor EIT recordings and no body box data recorded).

Subject		Tidal volume (VT)		
		Body Box (litre)	**EIT (litre)**	**Absolute Error**
Females	**1**	0.66	0.81	0.15
	2	0.36	0.68	0.32
	3	-	0.62	-
	4	0.76	1.38	0.62
Males	**5**	0.62	0.96	0.34
	6	0.45	0.46	0.01
	7	0.66	0.94	0.28
	8	-	0.44	-
	9	0.96	0.54	0.42
	10	0.68	-	-
	11	1.06	0.76	0.30
	12	0.58	0.51	0.07

Table 3.11: FRC from aEIT against the FRC from the body box (-: data missed due to poor EIT recordings and no body box data recorded).

Subject		Functional residual capacity (FRC)		
		Body Box (litre)	**EIT (litre)**	**Absolute Error**
Females	**1**	2.71	4.00	1.29
	2	3.13	0.16	2.97
	3	-	1.94	-
	4	2.41	2.34	0.07
Males	**5**	3.53	3.12	0.41
	6	3.02	3.95	0.93
	7	3.52	4.92	1.40
	8	-	3.49	-
	9	3.66	4.19	0.53
	10	2.29	-	-
	11	3.06	2.13	0.93
	12	2.20	4.92	2.72

Table 3.12: TLC from aEIT against the TLC from the body box (-: data missed due to poor EIT recordings and no body box data recorded).

Subject		Total lung capacity (TLC)		
		Body Box (litre)	**EIT (litre)**	**Absolute Error**
Females	**1**	5.53	6.60	1.07
	2	6.30	-	-
	3	-	4.78	-
	4	4.90	7.01	2.11
Males	**5**	6.03	6.99	0.96
	6	7.90	6.84	1.06
	7	7.49	9.88	2.39
	8	-	7.91	-
	9	8.07	7.02	1.05
	10	5.58	5.87	0.29
	11	7.62	6.53	1.09
	12	5.93	9.70	3.77

Table 3.13: RV from aEIT against the RV from the body box (-: data missed due to poor EIT recordings and no body box data recorded).

Subject		Residual volume (RV)		
		Body Box (litre)	**EIT (litre)**	**Absolute Error**
Females	**1**	1.81	2.39	0.58
	2	1.72	-	-
	3	-	1.78	-
	4	1.68	1.32	0.36
Males	**5**	2.10	1.68	0.42
	6	1.72	3.48	1.76
	7	1.77	3.15	1.38
	8	-	3.31	-
	9	2.00	3.30	1.30
	10	1.71	3.14	1.43
	11	1.64	3.37	1.73
	12	1.50	4.32	2.82

Table 3.14: VC from aEIT against the VC from the body box (-: data missed due to poor EIT recordings and no body box data recorded).

Subject		Vital capacity (VC)		
		Body Box (litre)	**EIT (litre)**	**Absolute Error**
Females	**1**	3.72	4.21	0.49
	2	4.58	-	-
	3	-	3.00	-
	4	3.23	5.69	2.46
Males	**5**	3.93	5.31	1.38
	6	6.19	3.36	2.83
	7	5.72	6.73	1.01
	8	-	4.60	-
	9	6.06	3.72	2.34
	10	3.87	2.73	1.14
	11	5.98	3.16	2.82
	12	4.43	5.38	0.95

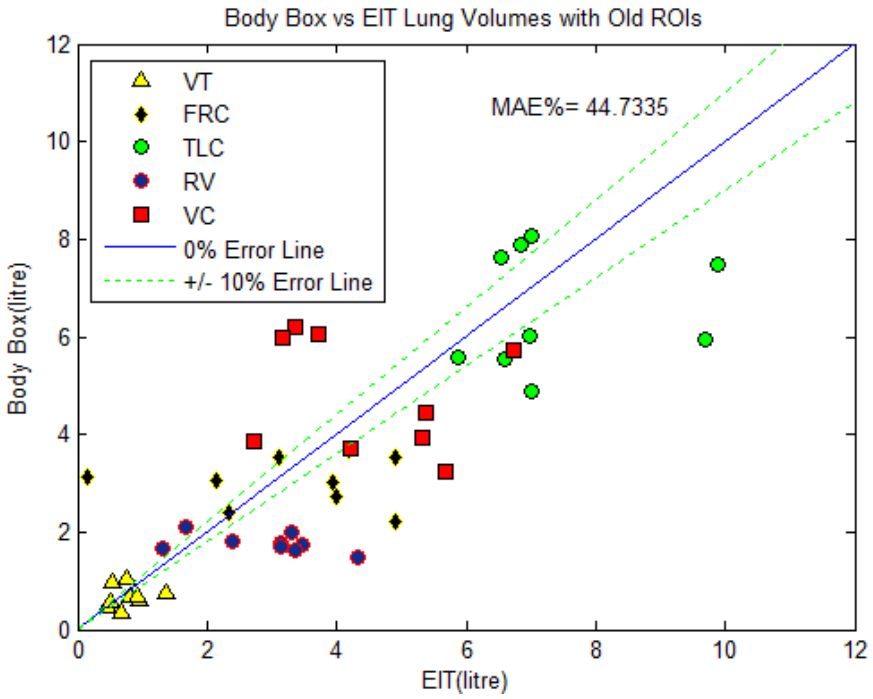

Figure 3.8: Scatter plot shows the VT, FRC, TLC, RV and VC calculated by the aEIT software against the one measured from the body box.

Table 3.15: Summary of the performance indices for aEIT in comparison with the the body box.

	Lung volumes				
	VT	FRC	TLC	RV	VC
MAE (%)	41.87	44.01	24.42	77.32	36.06
eSTD	0.28	1.45	1.50	0.92	1.29

From these results, it can be seen that the lung volumes from the aEIT system still diverge from the ones measured by the body box with the average accuracy of 55%. However, the accuracy of the aEIT system with the body box is better as compared with the accuracy of the aEIT system using spirometry.

3.5 Summary

It can be concluded from this comparative study that the aEIT system has shown the ability to measure lung volumes with range of errors depending on subject and its position. The aEIT measurement system has shown a very large diversion when compared with spirometry measurements in both body positions, especially measurements in the supine position. As for comparison between the aEIT system and the body box, the results are slightly better than the aEIT against spirometry but still with a high percentage of deviation. EIT is also seen to produce an over-estimate for most of the lung volumes. These over-estimates and large diversions of the aEIT measurements are reckoned to be triggered by the one fixed region of interest used in current aEIT system to estimate the absolute lung resistivity and volume. Therefore, in the next Chapter, research work on the improvement of the Region of Interest (ROI) using the MRI images of the studied healthy volunteer subjects will be performed. The results of the improved aEIT system with the new region of interest in comparison with spirometry and body box measurements will be presented.

CHAPTER 4

CALIBRATION AND IMPROVEMENTS OF THE SHEFFIELD MK 3.5 aEIT SYSTEM

4.1 Introduction

From the literature, it is known that current EIT systems suffer from some limitations that may prevent their adoption for routine medical diagnosis (Brown, 2003). A series of calibrations and improvements has been made by our Research Group to enhance the accuracy and consistency of the calculated absolute lung volume and resistivity in the aEIT system. In Chapter 3, the Sheffield Mk 3.5 aEIT v.1.047 software is used to calculate the absolute lung resistivity and volume. However, the results revealed that inter-individual differences had caused the absolute aEIT measurements to be very inaccurate. One possible source of error in determining absolute lung volume and resistivity is the usage of a fixed region of interest (ROI) in the Sheffield Mk 3.5 aEIT v.1.047 software for all the subjects considered.

In this Chapter, based on the calibration and improvement carried through by Panoutsos *et al*. (2007), further improvements on the Mk 3.5 aEIT system's software are made, whereby the ROI of the lung in relation to the thoracic shape is further

developed and the new sub-ROIs were introduced. This Chapter is organised as follows: first, previous attempts made by the Research Group to improve the accuracy and consistency of the estimated absolute lung volume and resistivity in the Sheffield Mk 3.5 aEIT software are reviewed; second, further developments of the zone of interest of the lungs and introduction of the new regions are presented and the improvement results are analysed and discussed; finally conclusions are drawn in relation to this newly proposed region of interest.

4.2 A review of amendments of the aEIT software

The aEIT software was initially modified to be compatible with the latest version of MATLAB. This would allow for easier software debugging in the future and at the same time it would allow for the transfer of work between the three research sites involved in this project (Dept. of Anaesthesia and Dept. of Medical Physics, The Royal Hallamshire Hospital and Dept. of Automatic Control and Systems Engineering, The University of Sheffield). Several functions in the software had to be updated and in certain cases codes for whole modules had to be re-written.

4.2.1 aEIT lung volume system calibration

The study on healthy subjects (Panoutsos *et al*., 2007) showed a large deviation between the aEIT lung volume estimation and the Spirometry based estimation. The error pattern revealed a consistent logarithmic relationship between the measured values and the values obtained from the aEIT. This prompted an investigation into the calculations of the Nopp adult lung model. The adult lung model described by Nopp *et al*. (1997) predicts a value for lung resistivity as a function of frequency. Instead of modifying the Nopp model, the output of the model is filtered using a calibration function. This calibration function has allowed not only correction of the model but

also absorb resistivity estimation errors created in the previous steps of the algorithm (i.e. Cole-Cole equation fit). The proposed calibration equation is given as follows:

$$y = \frac{ln\,(x) + 1.31}{0.47} \qquad \textbf{(4.1)}$$

Where x represents the absolute lung volume before calibration and y represents the absolute lung volume after calibration. The calibration equation was estimated by fitting the error data between the aEIT and Spirometry as shown in Figure 4.1.

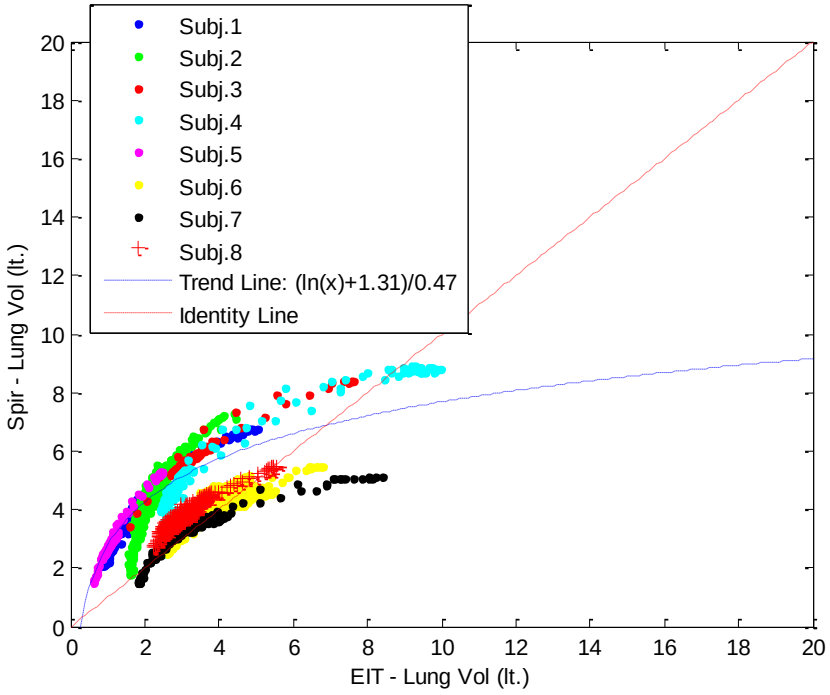

Figure 4.1: aEIT versus Spirometry Lung Volume Estimation**.**

Due to the importance of this function to the overall lung volume estimation of the system, the FRC for each subject was measured using body plethysmography (body box) measurements conducted at the Respiratory Unit of the Royal Hallamshire Hospital, Sheffield (UK).

4.2.2 Lung weight estimation

Part of the lung resistivity to volume calculation includes the estimation of the density of the lung tissue. The aEIT system assumes a fixed value of lung weight based on an average population mean model. This has lead to big errors in the estimation of lung volume in the case where the subject's physiology deviates from the population mean. A model based on reference data to estimate the lung weight had constructed in order to overcome this problem. By consulting large-scale post-mortem data on lung weight (Spencer, 2003; Grandmaison, 2001) the following model (Equations 4.2 and 4.3) was fitted to the data based on height and gender:

$$MaleLungWeight = 880 + BodyHeight^3/15000\ (in\ grams) \quad \textbf{(4.2)}$$

$$FemaleLungWeight = 850 + BodyHeight^3/20000\ (in\ grams) \quad \textbf{(4.3)}$$

The calibration equation (Equation 4.1) then had to be adjusted to account for the changes in the lung weight model. The final calibration function (used in the Mk3.5 aEIT system's software of version 1.047) is given by the following equation:

$$y = \frac{ln(x - 0.30)}{0.32} \quad \textbf{(4.4)}$$

Where *x* represents the absolute lung volume before calibration and *y* represents the absolute lung volume after calibration. The calibrated system showed significant improvement in performance with good agreement between the spirometry/body box measurements and aEIT calculated lung volumes. The calibrated aEIT system and the study on healthy subjects are presented in (Panoutsos *et al*., 2008). This calibrated aEIT system (software of version 1.047) also being used in the study on different

group of healthy subjects (8 males and 4 females) in sitting and supine positions as presented in Chapter 3. However, the analysis show some poor quality results, where most of the lung volumes calculated by the aEIT system has a large deviation from spirometry and body box measurements. It is hypothesised that the usage of one fixed region of interest in this version of aEIT system's software (v.1.047) has contributes to such results. In the next section, the work on creating the new ROI is presented.

4.3 The new region of interest (ROI)

The Sheffield Mk 3.5 aEIT system is able to produce a resistivity map of the human thorax. In the current aEIT system's software (v.1.047), one fixed region of interest (ROI) is used to locate the lung region and extract the resistivity of the lungs while filter out other organs. Due to inter-individual differences in the human thorax anatomy (heart size/location, lung size, body/organs fat content etc.) it is not possible to use one ROI that would be suitable for all subjects and in cases where there are significant anatomical differences (as compared to the average person) the aEIT system can produce significant errors in lung volume calculation as shown in the results from Chapter 3.

Therefore, in order to further enhance the accuracy and consistency of the calculated lung absolute volume and resistivity in the Sheffield Mk3.5 aEIT system (software of version 1.047) and improve the estimation of the lung ventilation distribution in the anterior/posterior left and right quadrants, a multiple ROIs were developed in relationship with the height and thoracic shape. Several scans of the thorax (Magnetic Resonance Imaging- MRI) of the volunteers involved in Chapter 3 were used to produce the new ROIs.

4.3.1 Step by step process of creating the new region of interest

MRI scans from twelve healthy volunteers (8 males and 4 females) were studied. Demographic information of all the subjects can be found in Chapter 3. The MATLAB-based image processing toolbox was used to extract the original lung region and calculate the 16x16 pixels ROI based on the MRI image taken at the level of approximately 5cm above the xyphoid process. The step by step process of creating the new region of interest is described as follows:

Step 1:

The exact lung region for each subject is extracted from each original MRI scan and the ellipse body shape was approximated (Figure 4.2).

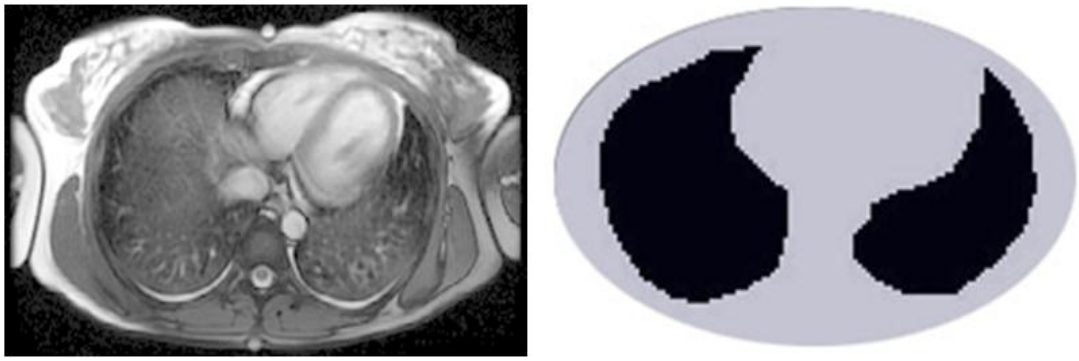

(a) (b)

Figure 4.2: (a) MR images taken at 5cm above xyphoid. (b) Extracted exact lung region and approximate ellipse body shape.

Step 2:

The current 16 x 16 pixels of EIT ROI is then mapped to each subject's extracted lung region and shape-wrap according to the approximate ellipse (Figure 4.3).

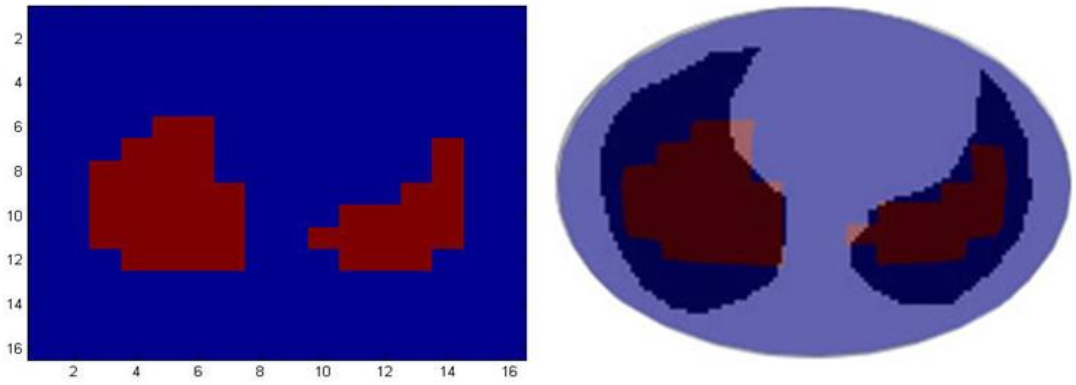

(a) (b)

Figure 4.3: (a) 16 x 16 pixel of ROI. (b) ROI (red) is shape-wrap to subject's approximate ellipse (blue).

Step 3:

The best fit new ROI is drawn using MATLAB 7.1 to cover the whole lung region (Figure 4.4).

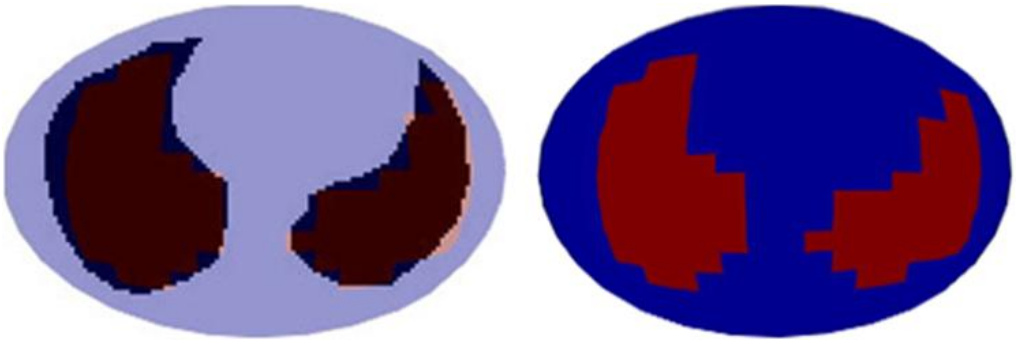

(a) (b)

Figure 4.4: (a) Best fit new ROI. (b) New ROI in ellipse shape.

Step 4:

In the final step, the best fit new ROI is remapped back to the original 16 x 16 pixels shape (Figure 4.5).

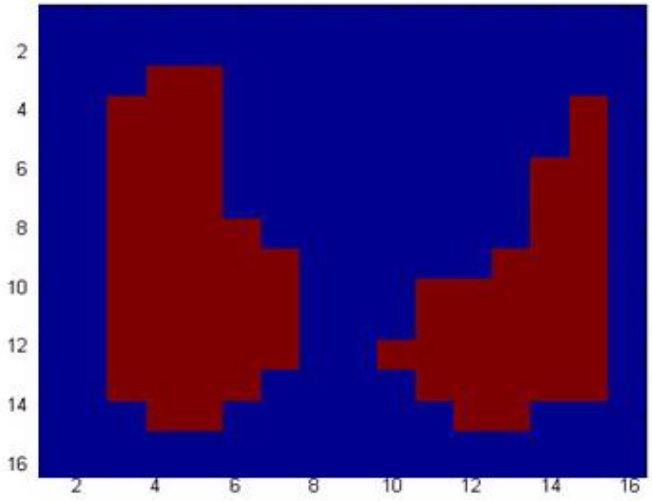

Figure 4.5: The new 16 x 16 pixels of EIT ROI.

4.3.2 Multiple regions of interest (ROIs)

To improve the performance of current aEIT system, the employment of multiple ROIs were proposed in contrast with the current aEIT system which used only one fixed ROI to locate the lung region and extract the resistivity of the lungs. The new 16 x 16 pixels of EIT ROI from twelve healthy volunteers (8 males and 4 females) were studied. Hepper *et al*. (1996) revealed in his study that among the anthropometric information of the subjects (eg: height, weight, body surface area, etc), height is correlated best with lung volume. In the light of this finding and upon consulting with the clinical expert, three (3) new ROIs are selected to represent the 'SMALL', 'MEDIUM' and 'LARGE' group of subjects depending on subject's height and body shape. Before the decision on the three (3) ROIs were made, a fit test was carried-out, whereby one ROI for each group of subjects was randomly chosen and mapped into

the other subject's approximate ellipse ratio that belongs to the same group. The ROI which best fits all other subject's approximate ellipse ratio was then chosen to represent the ROI for that particular group. Figure 4.6 shows the example of selected ROI that is mapped to the subjects' approximate ellipse in the 'MEDIUM' group.

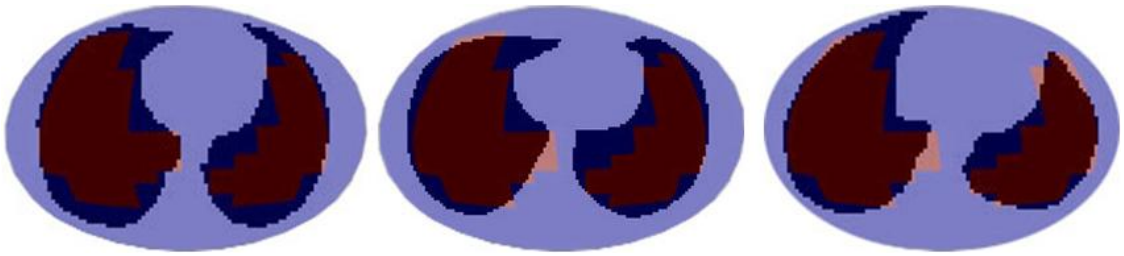

Subject 1 Subject 2 Subject 3

Figure 4.6: Example of the fit test performed for the 'MEDIUM' group.

These three (3) selected ROIs are then used in the aEIT software to calculate for lung resistivity and volumes. Figure 4.7 shows the three (3) selected ROIs and Figure 4.8 shows the flow chart for selection of these ROIs in the aEIT software.

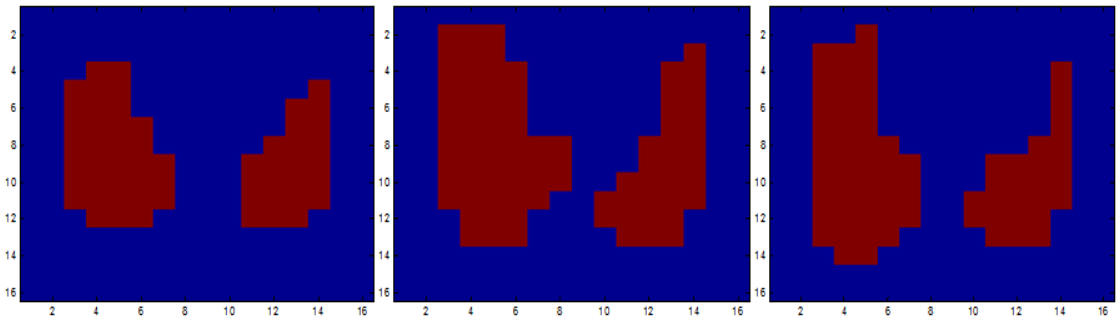

(a) (b) (c)

Figure 4.7: (a) ROI 1 (Small), (b) ROI 2 (Medium), (c) ROI 3 (Large).

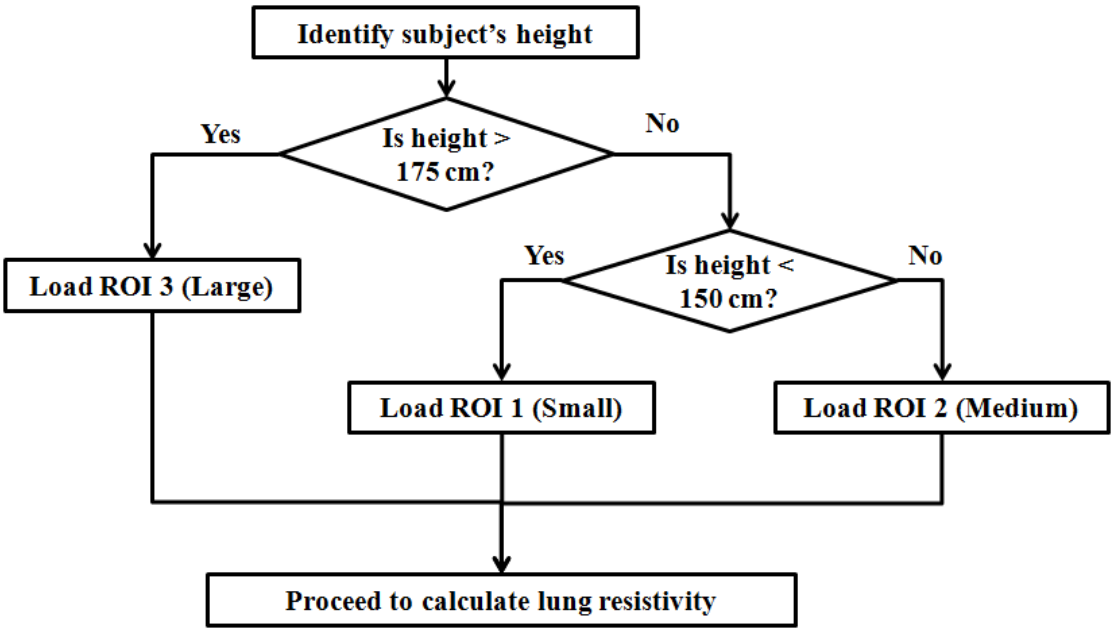

Figure 4.8: Flow chart of the ROI selection.

In the current aEIT software (version 1.047), the estimation of regional lung ventilation is based on the four (4) sub-ROIs (left lung anterior, left lung posterior, right lung anterior and right lung posterior). In this work, another two (2) sub-ROIs are introduced (left middle and right middle). These additional sub-ROIs allow for more specific analysis on what happened in the lung regional and has been of the most clinical interest. The anterior and the posterior parts of the lung correspond to non-dependent and dependent lung respectively, while the middle part corresponds to the normal region of the lung. Therefore, the graphical user interface (GUI) has been amended to visualise the ROI and the new regional lung ventilation. Index for the regional lung ventilation has also been made visible on the graph for the ease of clinician's analysis as opposed to the old GUI. Figure 4.9 shows an example of the screenshot of the old and the new GUI showing image of old (4 sub-ROIs) and new (6 sub-ROIs) together with the regional ventilation graphs.

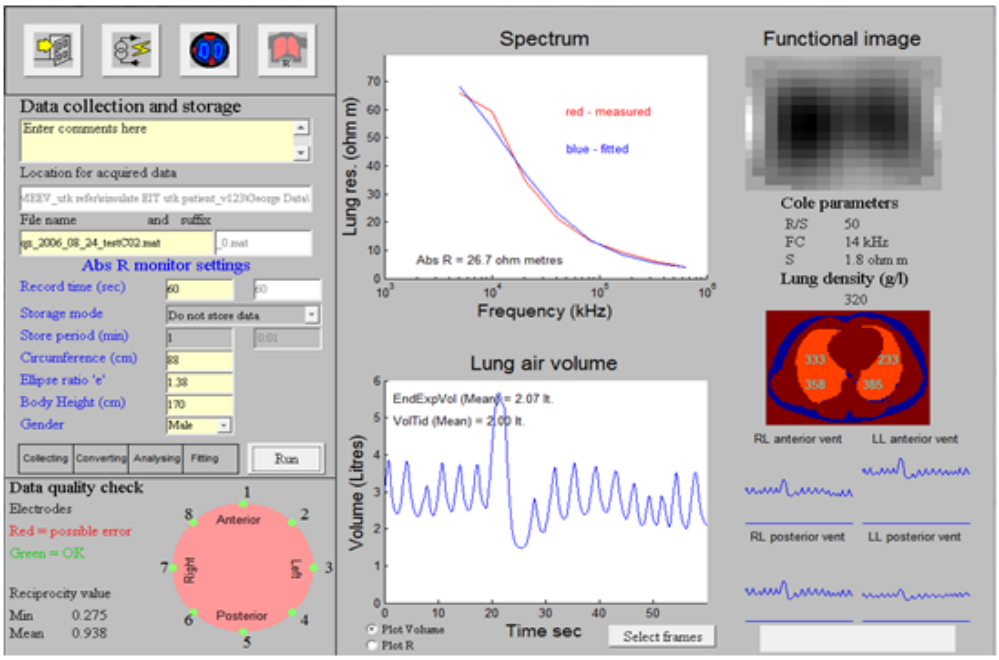

(a)

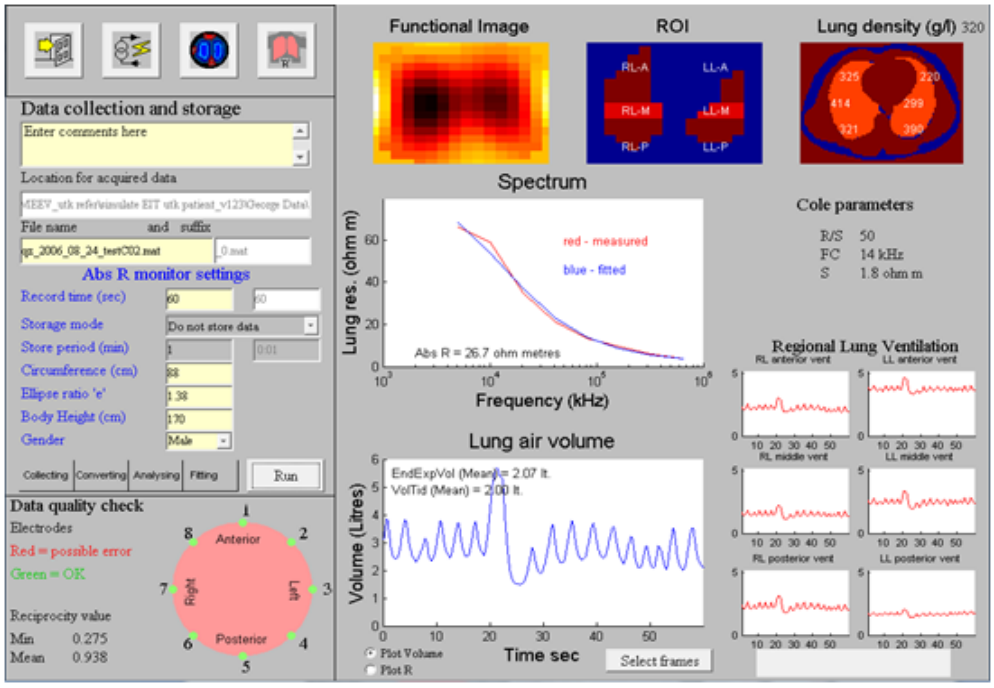

(b)

Figure 4.9: Example of the screenshots taken from the Sheffield Mk 3.5 aEIT software; (a) Old GUI with 4 sub-ROIs. (b) New GUI with 6 sub-ROIs.

4.4 Improved results and discussions

The new lung volumes obtained from the 12 healthy volunteers using the improved Sheffield Mk3.5 aEIT software (with multiple ROIs) were analysed and compared with the spirometry and body box measurements during quiet breathing at functional residual capacity (FRC), 1 litre breathing and maximum breathing manoeuvres. The method of comparison between aEIT measurement and spirometry measurement are the same as previously presented in Chapter 3. The percentage of mean absolute error (MAE%) and standard deviation of the errors (eSTD) were used as the performance indices for all the analyses. The '-' indicates that there are no data due to the error from one of the electrodes. This electrode must have been not adequately attached to the subject's body during the exercise.

4.4.1 Comparison between spirometry lung volumes and the aEIT lung volumes in sitting and supine position

The mean tidal volume (VT), 1 litre breaths and vital capacity (VC) calculated by aEIT were recorded for each subject, and compared with the mean tidal volume (VT), 1 litre breaths and vital capacity (VC), measured from the spirometry. Tables 4.2-4.4 summarise the results for analysis of these lung volumes in the sitting position while Tables 4.6-4.8 summarise the analysis results in supine position. The performances of the aEIT with the old ROI and the aEIT with new ROIs in the sitting position are compared and shown in Figure 4.10 and Table 4.4, while Figure 4.11 and Table 4.8 show the performances of aEIT with the old and the new ROIs in the supine position.

4.4.1.1 Results in sitting position

Table 4.1: Comparison between VT from aEIT and the VT from spirometry in the sitting position (-: data missed due to poor EIT recordings).

Subject		Tidal volume (VT)		
		Spirometry (litre)	**EIT (litre)**	**Absolute Error**
Females	**1**	0.29	0.66	0.37
	2	0.22	0.56	0.34
	3	0.63	0.65	0.02
	4	0.81	1.16	0.36
Males	**5**	0.36	0.68	0.32
	6	1.01	0.47	0.54
	7	0.60	0.74	0.14
	8	0.21	0.36	0.15
	9	0.80	0.50	0.30
	10	0.33	-	-
	11	1.48	1.07	0.41
	12	0.68	0.50	0.18

Table 4.2: Comparison between 1 litre breaths from aEIT with 1 litre breaths from spirometry in the sitting position.

Subject		1 Litre breaths		
		Spirometry (litre)	**EIT (litre)**	**Absolute Error**
Females	**1**	0.74	1.50	0.76
	2	0.80	1.05	0.25
	3	1.11	0.98	0.13
	4	0.88	1.58	0.70
Males	**5**	0.82	1.03	0.21
	6	1.18	0.66	0.52
	7	1.10	1.17	0.07
	8	0.89	0.98	0.09
	9	0.99	0.54	0.45
	10	0.73	0.93	0.20
	11	1.24	0.79	0.45
	12	0.94	1.04	0.10

Table 4.3: Comparison between VC from aEIT against the VC from spirometry in the sitting position.

Subject		Vital capacity (VC)		
		Spirometry (litre)	**EIT (litre)**	**Absolute Error**
Females	**1**	3.00	3.48	0.48
	2	4.05	4.10	0.05
	3	2.35	2.80	0.46
	4	2.88	4.40	1.52
Males	**5**	3.63	3.10	0.53
	6	5.24	3.14	2.10
	7	4.59	5.77	1.19
	8	4.55	4.42	0.13
	9	5.97	3.40	2.57
	10	2.25	2.80	0.55
	11	5.66	3.61	2.05
	12	3.90	4.90	1.00

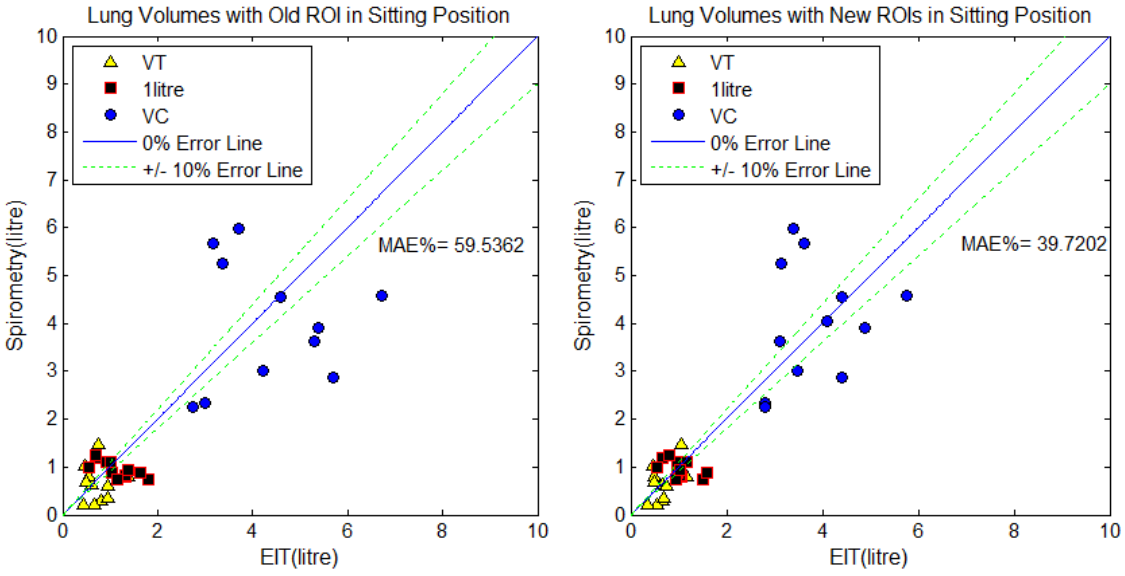

Figure 4.10: Scatter plot shows the VT, 1 litre breaths and VC calculated by the aEIT software against the one measured from the spirometry in sitting position. The left figure shows the aEIT results with the old ROI while the right figure shows the aEIT results with the new ROIs.

Table 4.4: Summary of the performance indices comparing the aEIT with old ROI and the aEIT with the new ROIs in the sitting position.

	Sitting					
	Tidal volume (VT)		1 litre breaths		Vital capacity (VC)	
	Old	New	Old	New	Old	New
MAE (%)	86.71	59.76	52.75	35.93	39.68	25.15
eSTD	0.28	0.15	0.39	0.24	1.29	0.84

4.4.1.2 Results in supine position

Table 4.5: VT from aEIT against the VT from spirometry in the supine position.

Subject		**Tidal volume (VT)**		
		Spirometry (litre)	**EIT (litre)**	**Absolute Error**
Females	**1**	0.44	0.80	0.36
	2	0.18	0.51	0.33
	3	0.53	0.54	0.01
	4	0.78	1.33	0.55
Males	**5**	0.41	0.65	0.24
	6	1.66	0.77	0.89
	7	0.51	0.56	0.06
	8	0.24	0.33	0.09
	9	1.25	1.32	0.07
	10	0.40	0.52	0.12
	11	1.25	0.94	0.31
	12	1.01	1.09	0.08

Table 4.6: 1 litre breaths from aEIT against the 1 litre breaths from spirometry in the supine position.

Subject		1 Litre breaths		
		Spirometry (litre)	**EIT (litre)**	**Absolute Error**
Females	**1**	1.15	1.37	0.22
	2	0.82	0.83	0.01
	3	1.10	1.20	0.10
	4	0.78	1.53	0.75
Males	**5**	1.03	1.64	0.61
	6	1.31	0.74	0.57
	7	1.36	1.38	0.02
	8	0.60	0.84	0.24
	9	1.43	0.94	0.49
	10	0.70	0.78	0.08
	11	1.20	1.00	0.20
	12	1.13	1.10	0.03

Table 4.7: VC from aEIT against the VC from spirometry in the supine position.

Subject		Vital capacity (VC)		
		Spirometry (litre)	**EIT (litre)**	**Absolute Error**
Females	**1**	2.93	3.50	0.57
	2	4.14	5.08	0.94
	3	2.76	3.30	0.54
	4	3.09	6.12	3.03
Males	**5**	3.18	4.20	1.02
	6	5.35	2.48	2.87
	7	4.14	4.30	0.16
	8	4.29	4.38	0.09
	9	5.76	4.40	1.36
	10	1.65	1.87	0.22
	11	5.54	4.50	1.04
	12	3.76	4.18	0.42

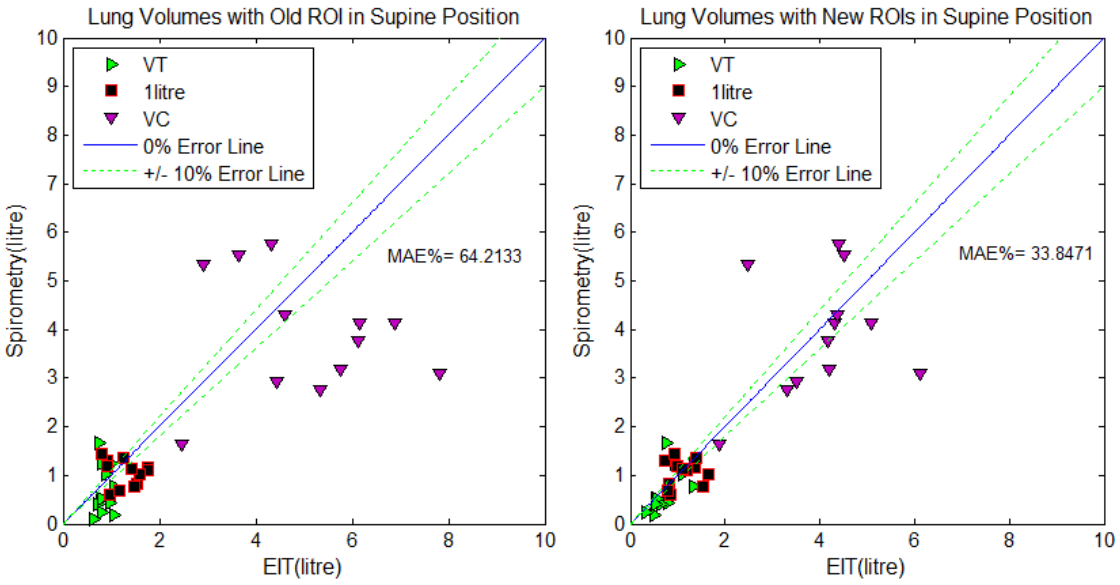

Figure 4.11: Scatter plot shows the VT, 1 litre breaths and VC calculated by the aEIT software against the one measured from the spirometry in supine position. The left figure shows the aEIT results with the old ROI while the right figure shows the aEIT results with the new ROIs.

Table 4.8: Summary of the performance indices comparing the old aEIT and the improved aEIT software in the supine position.

	Supine					
	Tidal volume (VT)		1 litre breaths		Vital capacity (VC)	
	Old	New	Old	New	Old	New
MAE (%)	77.03	47.11	50.35	27.90	65.26	26.53
eSTD	0.14	0.26	0.34	0.26	1.61	0.98

The overall results of absolute lung volumes calculated by the aEIT with the new ROIs show an increase in accuracy with the spirometry measurements in both sitting and supine positions. The average accuracy for aEIT with the new ROIs is about 60% in sitting position and 66% in supine position as compared to 40% and 36% with the old ROI in sitting and supine position respectively.

4.4.2 Comparison between body box lung volumes and the aEIT lung volumes

The mean tidal volume (VT), functional residual capacity (FRC), total lung capacity (TLC), residual volume (RV) and vital capacity (VC) calculated by aEIT were recorded for all subjects and compared with the mean tidal volume (VT), functional residual capacity (FRC), total lung capacity (TLC), residual volume (RV) and vital capacity (VC), measured from the body box. Tables 4.10-4.14 summarise the results for analysis of these lung volumes. The performances of the aEIT with the old ROI and the aEIT with new ROIs are compared and shown in Figure 4.12 and Table 4.14. The '-' sign indicates that there are no body box measurements done and also poor EIT data recordings for that particular subject.

Table 4.9: VT from aEIT against the VT from the body box (-: data missed due to poor EIT recordings and no body box data recorded).

Subject		**Tidal volume (VT)**		
		Body Box (litre)	**EIT (litre)**	**Absolute Error**
Females	**1**	0.66	0.66	0.00
	2	0.36	0.56	0.20
	3	-	0.65	-
	4	0.76	1.16	0.40
Males	**5**	0.62	0.68	0.06
	6	0.45	0.47	0.02
	7	0.66	0.74	0.08
	8	-	0.36	-
	9	0.96	0.50	0.46
	10	0.68	-	-
	11	1.06	1.07	0.01
	12	0.58	0.50	0.08

Table 4.10: FRC from aEIT against the FRC from the body box (-: data missed due to poor EIT recordings and no body box data recorded).

Subject		Functional residual capacity (FRC)		
		Body Box (litre)	**EIT (litre)**	**Absolute Error**
Females	**1**	2.71	3.22	0.51
	2	3.13	1.40	1.73
	3	-	1.78	-
	4	2.41	2.43	0.02
Males	**5**	3.53	3.65	0.12
	6	3.02	3.10	0.08
	7	3.52	3.60	0.08
	8	-	2.84	-
	9	3.66	3.25	0.41
	10	2.29	-	-
	11	3.06	3.76	0.70
	12	2.20	3.70	1.50

Table 4.11: TLC from aEIT against the TLC from the body box (-: data missed due to poor EIT recordings and no body box data recorded).

Subject		Total lung capacity (TLC)		
		Body Box (litre)	**EIT (litre)**	**Absolute Error**
Females	**1**	5.53	5.96	0.43
	2	6.30	5.00	1.30
	3	-	4.59	-
	4	4.90	5.20	0.30
Males	**5**	6.03	5.70	0.33
	6	7.90	5.85	2.05
	7	7.49	8.00	0.51
	8	-	6.87	-
	9	8.07	6.00	2.07
	10	5.58	5.10	0.48
	11	7.62	5.21	2.41
	12	5.93	7.90	1.97

Table 4.12: RV from aEIT against the RV from the body box (-: data missed due to poor EIT recordings and no body box data recorded).

Subject		Residual volume (RV)		
		Body Box (litre)	**EIT (litre)**	**Absolute Error**
Females	**1**	1.81	2.08	0.27
	2	1.72	1.00	0.72
	3	-	1.60	-
	4	1.68	1.07	0.61
Males	**5**	2.10	2.60	0.50
	6	1.72	2.70	0.98
	7	1.77	1.80	0.03
	8	-	2.37	-
	9	2.00	2.68	0.68
	10	1.71	1.70	0.01
	11	1.64	1.60	0.04
	12	1.50	3.00	1.50

Table 4.13: VC from aEIT against the VC from the body box (-: data missed due to poor EIT recordings and no body box data recorded).

Subject		Vital capacity (VC)		
		Body Box (litre)	**EIT (litre)**	**Absolute Error**
Females	**1**	3.72	3.48	0.24
	2	4.58	4.10	0.48
	3	-	2.80	-
	4	3.23	4.40	1.17
Males	**5**	3.93	3.10	0.83
	6	6.19	3.14	3.05
	7	5.72	5.77	0.05
	8	-	4.42	-
	9	6.06	3.40	2.66
	10	3.87	2.80	1.07
	11	5.98	3.61	2.37
	12	4.43	4.90	0.47

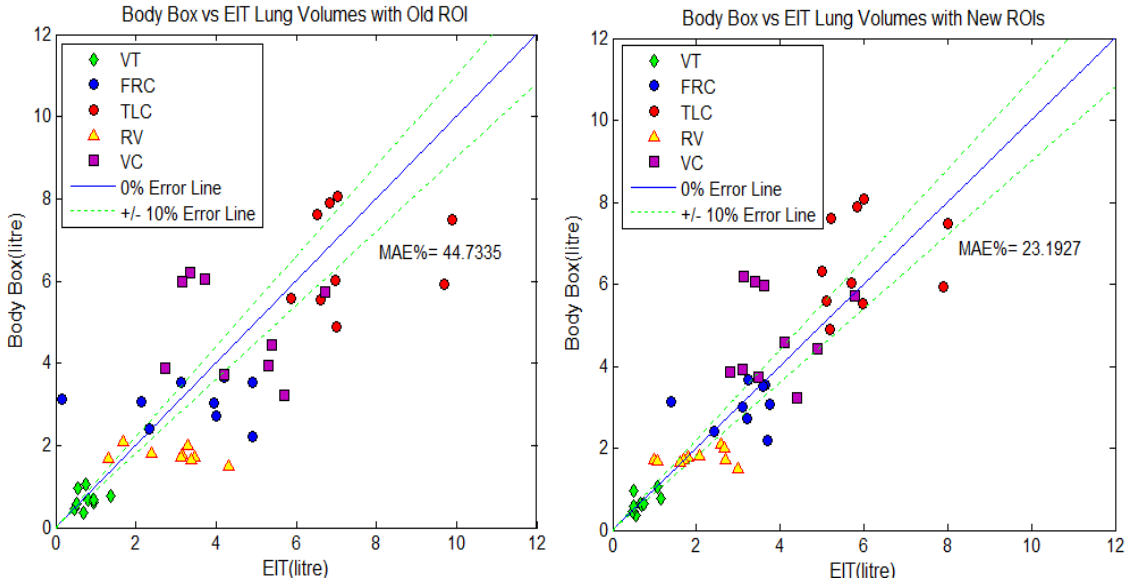

Figure 4.12: Scatter plot shows the VT, FRC, TLC, RV and VC calculated by the aEIT software against the one measured from the body box. The left figure shows the aEIT results with the old ROI while the right figure shows the aEIT results with the new ROIs.

Table 4.14: Summary of the performance indices comparing the old aEIT and the improved aEIT software in the sitting position

	Sitting									
	VT		FRC		TLC		RV		VC	
	Old	New	Old	New	Old	New	Old	New	Old	New
MAE (%)	41.87	21.89	44.01	20.61	24.42	17.19	77.32	31.26	36.06	24.62
eSTD	0.28	0.17	1.45	0.64	1.50	0.86	0.92	0.48	1.29	1.07

When comparing the measurements from the improved aEIT software with the new ROIs with measurements from the body box, it can be seen that the accuracy of the absolute lung volumes also increased. In all the lung volumes calculated by aEIT with the new ROIs, the average accuracy is about 77% as compared to 55% with the old ROI.

4.5 Summary

In this chapter, investigations to improve the Sheffield Mk 3.5 aEIT software through a series of calibrations and improvements to enhance the accuracy and consistency of the calculated absolute lung volume were carried-out. In the latest work of improvement, a study involving MRI scans was conducted on a population of healthy subjects to assess and redefine new regions of interest (ROIs) for the lungs taking into account the individual height and thoracic shape. The new sub-ROIs for estimation of regional lung ventilations were also introduced. The aEIT software with the new ROIs has shown an improved performance in accuracy in both spirometry and body box studies as compared to the old ROIs. Although the improved aEIT system is now able to provide good estimates of lung volumes, there is still active research in the area of validating and improving the accuracy and consistency of the aEIT estimation of lung volumes towards characterising the system as suitable for clinical use. In the light of all the promising development in the aEIT system, it is believed that such a system may be used as a continuous bedside monitoring tool to monitor lung function in mechanically ventilated ICU patients, where other means of lung function/condition measurement (MRI, CT) fail to provide portability and continuous measurement ability. Therefore in the next Chapter, the improved aEIT with the new ROIs will be employed to reflect the PEEP settings-induced changes on the lung absolute volume and densities in the real ICU patients.

CHAPTER 5

EIT CLINICAL TRIALS ON ICU PATIENTS

5.1 Introduction

In treating patients with severely impaired respiratory system, the use of positive end expiratory pressure (PEEP) and tidal volume have been identified as key ventilation parameters (Sundaresan and GeoffreyChase, 2010). PEEP was introduced to maintain the open atelectatic areas and thereby reduce the risk of hypoxemia and cyclic recruitment/derecruitment. Although the application of PEEP is widely used in clinical practice, selecting the most appropriate level of PEEP for the critically-ill patient is still a matter for debate. Increasing PEEP further prevents derecruitment in the dependent areas but may lead to overdistension in the non-dependent areas as well. To find a balance between these two aspects is one goal of setting such as PEEP level.

Lung overdistension has been defined in various ways, but usually referred to as a rise above normal resting functional residual capacity (FRC) or end-expiratory lung volume (EELV) (Ferguson, 2006). As reported in the current literature, the information provided by the global parameters of lung function, such as blood gases

values and the slope of the static pressure-volume curve (P/V) did not consider the inhomogeneity of lung region, and therefore may be at times misleading. As already stated in Sections 2.1.6.2 and 2.1.6.3 in Chapter 2, EIT has the potential of qualitatatively and quantitatively assessing various conditions of the lung during mechanical ventilation in critically-ill patients but most of the reported studies are mainly focusing on functional EIT (fEIT) not the absolute value.

Hence, in this Chapter, the ability of the improved Sheffield Mk3.5 aEIT system to reflect PEEP settings-induced changes on the aEIT quantitative parameters in ICU patients was investigated. The aEIT quantitative parameters were identified as the mean end-expiratory lung volume (MEEV), mean tidal volume (MVT), mean arterior density (MAD), mean middle density (MMD) and mean posterior density (MPD). The relationship between aEIT quantitative parameters and ratio of arterial partial pressure of oxygen to fraction of inspired oxygen (PaO2/FiO2) are also studied. This Chapter is organised as follows; first, the study protocol and data collection methods are presented; second, the results on PEEP settings-induced changes on aEIT quantitative parameters are analysed and discussed. The relationship between the aEIT quantitative parameters and PaO2/FiO2 ratio in all studied ICU patients is also investigated; finally, conclusions are drawn in relation to this overall study.

5.2 Study protocol and data collection methods

The study was conducted at the Northern General Hospital, Sheffield (UK). The ethical clearance was sought and obtained from the Sheffield Teaching Hospitals NHS Trust and approved by the local research office.

5.2.1 Identifying Participants

Any patients fulfilling the inclusion/exclusion criteria (as shown below) and ventilated on ICU are included in the study. In patients who are sedated and ventilated and unable to provide consent for themselves, their relatives will be approached to give consent and when the patient recovers consciousness and is able to understand the study, he/she will be asked to give retrospective consent for the data to be included within the research.

The principal inclusion criteria:

i) All: − 18 years or over
ii) Cases: - Receiving ventilatory support in Critical Care.

The principal exclusion criteria:

i) Pregnant or lactating;
ii) Unable to understand English;
iii) Been involved in any other interventional clinical trial within the last 3 months.

5.2.2 Data collection methods

Data from patients with BIPAP (Bilevel Positive Airway Pressure) and CPAP (Continuous Positive Airway Pressure) were considered in this study to investigate the effect of changing PEEP to the absolute lung volume and lung density of patients evaluated via the aEIT system.

The same equipments as shown in Section 3.2 in Chapter 3 were used in this study to measure the chest circumferences and chest width and depth. The same Skintact Premier ECG electrodes were used with the aEIT system's data collection unit. The aEIT data were acquired via the 8-electrode Sheffield Mk3.5 aEIT system which is the latest of a number of EIT systems developed in Sheffield (Wilson *et al*., 2001). The improved Sheffield Mk3.5 aEIT software of version 1.049 (written in MATLAB) was used to run the Mk3.5 system and estimate the absolute lung resistivity and volume.

The EIT data were recorded using a total of ten (10) male patients and four (4) female patients. However, seven (7) patients (3 males and 4 females) were excluded in the study due to; i) errors in all the recorded EIT data and ii) they were being weaned from the ventilator. As a result, only seven (7) mechanically ventilated male patients were left for the study. Demographic information of the indentified patients such as gender (G), height (H), weight (W) and chest circumference (C) were recorded. The ellipse ratio (E) was calculated based on the chest width and depth. Ventilation mode (Vent. Mode), patient's position and diagnosis were also recorded as a reference. Table 5.1 shows the summary of information for all the studied patients.

Table 5.1: Information summary of the studied patients.

Patient	G	H (cm)	W (Kg)	Chest		Vent. Mode	Position	Diagnosis
				E	C(cm)			
1	M	170	67	1.36	82	BIPAP	Supine	Severe SEPSIS
2	M	175	73	1.36	89	BIPAP	Prone	Respiratory failure
3	M	173	70	1.39	88	CPAP/BIPAP	Prone	Pulmonary oedema
4	M	171	71	1.19	86	CPAP	Supine	Respiratory failure
5	M	162	68	1.5	94	CPAP	Supine	Bilateral pneumonia
6	M	170	75	1.18	113	BIPAP	Prone	Respiratory failure
7	M	160	55	1.52	94	CPAP	Supine	Pneumocystis pneunomia

5.2.2.1 Routine changes in pressure and EIT recordings

The patients were connected to the Mk3.5 aEIT system via the 8-electrode array placed around the thorax, 5cm above the xyphoid process in different positions (i.e. supine or prone) depending on the needs of the patients at that particular time. EIT recordings were performed at a frequency of 25 Hz over one minute in identified patients, each day prior to physiotherapy in the morning. In the event where a routine change in ventilator settings (such as PEEP change) was made, EIT data were recorded for one minute prior to a change in pressure setting and then at every 30 minutes after any subsequent change. The 30-minute interval is to allow the patients to be in a stable condition after every change was made. The number of recording days depends on the availability of the nurses who were responsible for the data recordings and also how long the patients were being ventilated for in the ICU.

5.2.2.2 Ventilator parameters and blood gasses measurements

Ventilator parameters such as PEEP and tidal volume (VT) were retrieved at the time when the EIT recordings of the patient were executed. In this study, the tidal volume (VT) were measured by the ventilator and not set because the patients were ventilated in pressure-control ventilation. Blood gasses data i.e. arterial partial pressure of oxygen (PaO2), arterial partial pressure of carbon dioxide (PaCO2) and ratio of arterial partial pressure of oxygen to fraction of inspired oxygen (PaO2/FiO2) were also extracted from the Patient Data Monitoring System (PDMS). Because these data (PaO2, PaCO2) are not measured frequently and regularly, obtaining blood gases data at the same time as the EIT measurement is being performed is a difficult task. Therefore, the clinician has suggested taking the nearest blood gases data to be used in this study.

5.3 Results and discussions

In this section, the effects of changing PEEP to the MEEV, MAD, MMD and MPD in all patients were analysed. Relationships between MEEV, MAD, MMD and MPD with the PaO2/FiO2 and PaCO2 values were analysed. VT measured by the ventilator was also compared with MVT calculated by the aEIT system.

5.3.1 PEEP, MEEV and MVT

PEEP refers to the application of a fixed amount of positive pressure applied during the mechanical ventilation cycle (Figure 5.1) (Butcher and Boyle, 1997). The major benefit of PEEP is achieved through their ability to increase functional residual capacity (FRC) and keep this value above closing capacity. In critically ill patients receiving mechanical ventilation, FRC is determined by the level of PEEP and it is

therefore normally referred to as end-expiratory lung volume (EELV). The increase in EELV is realised by increasing alveolar volume and through the recruitment of alveoli that would contribute to gas exchange, hence, increasing oxygenation and lung compliance.

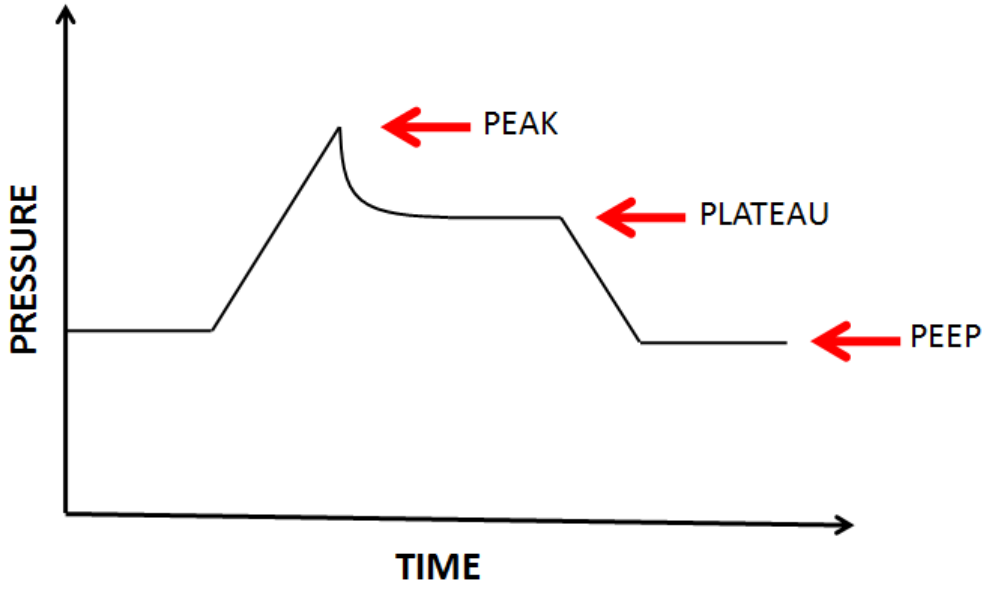

Figure 5.1: Pressures relating to mechanical ventilation [Butcher and Boyle, 1997].

In the aEIT system, EELV is represented by the mean of lung volume at the end of expiratory and known as the mean end-expiratory lung volume (MEEV). This value is calculated based on the absolute lung volume produced by the aEIT system. The steps of producing this absolute lung volume are shown in Section 3.4.1 in Chapter 3. Another quantitative parameters calculated by aEIT system from the absolute lung volume is the mean tidal volume (MVT). This value is the mean of the difference between the absolute lung volume at the end of inspiratory and end of expiratory. An example of the MEEV and MVT produced by the aEIT system can be seen in Section 3.4.2. In the aEIT system, MEEV only gives a general information about the lung volume of the measured patients.

5.3.2 Mean regional densities

To investigate the regional ventilation distribution of the lung, the aEIT system produced regional densities which have the potential to provide information about the regional lung abnormalities in the patients. In the current aEIT system, the model of lung density ($\rho lung$), as a function of absolute lung resistivity ($absR$) obtained by Nopp *et al*. (1997), is used to calculate the overall absolute lung density (refer to Equation (3.1 in Chapter 3). To obtain the regional lung density, the pre-determined region of interest (ROI) is used and the lung densities are estimated for 6 lung regions defined as right lung anterior density (RLAD), right lung middle density (RLMD), right lung posterior density (RLPD), left lung anterior density (LLAD), left lung middle density (LLMD) and left lung posterior density (LLPD) as shown in Figure 5.2.

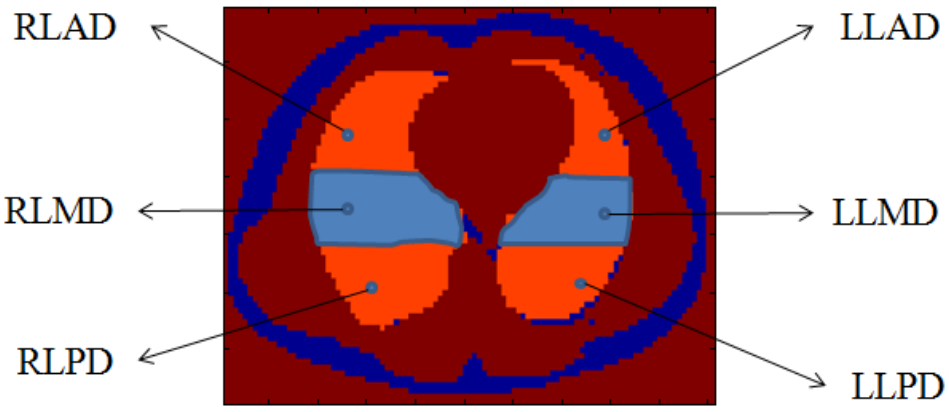

Figure 5.2: Definition of regional absolute lung densities.

To simplify the analysis, the densities of the left lung and the right lung were combined to become Mean Anterior Density (MAD), Mean Middle Density (MMD) and Mean Posterior Density (MPD) (Figure 5.3).

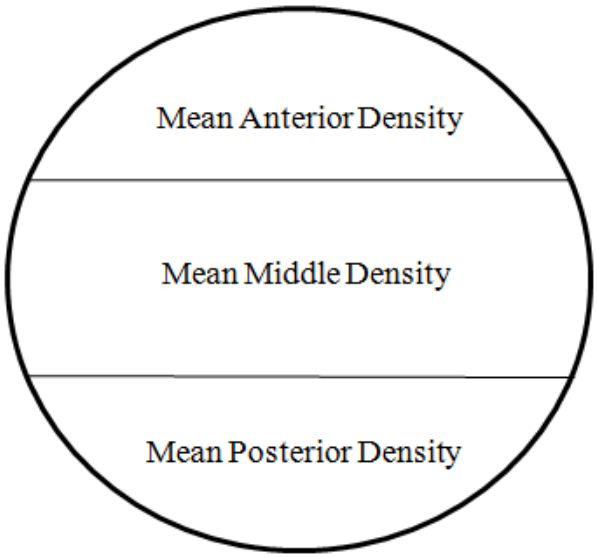

Figure 5.3: MAD, MMD and MPD regions of the lung.

5.3.3 PEEP induced changes in aEIT quantitative parameters

Table 5.2 summarises the results of changing PEEP to MEEV, MAD, MMD and MPD values for all the patients with different ventilation modes on different days. The tidal volume (VT) measured by the ventilator and MVT derived from the aEIT system were also included. The errors in aEIT readings were due to some technical problem i.e. electrode problems and electrode disconnected during the measurement. The reason for no VT values recorded for patient 5 is because the patient was ventilated using the external CPAP. In this particular case, only readings for PEEP were available.

Table 5.2: Summary of PEEP settings, VT and aEIT quantitative parameters in all patients with different ventilation modes on different days.

Pt.	Day	Mode	VENTILATOR SETTINGS/ MEASUREMENT		aEIT QUANTITATIVE PARAMETERS				
			PEEP	VT	MEEV	MVT	MAD	MMD	MPD
			(cmH2O)	(ml)	(litre)	(ml)	(g/l)	(g/l)	(g/l)
1	1	BIPAP	7	340	Error				
	2	BIPAP	6	930	2.70	610	335	1213	598
	3	BIPAP	6	850	2.20	680	570	1302	577
2	1	BIPAP	12	640	6.39	650	250	352	198
		BIPAP	12	730	6.30	710	255	361	200
	2	BIPAP	12	750	6.32	770	334	410	161
		BIPAP	10	660	5.71	600	383	476	187
		BIPAP	10	550	5.78	540	375	469	188
		BIPAP	10	530	5.68	540	370	455	197
		BIPAP	10	560	5.64	600	378	472	200
	3	BIPAP	10	1190	4.97	1330	550	653	155
		BIPAP	10	390	4.93	480	548	656	155
	4	BIPAP	10	1210	5.67	950	501	655	165
		BIPAP	10	700	5.46	530	513	683	171
3	1	CPAP	15	600	6.11	660	309	354	242
		CPAP	15	600	5.99	600	304	370	230
	2	BIPAP	12	410	6.94	500	213	291	146
		BIPAP	12	410	6.93	500	212	291	151
4	1	CPAP	5	320	3.05	360	408	779	626
			5	360	3.20	340	381	756	631
			5	360	3.21	420	394	780	615
			5	370	2.95	350	363	671	551
5	1	CPAP	5	NO TIDAL VOLUME RECORDED	0.74	1180	1194	1203	477
			5		0.80	1150	1130	1143	482
			0		0.23	100	1379	1432	520
			0		0.51	100	1250	1440	472
6	1	BIPAP	8	600	5.80	450	553	400	353
		BIPAP	8	430	5.80	480	561	403	353
7	1	CPAP	8	900	Error				
	2	CPAP	10	530	Error				
	3	CPAP	5	520	3.73	400	464	377	683
		CPAP	5	490	5.87	310	127	530	400
		CPAP	5	660	5.72	320	134	543	414
		CPAP	5	534	1.79	670	446	1113	701

5.3.3.1 MEEV versus PEEP

Figure 5.4 shows the variation of MEEV as the results of PEEP change in all patients. A linear regression analysis was carried-out on the data and the correlation was 0.911 ($P<0.05$). It can be seen from the results that the MEEV increases proportionally with the increase of PEEP. This result agrees with the findings reported from the human study (Hinz *et al*., 2003; Wang, 2008).

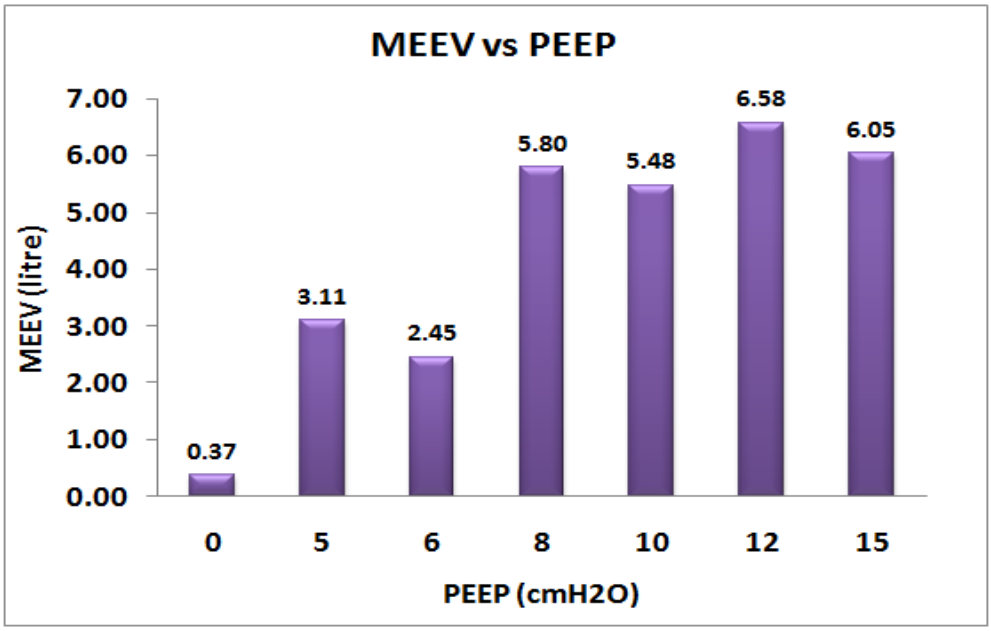

Figure 5.4: PEEP induced changes in MEEV in all patients.

Apart from this general observation, the effect of PEEP changes to individual patient was also made. In this case, data for PEEP and MEEV from Patients 2 and 3 were selected and analysed. Patient 2 was selected because recordings included the changes in PEEP in the same day, while Patient 3 recordings included changes in PEEP as well as the ventilation mode; both patients included no errors in all the aEIT readings. In this analysis, it was assumed that no variations in electrodes placement exist during the aEIT measurement in all the days.

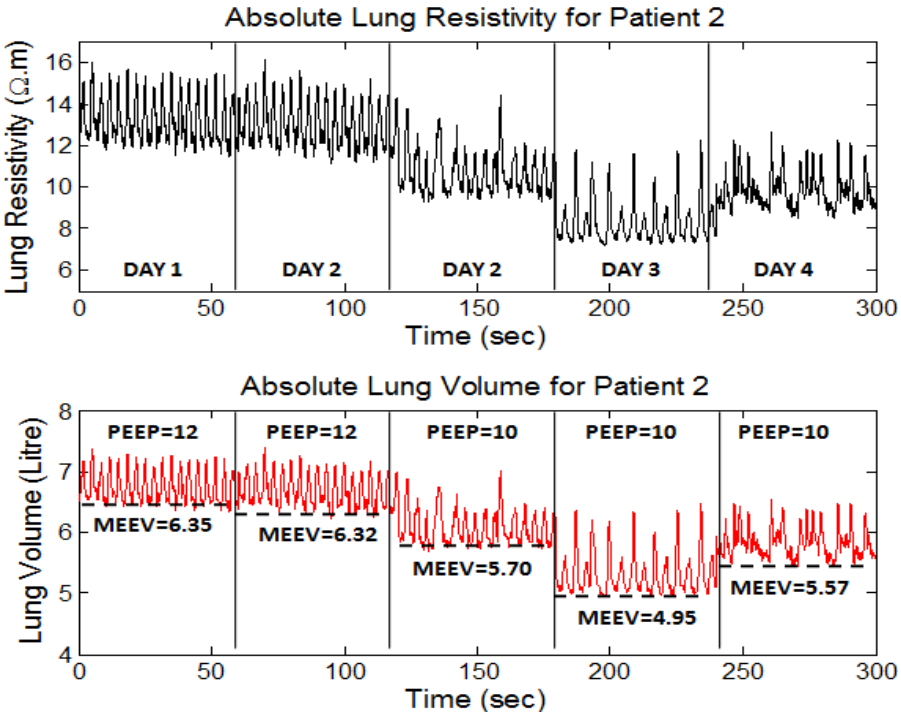

(a)

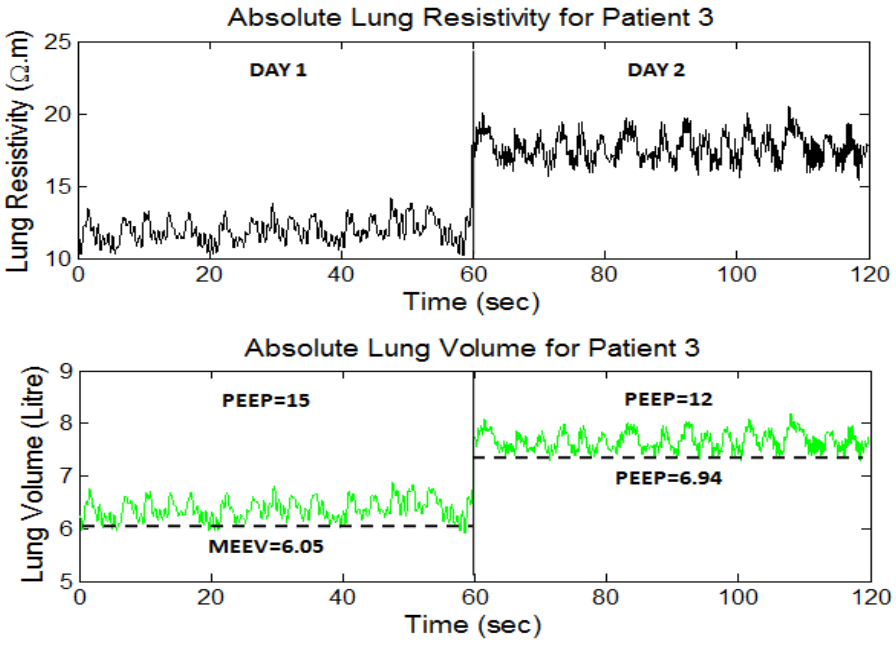

(b)

Figure 5.5: Absolute lung resistivity and lung volume measured by the aEIT system at different PEEP settings for (a): Patient 2 in four days and (b): Patient 3 in two days.

It can be seen that variations in PEEP values in both patients does lead to changes in MEEV values measured by the aEIT system. It is also discovered that MEEV can also increase or decrease without any changes made to the PEEP as depicted in Patient 2 on Days 3 and 4. On Day 3, MEEV readings for Patient 2 decreased as compared to the readings on Day 2. According to the expert clinician, this scenario is deemed possible in patients as an indication of insufficient PEEP to keep the lung open. In Day 4, the patient's MEEV was found to increase even with the same PEEP setting as Day 3. According to the expert clinician, on Day 3, the patient had gone through a surgical procedure called the 'percutaneous tracheotomy' to improve the patient's airway access and breathing. Therefore, the result of increasing MEEV in Day 4 was found to support the fact that surgery had improved the overall patient's ventilation.

In Patient 3, reducing PEEP was seen to increase the MEEV. This scenario happened because the patient had a change in ventilation mode from CPAP to BIPAP. According to the expert clinician, this patient was experiencing collapsed lung during the CPAP mode and having realised this, the patient was then turned to the BIPAP mode, where they had more support and which increased the MEEV reading, even with less PEEP applied.

5.3.3.2 Mean regional densities versus PEEP

Figure 5.6 shows the variation of MAD, MMD and MPD values as a result of PEEP changes in all patients. Linear regression analysis was carried-out on the data and the results are summarised in Table 5.3. It can be seen from the results that generally, as PEEP increased the mean regional densities (MAD, MMD and MPD) decreased proportionally.

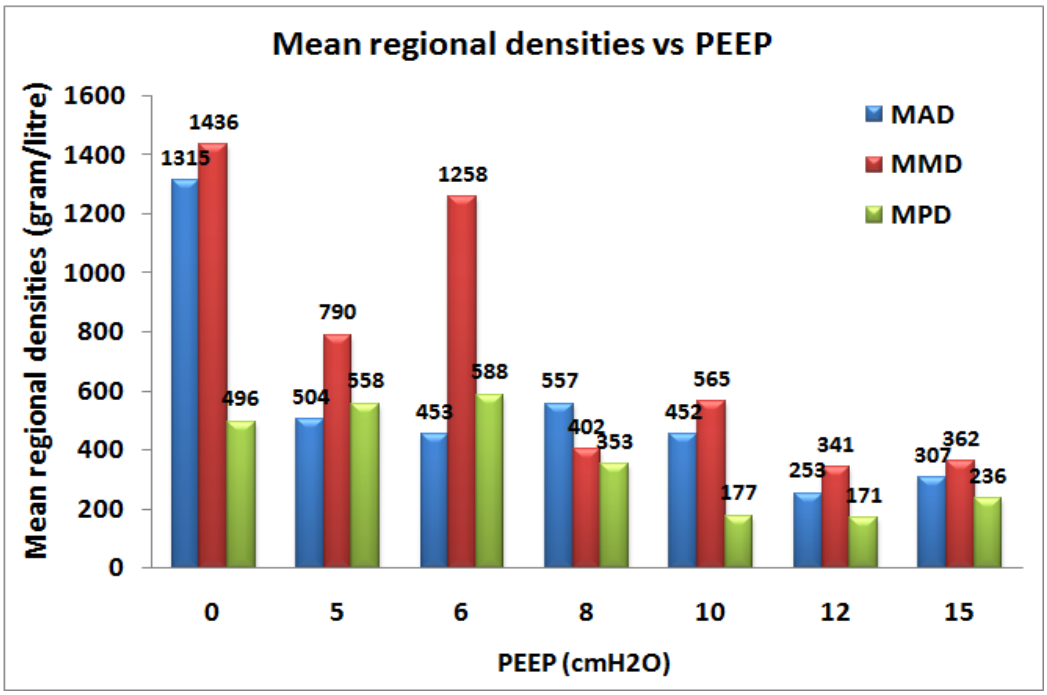

Figure 5.6: PEEP induced changes in MAD, MMD and MPD in all patients

Table 5.3: Linear regression analysis results for the data

	MAD (g/l)	MMD (g/l)	MPD (g/l)
PEEP (cmH2O)	-0.846 (P<0.05)	-0.856 (P<0.05)	-0.776 (P<0.05)

5.3.4 Relationship between MEEV, MAD, MMD and MPD with blood gasses parameters

Over the years, the ratio of the arterial partial pressure of oxygen to the fraction of inspired oxygen (PaO2/FiO2) has been used to assess the level of gas exchange abnormalities in the lungs (Karbing *et al*., 2007), including classification of patients with acute lung injury (ALI) and adult respiratory distress syndrome (ARDS)

(Bernard *et al*., 1994; Artigas *et al*., 1998). In this section, the relationship between PaO2/FiO2 ratio and MEEV, MAD, MMD and MPD produced by the aEIT system is investigated. Table 5.4 shows all the patients' data which include MEEV, MAD, MMD, MPD and all the blood gasses values. Note that Patients 4 and 5 were excluded from this analysis because both patients' records did not include the blood gasses values; data with errors were also excluded.

Table 5.4: Summary of blood gasses values and aEIT quantitative parameters for all patients

Pt.	**Day**	**BLOOD GASSES PARAMETERS**			**aEIT QUANTITATIVE PARAMETERS**			
		PaO2/FiO2 (kPa)	**PaO2 (kPa)**	**PaCO2 (kPa)**	**MEEV (litre)**	**MAD (g/l)**	**MMD (g/l)**	**MPD (g/l)**
1	1	54	16.1	5.09	2.70	335	1213	598
	2	54	16.1	4.68	2.20	570	1302	577
2	1	34	18.6	4.28	6.35	253	357	199
	2	30	11.9	4.29	6.32	334	410	161
		26	10.3	4.44	5.70	377	468	193
	3	26	13.1	4.87	4.95	549	655	155
	4	23	10.3	3.95	5.57	507	669	168
3	1	21	14.7	5.53	6.05	307	362	236
	2	15	9.7	8.57	6.94	213	291	149
6	1	26	10.3	5.18	5.80	557	402	353
7	1	29	11.6	4.91	4.28	293	641	550

Figure 5.7 depicts the variations of MEEV, MAD, MMD, MPD, PaO2/FiO2 ratio and PaCO2 with days in all studied patients. The green dotted lines appeared on the PaO2/FiO2 ratio graph and the PaCO2 graph represents the acceptable range (lower and higher limits) of these parameters. These ranges were chosen following consultation with the ICU expert clinician. For MEEV, MAD, MMD and MPD, these green dotted lines correspond to the normal range (lower and higher limits) of these

parameters. After discussions with the expert clinician, it has been decided to acquire these lower and higher limits based on the data from another study relating to five patients that involved measurement of lung ventilation using the aEIT system (Tunney *et al*., 2008). These patients had undergone oesophagogastrectomy for oesophageal cancer, were smokers but had no chronic lung disease. The MEEV, MAD, MMD and MPD of these patients were calculated based on the improved aEIT system software (version 1.049). The MEEV, MAD, MMD and MPD values for these five patients are summarised in Table 5.5.

Table 5.5: The MEEV, MAD, MMD and MPD values the five patients undergone oesophagogastrectomy for oesophageal cancer

Patient	MEEV (litre)	MAD (g/l)	MMD (g/l)	MPD (g/l)
1	3.78	510	556	329
	3.39	570	624	356
2	3.12	576	987	357
	2.93	601	1064	358
3	4.61	313	465	315
	5.45	264	403	242
4	6.49	224	284	253
	6.75	205	265	246
5	4.18	435	588	397
	3.79	471	651	433
	3.67	474	684	454
Average	4.38	422	597	340

These average values of MEEV, MAD, MMD and MPD were chosen as the normal reference values for the patients involved in the current study. The lower and upper limits were then derived based on these reference values and the overall data of the current studied patients. The lower and upper red dotted lines on the MEEV graphs represent the limits for the lung to be collapsed or overinflated. A lower value than 1.75 litres means that the lung is collapsed, while a greater value than 6.25 litres indicates that the lung is overinflated. These limits were also set based on discussions with the ICU expert clinician.

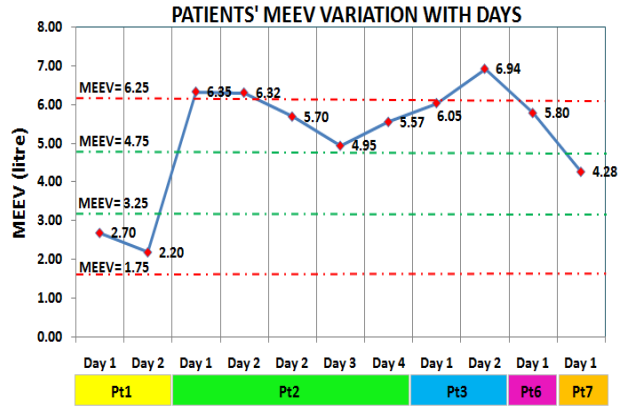

(a)

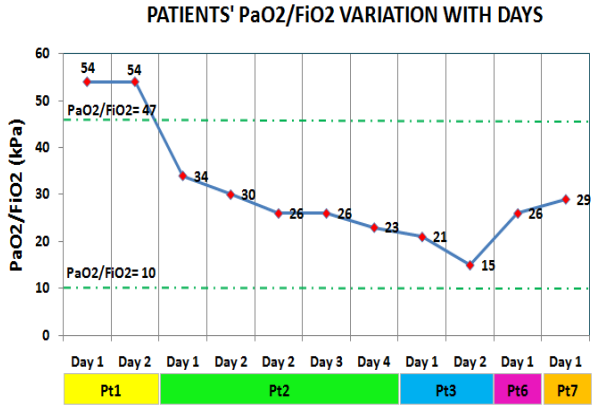

(b)

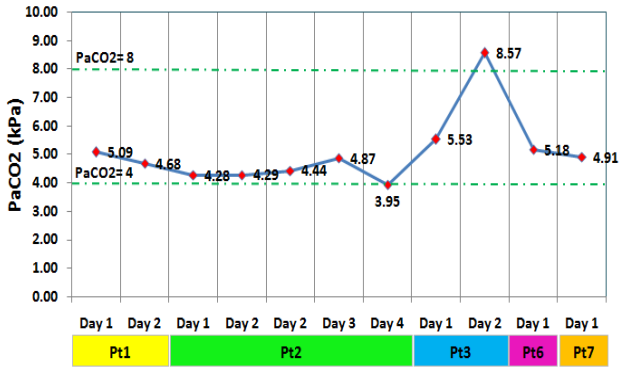

(c)

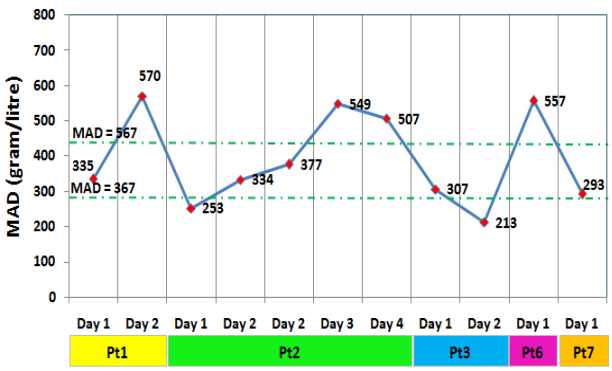

(d)

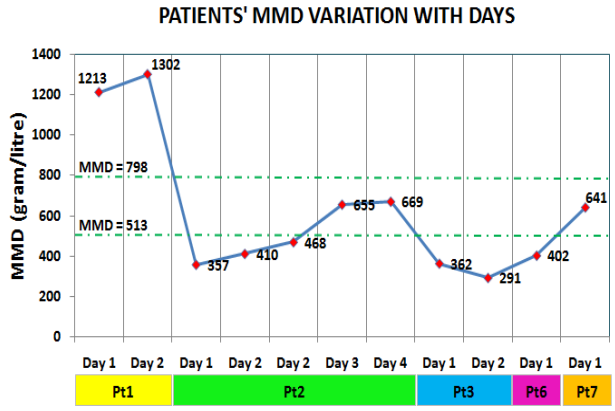

(e)

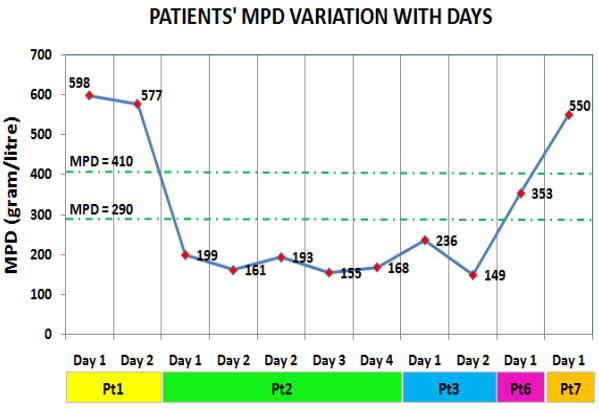

(f)

Figure 5.7: Variation of: (a) MEEV, (b) PaO2/FiO2, (c) PaCO2, (d) MAD, (e) MMD and (f) MPD with days in all studied patients.

The relationship between MEEV and PaO2/FiO2 ratios in overall patients' data was analysed. It was hypothesised at the beginning that increasing MEEV should improve oxygenation and pulmonary gas exchange. However, from the linear regression analysis that was conducted, the correlation was -0.6821 ($P<0.05$). In general, this result shows that MEEV has a significant negative correlation with the PaO2/FiO2 ratio. Nevertheless, when analysing the individual patients this finding was arguable. Results for Patient 2 on Day 2 show that MEEV was reduced from 6.32 litres to 5.70 litres as the effect of PEEP reduction and the PaO2/FiO2 ratio also seen to be reduced from 30kPa to 26kPa. This observation seems to support the previous hypothesis. But in Days 3 and 4, when the MEEV increased from 4.95 litres to 5.57 litres, the PaO2/FiO2 ratio was seen to decrease from 26 kPa to 23 kPa. The same observation was seen in Patient 3, whereby the PaO2/FiO2 ratio was decreased when MEEV increased from Day 1 to Day 2. In Patient 1, no change in PaO2/FiO2 ratio was observed when MEEV decreased from 2.70 litres to 2.20 litres.

From the previous observations, it was found that the relationship between the MEEV and the PaO2/FiO2 ratio does vary with the patient and also between patients because of several reasons: as stated by Heinze *et al*. (2010), an increase in the MEEV value may be due to alveolar recruitment, leading to improved oxygenation (PaO2/FiO2 ratio), or may also relate to overdistension of already open alveoli, leading to no PaO2/FiO2 change or even to a decrease. Under the condition of an overdistented lung, the blood vessels which surround the airspace were being compressed, causing an increase in dead space (wasted ventilation), hence leading to a reduction in PaO2/FiO2 ratio.

The results shown in Figure 5.7 also demonstrate the ability of the aEIT system in providing information about the ventilation inhomogeneity existing within the lung. Considering only the blood gas parameters (PaO2/FiO2 and PaCO2), one may assume that the patients were in a stable condition because most of the values were in the acceptable limits. But when investigating the quantitative parameters provided by the

aEIT system more closely, it can be seen that the patients were not really ‘stable’ as some of the values of these parameters were out of the normal range. For example, the MPD values for Patients 2 and 3 in all the studied days were below the normal range, which means that the patients’ posterior lungs were having less density and hence a high lung volume. This observation is supported by the value shown in the MEEV graph, whereby the MEEV values for all these patients were above the normal lung volume range, which leads the lung to be in slightly overinflated or overinflated condition. According to the expert clinician, for patients with respiratory problem, it is acceptable for the patients’ lung to be slightly overinflated but not more than the allowable limits in order for the patients to receive sufficient oxygenation and be within the acceptable limits of PaO2/FiO2.

When patients were ventilated in the supine position (Figure 5.8 (a)), it is known that the alveoli in non-dependent zones (anterior region) are less likely to collapse at end expiration as compared with the middle region and the posterior region. This denotes that, the anterior region will tend to be less dense compared to the middle and posterior region. However, in current studies, Patients 2, 3 and 6 have shown that the MMD (middle) and MPD (posterior) regions are less dense compared to the anterior and the middle regions. This is because the patients were ventilated in the prone position (Figure 5.8 (b)).

(a) (b)

Figure 5.8: Illustration for the two different position of the studied patients: (a) Supine, (b): Prone.

In patients with acute respiratory problem, the prone position has proven to eliminate lung compression by the heart and abdominal contents, thus limiting actelactasis, especially in the posterior region and as a result can improve gas exchange (Albert *et al*., 2000; Mentzelopoulus *et al*., 2003; Mentzelopoulus *et al*., 2005).

5.3.5 Tidal volume from ventilator versus tidal volume from aEIT

Figure 5.9 compares the VT measured by the ventilator and VT calculated from aEIT system for all patients. It can be seen that there is a good correlation between the these two parameters with R=0.824 and percentage of mean absolute error (MAE%) of 15.9. This result shows that the aEIT system is able to provide VT readings closely to the one measured by the ventilator with 84% accuracy.

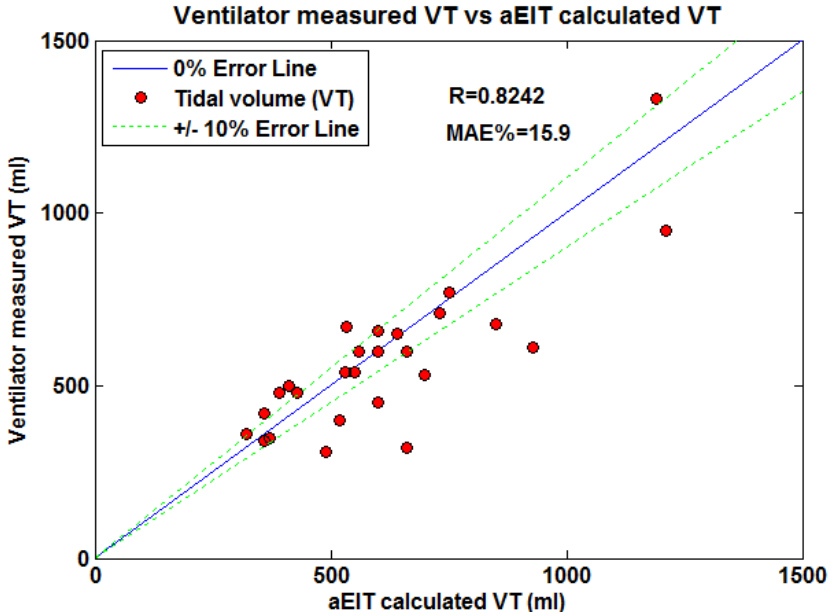

Figure 5.9: Comparison of the tidal volume (VT) measured by the ventilator and EIT for all subjects.

5.4 Summary

In conclusion, results from this study have shown that the improved Sheffield Mk3.5 aEIT system is able to identify PEEP-induced changes in patients under mechanical ventilation. Increasing PEEP leads to improved regional lung ventilation which is reflected on the values of aEIT quantitative parameters i.e. MEEV, MAD, MMD and MPD. The negative correlation between MEEV and PaO2/FiO2 cannot be taken as the final conclusion about the relationship since it varies within the patient and between patients. The PaO2/FiO2 ratio provides only a global information about patients' ventilation, however, regional densities given by MAD, MMD and MPD do have the potential to provide information about the regional lung ventilation distribution. Patients' position is also shown to affect the results of regional ventilation distribution which is reflected in the higher values of MPD and MMD as compared to MAD in Patients 2, 3 and 6. A good correlation between ventilator measured VT and aEIT calculated VT indicates that the current aEIT system is able to provide good estimates of VT readings in ventilated patients.

Certainly, this study has demonstrated the potential of the improved aEIT system to provide not only information on the overall lung volume but also on the regional lung ventilation distribution. These sets of information together with PaO2/FiO2 should lead to a better understanding of phenomena surrounding ventilated patients in order to support decision-making and guide ventilator therapy. However, more data on ICU ventilated patients are needed to confirm the findings in this study and established methods such as nitrogen wash-in-wash-out to quantify the patients' lung volume needs to be used to compare with the values of the MEEV provided by the aEIT system. In the next Chapter, MEEV and mean regional densities' models are developed to map these parameters from ventilator and blood gas parameter.

CHAPTER 6

MODELLING OF aEIT-BASED QUANTITATIVE PARAMETERS USING A NEURAL FUZZY SYSTEM

6.1 Introduction

The aEIT clinical trials on ICU patients presented in Chapter 5 have shown that the system is now able to provide useful information about changes in aEIT quantitative parameters such as mean end-expiratory lung volume (MEEV), mean anterior density (MAD), mean middle density (MMD) and mean posterior density (MPD) as the results of changes in PEEP settings These identified parameters, have the potential to represent the overall lung volume and regional lung distribution of the patient and can be integrated with the information of the blood gas parameters to achieve the optimal ventilator management strategy in the ICU. Modelling the relationship between these parameters should indeed represent a step forward to represent the acute-ventilated patients with EIT.

In patients with acute phase, there are other ventilator parameters that need to be monitored in addition to PEEP, such as peak inspiratory pressure (PIP), inspiratory

pressure (Pinsp), fraction of inspired oxygen (FiO2) and respiratory rate (RR). Therefore, in this Chapter, the relationship between these identified aEIT quantitative parameters with PIP, Pinsp, FiO2 and RR were studied based on data from the acute-ventilated patients with EIT in the ICU. Four data-driven models were developed and these models represent the relationships between ventilator parameters and blood gas parameter with the MEEV, MAD, MMD and MPD. The relationships will mimic the behaviour of the overall lung volume and ventilation distribution of the patients in response to the changes in ventilator parameters as well as blood gas parameter. This Chapter is organised as follows: first, the modelling and the data collection methods are presented, second; the development of MEEV, MAD, MMD and MPD models is reviewed and the modelling results are shown, analysed and discussed. Finally, the overall results are summarised and conclusion are drawn based on the results hence obtained.

6.2 Modelling method

Neural-Fuzzy modelling falls under the umbrella of Computational Intelligence (CI) modelling and can be used as a non-linear method for mapping a certain number of inputs to a certain number of outputs. This non-linear mapping can be learned from process data using various algorithms. The two most popular types of fuzzy rules processing are the Mamdani-type (Mamdani, 1974) and the Sugeno-type (Takagi and Sugeno, 1985). Such models include a number of linguistic descriptions of the process under investigation (rules). The architecture used in this work is the Adaptive Neural-Fuzzy Inference System or also known as ANFIS (proposed by Jang (1993)) and consists of a set of TSK-type fuzzy IF-THEN rules (proposed by Takagi, Sugeno and Kang (Sugeno and Kang, 1988; Takagi and Sugeno, 1985)). A typical fuzzy rule in Sugeno fuzzy model has the following form:

IF *x* is **A** and *y* is **B THEN** *z* = *f(x,y)* **(6.1)**

Where *x* and *y* are the inputs to the system, **A** and **B** are linguistic labels such as: *low*, *moderate* and *high*, while *z* = *f(x,y)* is a crisp function in the consequent. The structure of an ANFIS model for a 2-input and 1-output system includes the following layers (as shown in Figure 6.1):

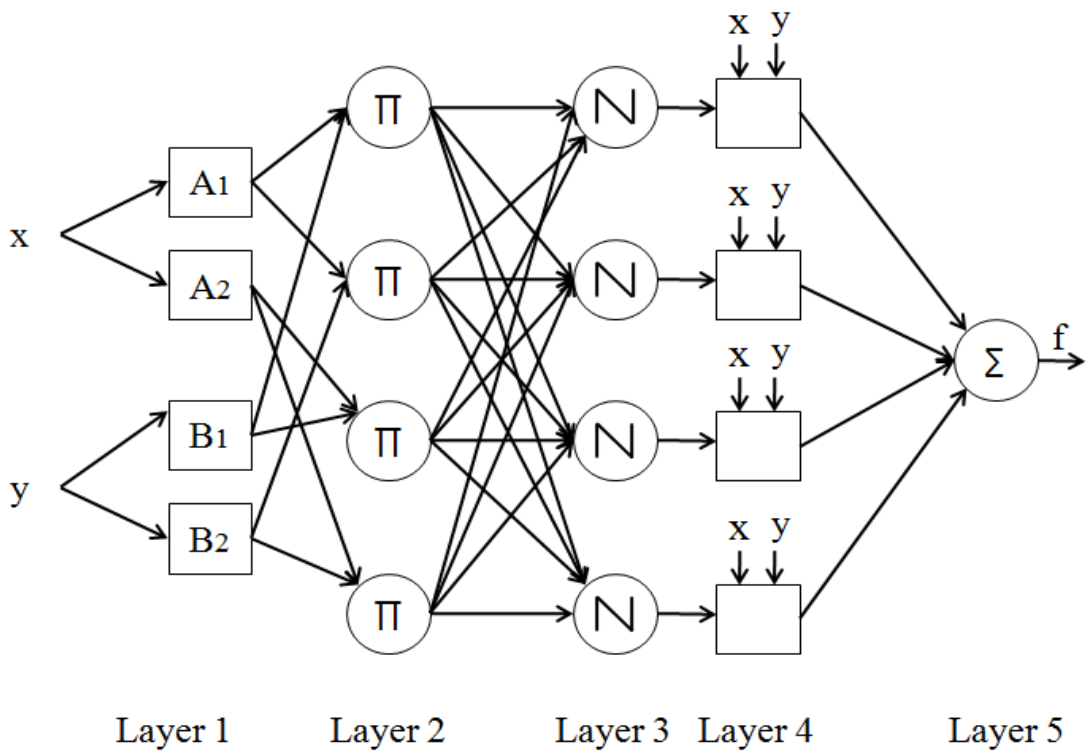

Figure 6.1: An example of a two input-one output ANFIS with four rules.

Layer 1: The membership functions layer. The output of any node in this layer gives the membership degree of an input (crisp value). A1, A2, B1 and B2 are the fuzzy membership functions.

Layer 2: The multiplication layer. Every node here multiplies the inputs of membership degrees and produces the firing strength of the rule.

Layer 3: The normalisation layer. It calculates the ratio of the particular rule-firing degree to the sum of all rule degrees.

Layer 4: This applies the sugeno processing rule and is therefore an output calculating layer.

Layer 5: It consists of only one node which calculates the overall outputs as the sum of all incoming signals.

A hybrid learning procedure proposed by Jang (1993) is used. It consists of two passes. In the forward pass, the node outputs propagate forward until Layer 4 and the consequent parameters are identified using a least-squares method. Then, a backward pass is performed with the consequent parameters fixed and the parameters of the input membership functions (which are represented by the weights and biases in Layer 1) adjusted using a gradient descent method.

6.3 Patient's data

In this modelling work, only data from patients with BIPAP (Bilevel Positive Airway Pressure) and with no or very little spontaneous breathing were considered to ensure that they were in the acute phase. Based on data from the clinical trials on ICU patients in Chapter 5, four (4) ventilated patients with EIT were identified (Patients 1, 2, 3 and 6). However, due to the limited size of EIT data relating to Patients 1, 3 and 6, only data from Patient 2 are considered in this work. MEEV, MAD, MMD and MPD were extracted from aEIT measurements and the ventilator parameters (FiO2, PEEP, RR, PIP, Pinsp) together with PaO2/FiO2 ratio values which were retrieved from the Sheffield Patient Data Monitoring System (PDMS).

6.4 Development of MEEV model

The MEEV model is designed to predict the aEIT Mean-End Expiratory Lung Volume (MEEV) directly from ventilator and blood gasses data obtained from the Sheffield Patient Data Monitoring System (PDMS).

6.4.1 Model's inputs selection

Prior to modelling, an inputs selection operation for the MEEV model was carried-out by consulting the expert clinician and by also performing correlation analyses. From Patient 2 data, 55% of the data were randomly chosen as the training data. The remaining 45% from the same data set were selected as the testing data. The correlation analysis was conducted for the data and the results are shown in Table 6.1.

Table 6.1: The correlation analysis results for MEEV model inputs selection.

	PIP	***PEEP***	***Pinsp***	***RR***	***FiO2***	***PaO2/FiO2***
MEEV	0.65	0.81	0.39	0.55	0.07	0.72

It can be seen from this correlation analysis that PIP, PEEP, Pinsp, RR and PaO2/FiO2 ratio are likely to have a significant relationship with MEEV. However, in this modelling work, only parameters with a correlation coefficient >0.6 will be selected as the input to the model. Therefore, in this case, PIP, PEEP and PaO2/FiO2 ratio were chosen as the inputs to the MEEV model. The MEEV model structure is summarised in Figure 6.2.

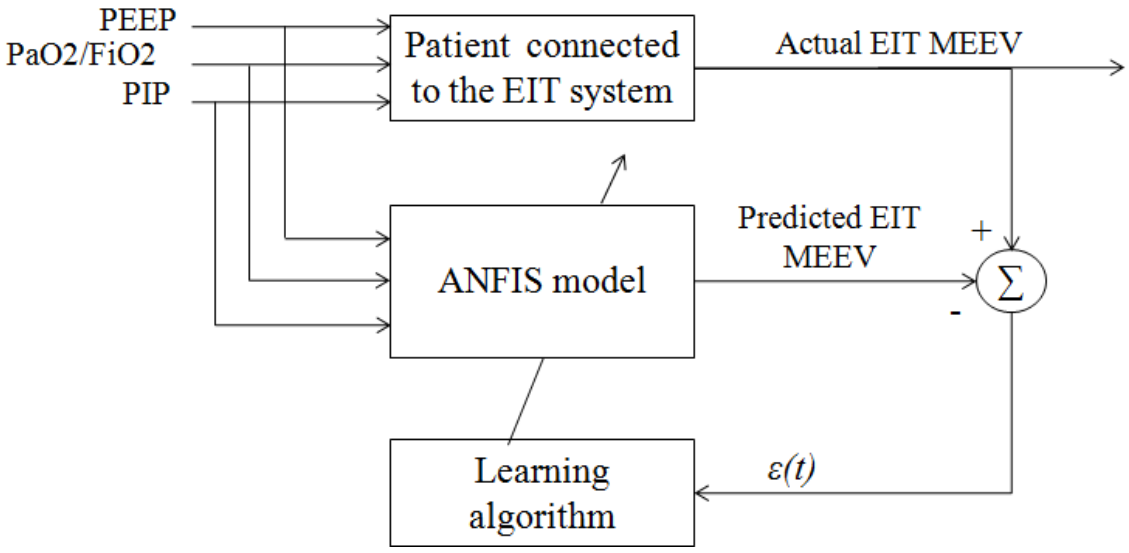

Figure 6.2: The MEEV model structure.

The MEEV-ANFIS model was trained using MATLAB® v7.1 fuzzy logic toolbox. The initial fuzzy system structure was decided upon using subtractive clustering method (Chiu, 1994). The membership functions and linear parameters of the output were further optimised via the hybrid Levenberg-Marquardt (Hagan and Menhaj, 1994) and the back-propagation algorithms (Horikawa *et al.*, 1992).

6.4.2 MEEV model training and testing results

The training data distribution is summarised in Table 6.2. The modelling results are summarised in Table 6.3 and Figure 6.3. The root mean square error (RMSE), the mean absolute error (MAE%), the correlation coefficient (Cor.) and the standard deviation of the errors (eSTD) were used as the performance indices for model assessment.

Table 6.2: Summary of the training data for MEEV model

	Mean ± S.D.	***Minimum***	***Maximum***
PEEP (cmH2O)	11 ± 0.93	10	12
PaO2/FiO2	27 ± 3.80	23	34
PIP (cmH2O)	25 ± 5.22	20	36
MEEV (litre)	5.71 ± 0.49	4.93	6.35

Table 6.3: The MEEV model training and testing results

	Training	***Testing***
RMSE	0	0.07
MAE (%)	0	1.04
Cor.	1	0.99
eSTD	0	0.07

As shown in Figure 6.3, the ANFIS model can predict the MEEV with a good accuracy in both training (100%) and testing (99%). The current modelling results show that ANFIS is a good modelling method to learn the relationship between the MEEV and the ventilator parameters and blood gas parameter.

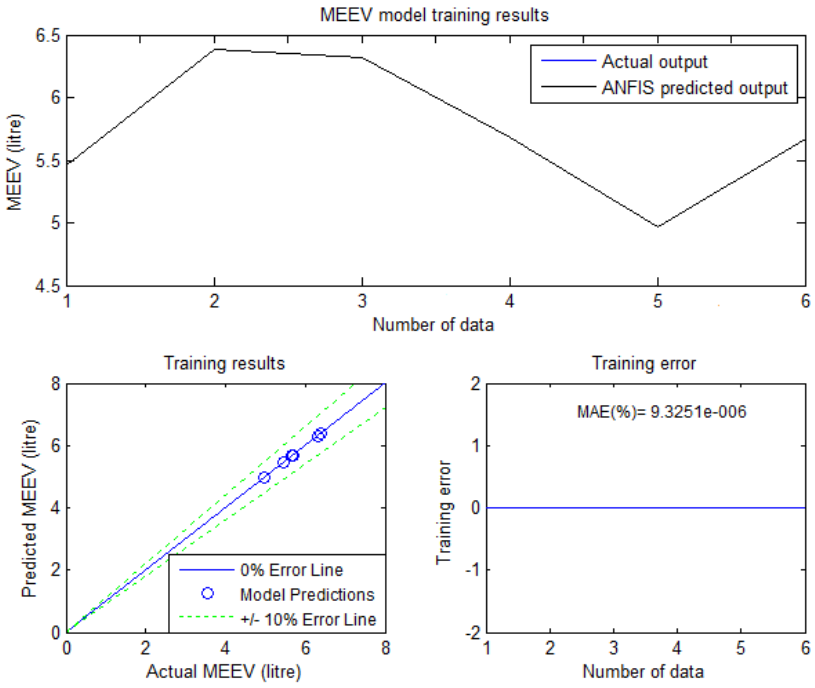

(a)

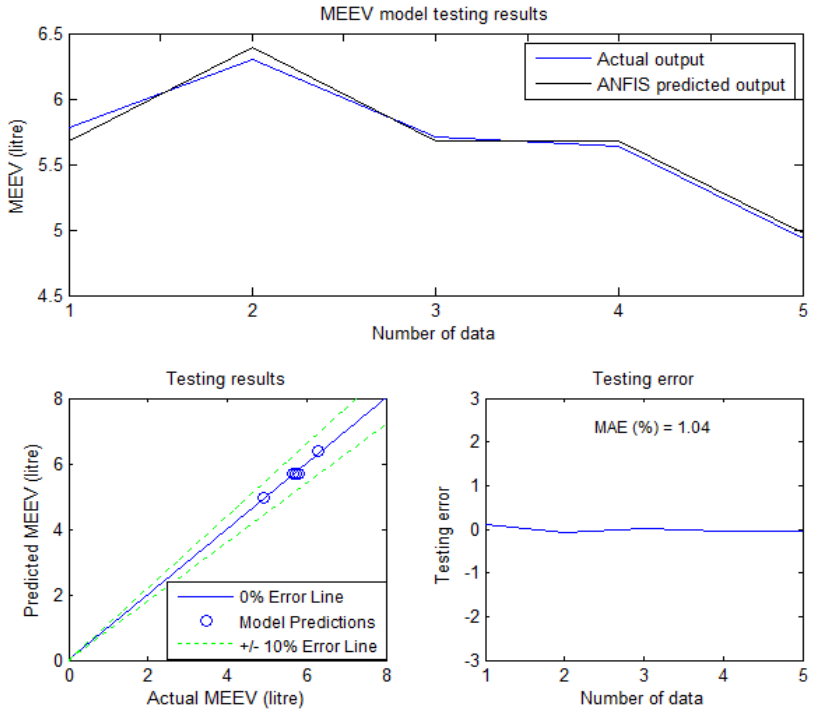

(b)

Figure 6.3: The MEEV ANFIS model: (a) training results and (b) testing results.

6.5 Development of MAD, MMD and MPD models

These models are developed to map mean regional densities (MAD, MMD and MPD) of patients' lung from ventilator parameters and blood gas parameter using ANFIS. Data of regional densities for Patient 2 were retrieved from the aEIT system and used as the output in these models.

6.5.1 Models' inputs selection

After consulting the clinicians and conducting the correlation test, PEEP, PaO2/FiO2 and RR were selected as inputs to the models, which on average, had a good correlation with MAD, MMD and MPD. The correlation analysis results are shown in Table 6.4 and the MAD, MMD and MPD model structure is shown in Figure 6.4.

Table 6.4: The correlation analysis results for MAD, MMD and MPD models' inputs selection.

	PIP	***PEEP***	***Pinsp***	***RR***	***PaO2/FiO2***
MAD	-0.21	-0.74	-0.09	-0.30	-0.81
MMD	-0.05	-0.71	0.09	-0.13	-0.81
MPD	0.07	0.23	0.03	-0.30	0.43
Average	-0.06	-0.41	0.01	-0.24	-0.40

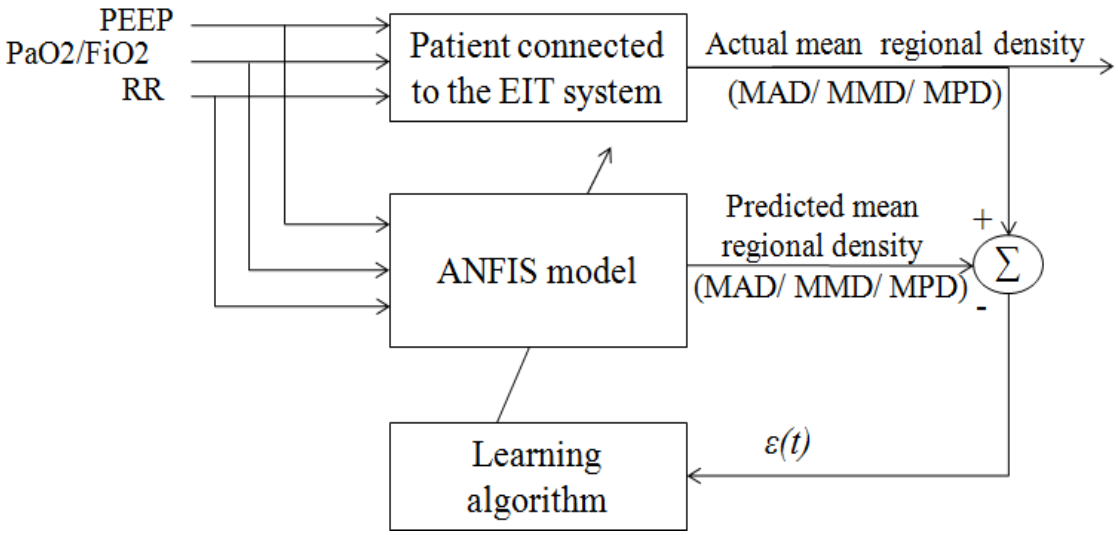

Figure 6.4: The model structure for MAD, MMD and MPD.

The initial fuzzy inference system structure has been determined using the subtractive clustering method. The hybrid algorithm was used to optimise the membership functions and output parameter.

6.5.2 MAD, MMD and MPD models training and testing results

The training data distribution for all the models are summarised in Table 6.5. The performance of the models are summarised in Table 6.6, Figure 6.5, Figure 6.6 and Figure 6.7. The root mean square error (RMSE), the mean absolute error (MAE%), the correlation coefficient (Cor.) and the standard deviation of the errors (eSTD) were used as the performance indices for model assessment.

Table 6.5: Summary of the training data for MAD, MMD and MPD models

	Mean ± S.D.	***Minimum***	***Maximum***
PEEP (cmH2O)	11 ± 0.93	10	12
PaO2/FiO2	27 ± 3.80	23	34
RR (breath/min)	17 ± 1.81	14	20
MAD (gram/litre)	405 ± 108	250	550
MMD (gram/litre)	513 ± 125	352	683
MPD (gram/litre)	180 ± 18.55	155	200

Table 6.6: The MAD, MMD and MPD models training and testing results

	MAD		***MMD***		***MPD***	
	Training	**Testing**	**Training**	**Testing**	**Training**	**Testing**
RMSE	0	5.04	0	8.29	0	6.78
MAE (%)	0	1.31	0	1.63	0	2.42
Cor.	1	1	1	0.99	1	0.96
eSTD	0	5.26	0	9.10	0	5.77

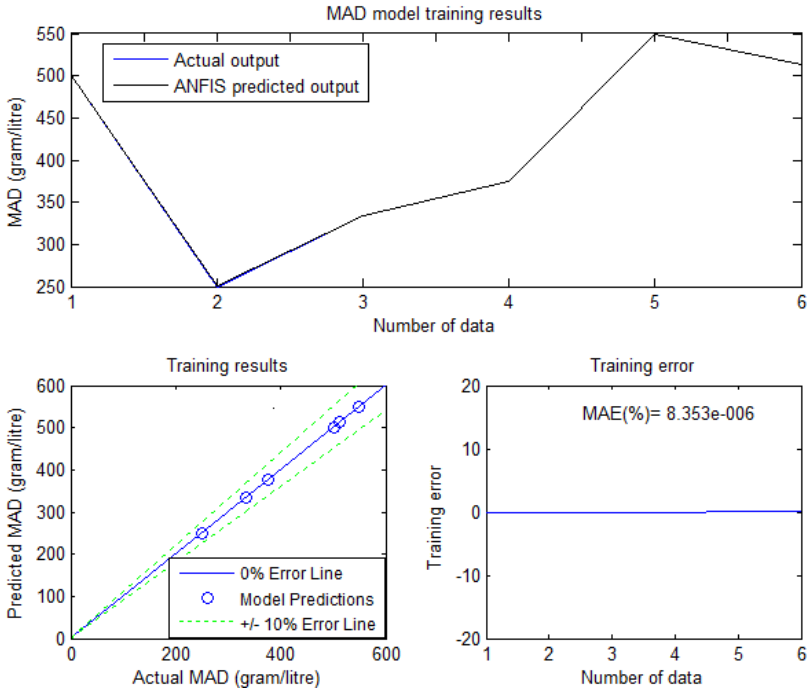

(a)

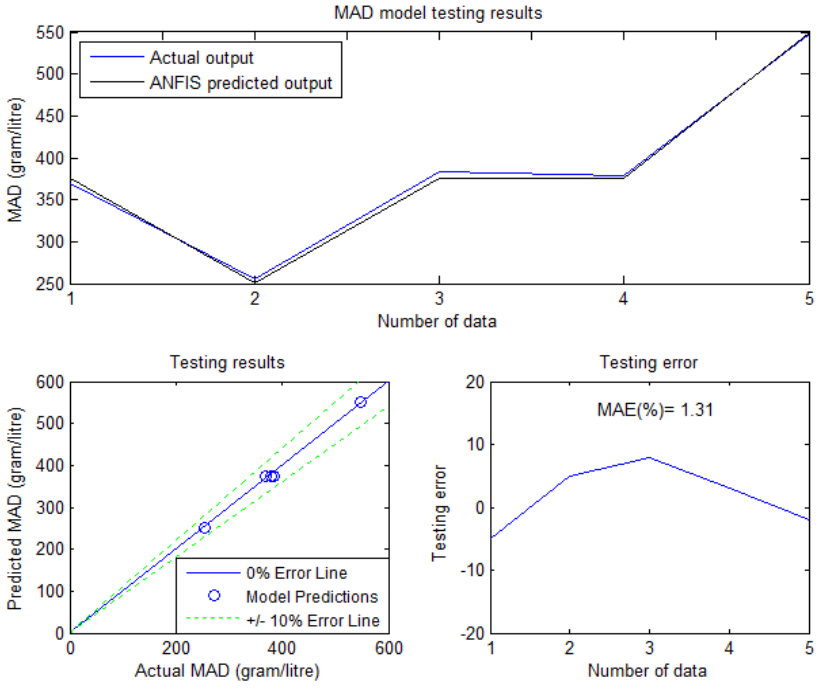

(b)

Figure 6.5: The MAD ANFIS model: (a) training results and (b) testing results.

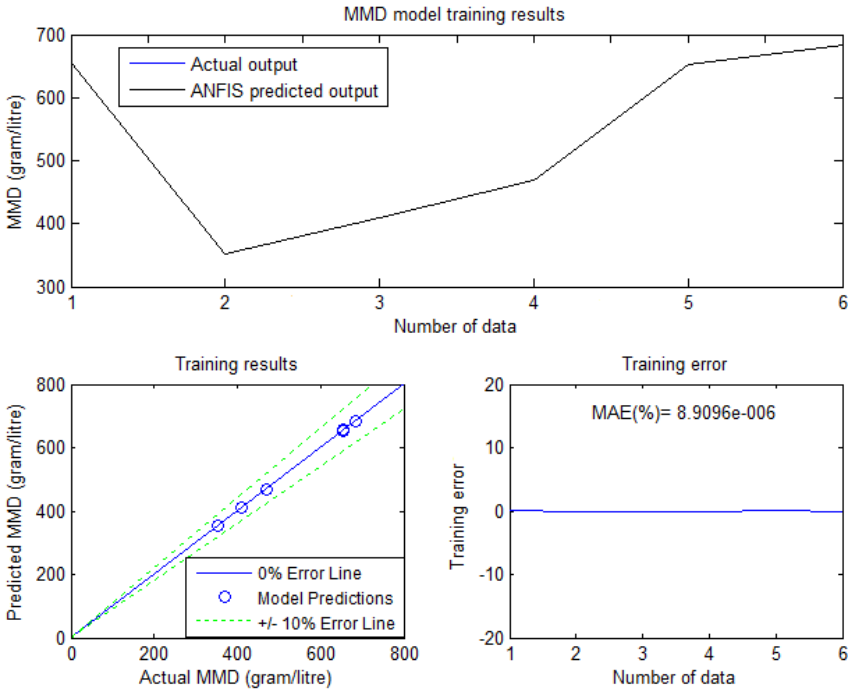

(a)

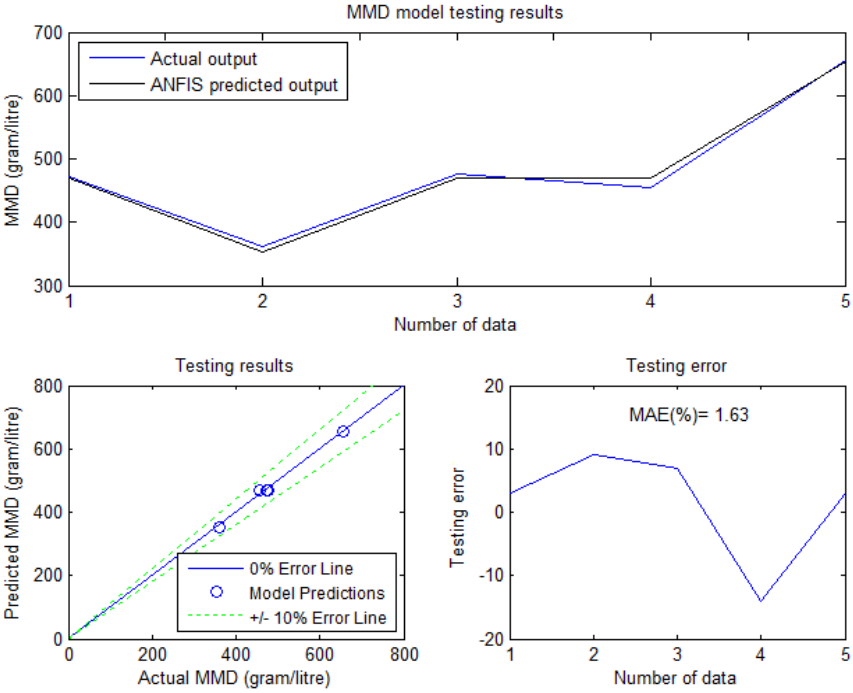

(b)

Figure 6.6: The MMD ANFIS model: (a) training results and (b) testing results.

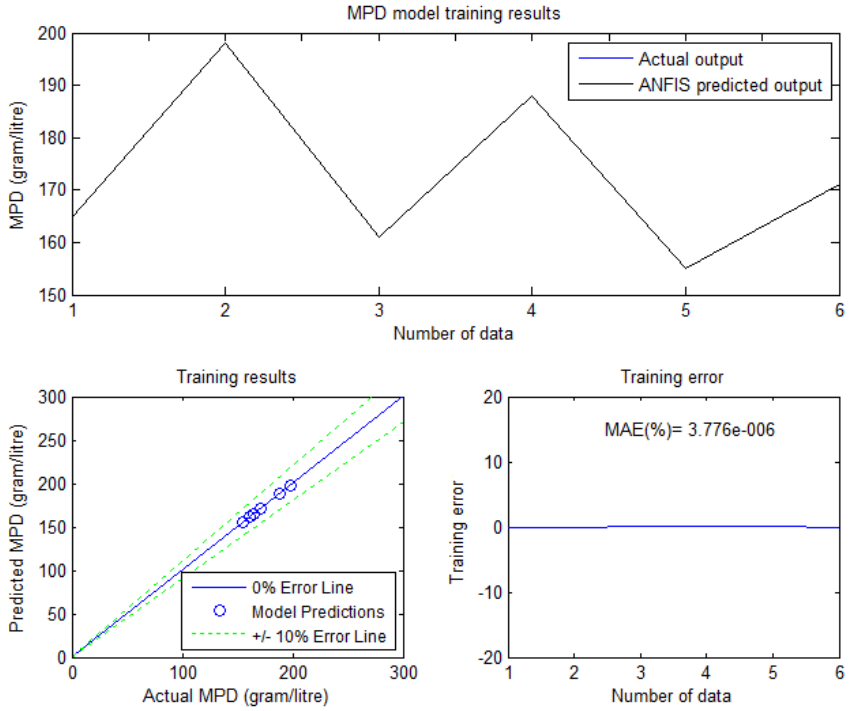

(a)

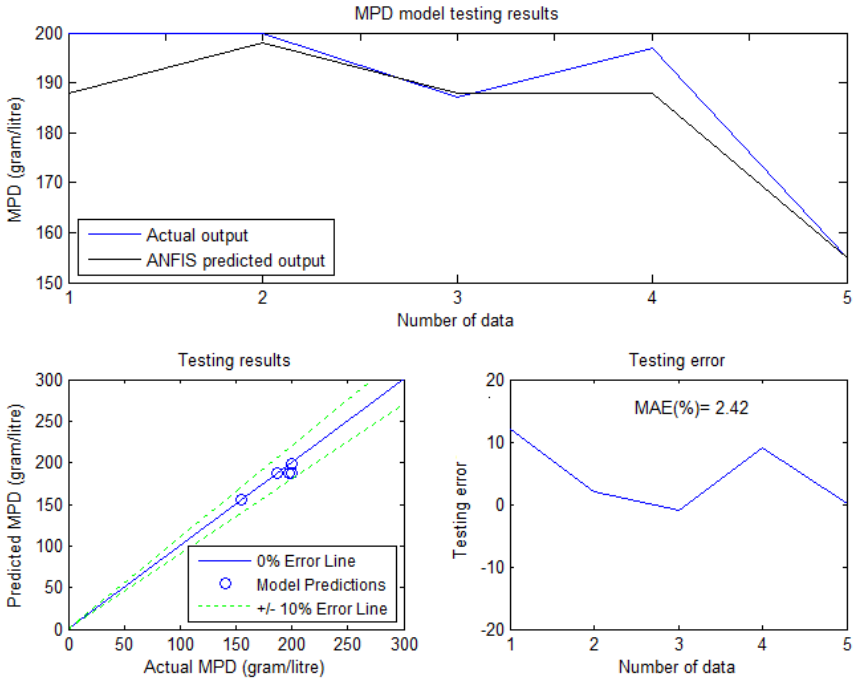

(b)

Figure 6.7: The MPD ANFIS model: (a) training results and (b) testing results.

From the modelling results previously summarised, all models show a good prediction of the regional lung density (MAD, MMD and MPD), with average accuracy of 100% for training and 98.2% for testing in all models. However, it is expected that more data are needed to ensure the consistency of results. In addition of having the global information of the lung, these models have the potential to be used in the study of regional lung behaviour as a result of changing the ventilator settings.

6.6 Summary

In summary, the MEEV, MAD, MMD and MPD models have been developed based on the data from real ventilated patient with EIT using ANFIS. All the modelling results show that ANFIS represents a good modelling tool to learn the relationships between the aEIT quantitative parameters (MEEV, MAD, MMD and MPD), the ventilator and the blood gas parameters. Although the selected model structures have proven to be sufficient in predicting the MEEV, MAD, MMD and MPD with a good accuracy, these models still need to be improved due to the small amount of training and testing data available and further validation of the models still need to be carried-out in the future. In the next Chapter, these models will be used in combination with a totally non-invasive blood gas model of ventilated patients (SOPAVent) to validate the fuzzy rules for the decision support system via a series of simulation scenarios to mimic the real patients' state evolution in the intensive care unit (ICU).

CHAPTER 7

AN INTELLIGENT EIT-BASED DECISION SUPPORT SYSTEM FOR CRITICALLY-ILL VENTILATED PATIENTS IN INTENSIVE CARE UNIT

7.1 Introduction

In Chapter 6, four (4) models of aEIT quantitative parameters were developed and validated. These models represent the relationship between ventilator settings (PEEP, PIP, RR) and blood gas parameter (PaO2/FiO2 ratio) with the mean end expiratory lung volume (MEEV), mean anterior density (MAD), mean middle density (MMD) and mean posterior density (MPD) in critically-ill ventilated patients. Despite the relatively small size of the data used to elicit such models, the training and testing results showed that the models are able to provide a good prediction of the required parameters (MEEV, MAD, MMD and MPD). As a result, these models formed the basis for both the design and evaluation of decision support system (DSS) for critically-ill ventilated patients in ICU.

In this Chapter, the work on the development of prospective intelligent EIT-based decision support system (IEDSS) that integrates information from a totally non-invasive blood gas model of ventilated patients (SOPAVent) in ICU with models of aEIT quantitative parameters is presented. The SOPAVent (Simulation of Patient under Artificial Ventilation) model was initially designed to predict steady-state blood gas measurements of patients in stable conditions. The model was then extended to allow real-time continuous predictions of the patient's blood gases and tidal volume. This particular Chapter is organised as follows: first, the work on designing the intelligent EIT-based decision support system is presented which consists of the FiO2/PEEP and Pinsp/RR sub-units and rule-based derivation that incorporates the expert knowledge with the fuzzy inference system in the analysis of the physiological and aEIT parameters for therapy optimisation. The validation of the IEDSS that simulates the hybrid aEIT-SOPAVent models according to designed patient's scenarios is then presented. Finally, conclusions are drawn based on the results hence obtained.

7.2 The intelligent EIT-based decision support system (IEDSS) design method

Mechanical ventilation is a complex process aimed at providing the adequate balance of oxygen levels and carbon dioxide built up in the circulation system. The levels of oxygen and carbon dioxide in the blood are reflected in both the arterial partial pressure of oxygen (PaO2) and the arterial partial pressure of carbon dioxide (PaCO2) which have long been used together with the pressure-volume curves for assessing the lung function and guiding the titration of mechanical ventilation for the critically-ill patients. The operation that consists of maximising the gas exchange and of minimising over-distension is not trivial which is compounded by the fact that there is very little information on guiding the clinicians to optimising the ventilator settings, especially PEEP, in mechanically ventilated patients (Moloney and Griffiths, 2004).

With the EIT system, it is now possible to have the information on the lung volumes and regional ventilation distribution at the patient's bedside, which will aid in providing advice on PEEP and other ventilator settings, to improve patient care in ICU. Therefore, in the development of the IEDSS, lung condition has been added as another therapeutic goal along with the blood gasses parameters, and as a result the IEDSS will be able to provide advice on FiO2, PEEP, Pinsp and RR settings. According to the expert clinician, it is well-known that FiO2 and PEEP mainly affect the patient's oxygenation while Pinsp and RR mainly influence the PaCO2 level. Therefore, it was decided to split the system into two sub-units, i.e. FiO2/PEEP and Pinsp/RR. In each sub-unit, suggestions for (advice on) changes in ventilator settings are produced by a fuzzy rule-base, thus, in total, four fuzzy rule-bases were developed.

7.3 Development of FiO2/PEEP sub-unit

7.3.1 Fuzzy partitions for the inputs and outputs

After discussions with the expert clinician, the main input variables to the FiO2/PEEP sub-unit were decided upon these include the PaO2, FiO2, MEEV, right lung anterior density (RLAD), right lung middle density (RLMD), right lung posterior density (RLPD), left lung anterior density (LLAD), left lung middle density (LLMD) and left lung posterior density (LLPD). Three input fuzzy sets were assigned to PaO2 and FiO2. While five were introduced to MEEV, RLAD, RLMD, RLPD, LLAD, LLMD and LLPD respectively. It is obvious that a relatively large number of rules will be produced from these variables. Therefore, in order to reduce this number, the nine input variables were grouped to lead only to three input variables which are the lung condition, PaO2 and patient condition. The structure of the fuzzy rule-bases in the FiO2/PEEP sub-unit is shown in Figure 7.1.

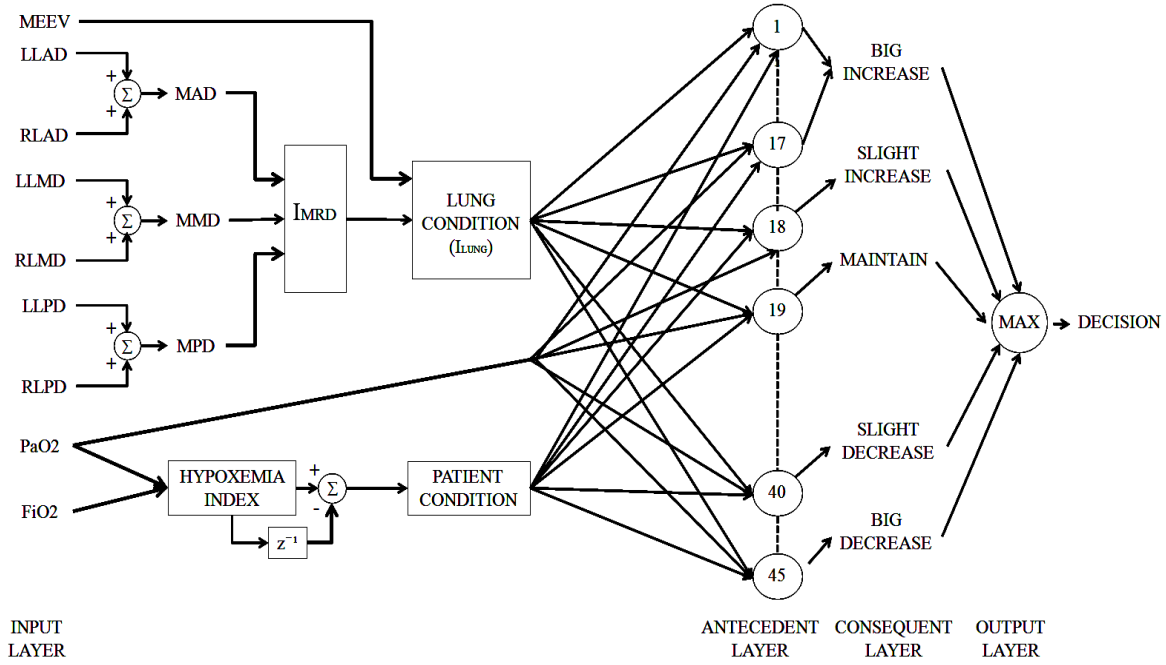

Figure 7.1: Structure of the fuzzy rule-base for FiO2/PEEP subunit.

Lung condition is an index (ranges from 0 to 1) that represents the behaviour of patient's lung (lung volumes and density) in response to various ventilator therapies. The lung densities were estimated for six lung regions defined as RLAD, RLMD, RLPD, LLAD, LLMD and LLPD. The densities of the left lung and the right lung calculated by the aEIT system are then combined to become mean anterior density (MAD), mean middle density (MMD) and mean posterior density (MPD) which become the secondary variables for the regional densities. This is realised by adding the mean density for the anterior left and right, middle left and right and posterior left and right as shown in Figure 7.1. The tertiary variable for the density is then introduced, that is the mean regional density index (IMRD). To produce the IMRD, each variable (MAD, MMD, MPD) and IMRD itself were assigned five fuzzy sets: VERY LOW (VL), LOW (L), MODERATE (M), HIGH (H) and VERY HIGH (VH) and by incorporating the knowledge of the expert clinician, fuzzy rules were developed using the MATLAB fuzzy logic toolbox to map the inputs (MAD, MMD

and MPD) into the output. In this case, a total of 125 fuzzy rules were generated and a sample example of these rules is as follows:

RULE 1: If (MAD is VL) and (MMD is VL) and (MPD is VL) then (IMRD is VL).

RULE 26: If (MAD is L) and (MMD is VL) and (MPD is VL) then (IMRD is VL).

RULE 53: If (MAD is M) and (MMD is VL) and (MPD is M) then (IMRD is M).

RULE 77: If (MAD is H) and (MMD is VL) and (MPD is L) then (IMRD is L).

RULE 125: If (MAD is VH) and (MMD is VH) and (MPD is VH) then (IMRD isVH).

By using the same method as realising the IMRD, the index of lung condition (ILUNG) is developed by combining the information of IMRD and normalised MEEV. Five fuzzy sets were used to represent MEEV: VERY LOW (VL), LOW (L), MODERATE (M), HIGH (H) and VERY HIGH (VH). The index of lung condition (ILUNG) is represented by five fuzzy sets: COLLAPSED (C), SLIGHTLY COLLAPSED (SC), MODERATE (M), SLIGHTLY OVERINFLATED (SO) and OVERINFLATED (O). It has been agreed with the clinician that these are the terms that best describe the patient's lung conditions. Therefore, a total of 25 rules were generated and a sample example of these rules is given as follows:

RULE 1: If (MEEV is VL) and (IMRD is M) then (LUNG_CONDITION is SC).

RULE 6: If (MEEV is L) and (IMRD is VH) then (LUNG_CONDITION is C).

RULE 10: If (MEEV is M) and (IMRD is H) then (LUNG_CONDITION is M).

RULE 14: If (MEEV is H) and (IMRD is M) then (LUNG_CONDITION is SO).

RULE 17: If (MEEV is VH) and (IMRD is M) then (LUNG_CONDITION is O).

For the PaO2 variable, the same method used by Kwok (2003) is repeated here with three fuzzy sets: LOW, NORMAL and HIGH. The hypoxemia index is well-known to clinicians as an indication of the level of lung injury. It is represented by the ratio of PaO2 (kPa) to fraction of FiO2. From Kwok (2003), the patient's condition was determined by the percentage change in the hypoxemia index and assigned three fuzzy sets: DETERIORATING, STATIC and IMPROVING. In this case, both the PaO2 and the percentage change in the hypoxemia index values are normalised to the range [0 1].

In the consequent layer, there are five fuzzy sets describing the actions that need to be performed on the ventilator settings, such as: SLIGHT INCREASE (SI), BIG INCREASE (BI), MAINTAIN (M), SLIGHT DECREASE (SD) AND BIG DECREASE (BD). The output member with the maximum membership value was then chosen as the actual output.

7.3.2 Parameters for fuzzy input membership functions

In this work, the Gaussian membership function was chosen to represent the fuzzy sets for MAD, MMD, MPD and MEEV. This membership function is specified by two parameters $\{m,\sigma\}$, where m and σ represent the centre and width of the Gaussian membership function respectively and has the following form:

$$\mu(x) = exp\left[-\frac{1}{2}\left(\frac{x-m}{\sigma}\right)^2\right] \quad \textbf{(7.1)}$$

Upon discussion with the expert clinician, the centre of Gaussian membership function which represents the fuzzy set VERY LOW, LOW, HIGH and VERY HIGH

were determined from the ICU patients' data gathered during the clinical trials of aEIT system. The centre for the MODERATE fuzzy set however, was taken from another study of five patients who were involved in single lung ventilation using the aEIT system (Tunney, 2008). These patients had undergone oesophagogastrectomy for oesophageal cancer, were current smokers but with no chronic lung disease. The mean values for MAD, MMD, MPD and MEEV were calculated from the patients and were used as the moderate value for all the variables respectively. Details on patients' MEEV, MAD, MMD and MPD values can be found in Chapter 5 (Section 5.3.4). In this work, the width of the Gaussian membership function for all these fuzzy sets was determined automatically by the MATLAB fuzzy logic toolbox. Figure 7.2 shows an example of the normalised membership functions for MAD with Gaussian membership functions.

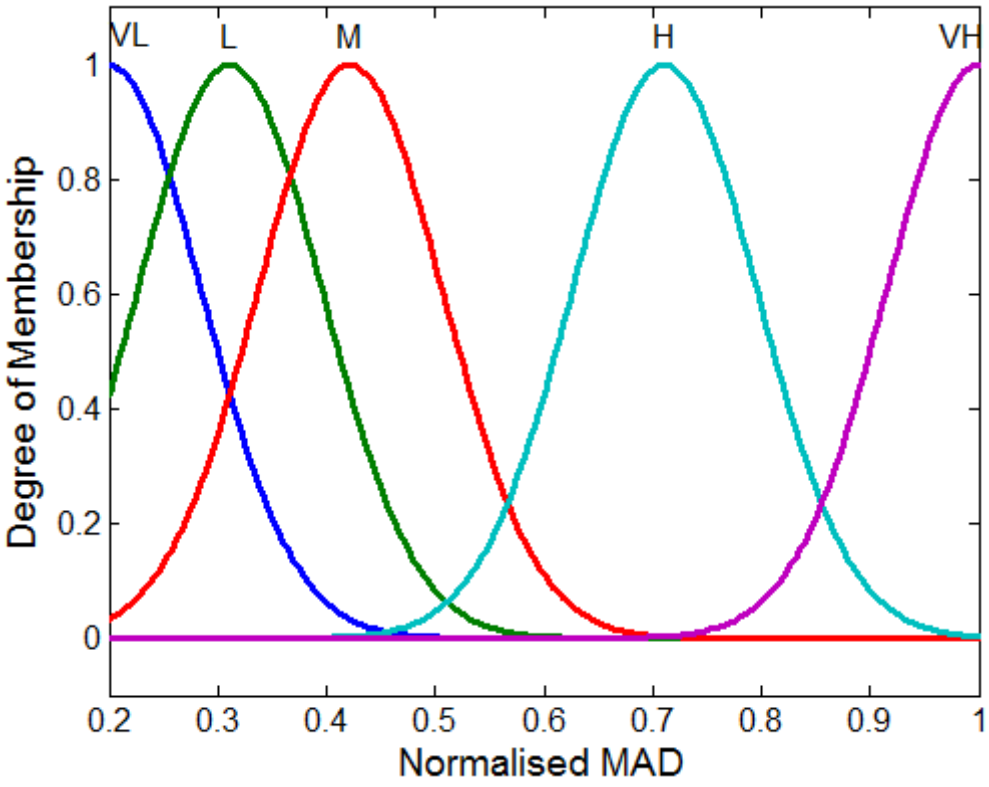

Figure 7.2: Fuzzy membership functions for the normalised MAD.

The fuzzy membership functions chosen to represent the fuzzy sets for PaO2 were based on the work conducted by Kwok (2003), where parameters of the membership functions were derived using an observational approach via a simulation study. Percentage changes in hypoxemia index were also studied and the parameters of the membership functions for this variable were derived based on the statistical distribution of the changes during the simulation studies conducted. For the PaO2 variable, Sigmoidal membership functions were used for LOW and HIGH, whereas Bell-shaped membership functions were used for fuzzy sets NORMAL. As for the percentage changes in hypoxemia index (patient condition), Gaussion membership function was used for STATIC condition, while Sigmoidal membership functions were used for DETERIORATING and IMPROVING (Figure 7.3 and Figure 7.4).

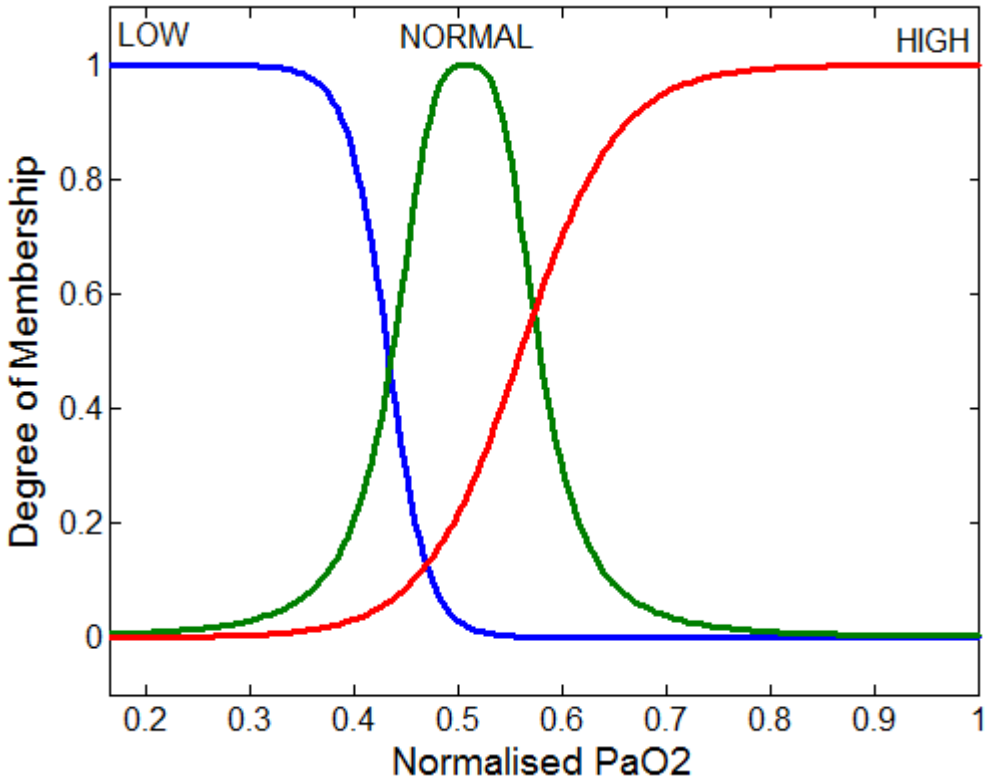

Figure 7.3: Fuzzy membership functions for the normalised PaO2.

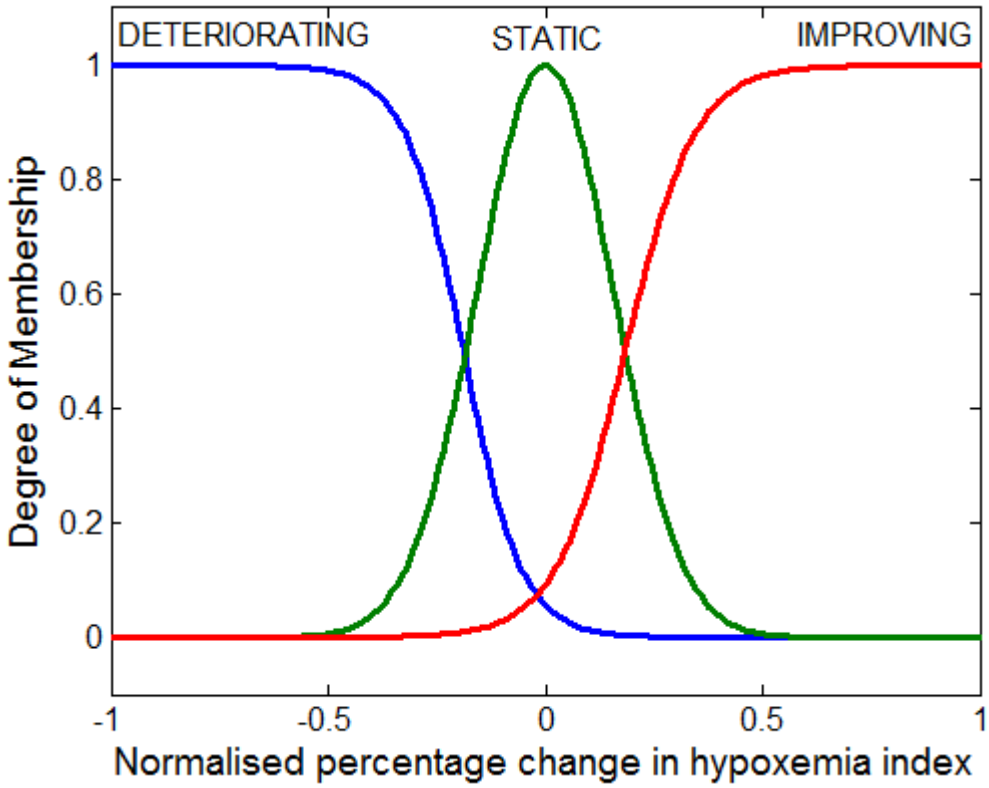

Figure 7.4: Fuzzy membership functions of patient condition described by the normalised percentage change in the hypoxemia index.

7.3.3 FiO2/PEEP fuzzy rule-base derivation

For the FiO2/PEEP sub-unit, the rule bases were provided by the expert clinician based on his experience in changing the ventilator settings. At present, this expert clinician makes decisions on patient's ventilation therapy based on blood gasses and airway pressure-volume graphical waveforms including often the lung condition when further diagnosis of the lung is needed, CT scan is used. For this study, the expert clinician was asked to incorporate the information on the lung condition extracted from the aEIT system (MEEV and regional lung densities) and the information of blood gasses (PaO2 and rate of change of the hypoxemia index) to make decisions on changing the ventilator settings for the two main variables presented in this sub-unit (FiO2 and PEEP). The clinician was given five settings to choose from: i) SMALL

DECREASE (SD), ii) BIG DECREASE (BD), iii) MAINTAIN (M), iv) SMALL INCREASE (SI) and v) BIG INCREASE (BI). Following discussions with this expert clinician, the membership functions for all the settings were selected based on each setting range, as shown in Figure 7.5. The positive and negative signs represent the direction of the settings change (i.e. increase or decrease) and the values represent the quantitative measures of how much such settings should change by. In this case, it has been agreed that the settings change advice for FiO2 and PEEP, should it include ranges of -0.6 to 0.6 and -6 to 6 respectively.

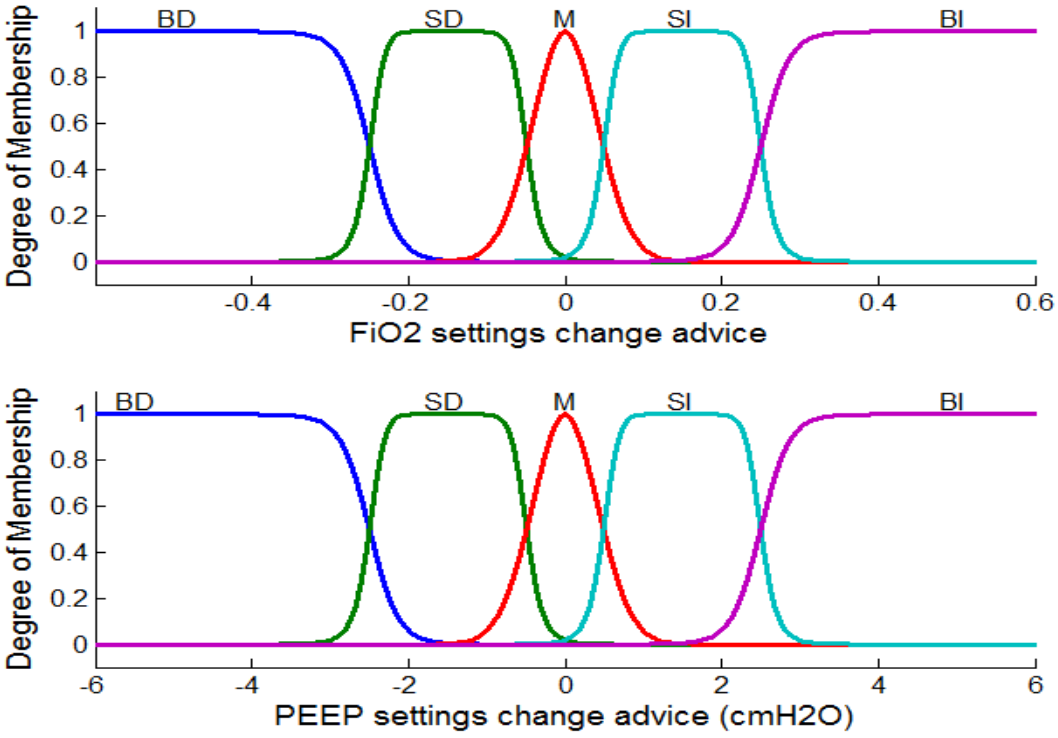

Figure 7.5: Membership functions for advice on changes in FiO2 and PEEP settings.

The clinician experience and know-how were then exploited to generate the consequence of FiO2 and PEEP rules based on the possible combinations of the inputs. Table 7.1 and Table 7.2 show the fuzzy rule-bases provided by the expert clinician for changing of FiO2 and PEEP respectively, encompassing possible AND combinations of the given input fuzzy values.

Table 7.1: The fuzzy rule-bases for the settings changes advice for FiO2 (SI: Small Increase, BI: Big Increase, M: Maintain, SD: Small Decrease, BD: Big Decrease).

PaO2 is LOW		**Patient Condition**		
		Deteriorating	Static	Improving
Lung Condition	Collapsed	BI	BI	SI
	Slightly Collapsed	BI	SI	M
	Moderate	BI	SI	M
	Slightly Overinflated	BI	SI	M
	Overinflated	BI	SI	M

PaO2 is NORMAL		**Patient Condition**		
		Deteriorating	Static	Improving
Lung Condition	Collapsed	BI	M	M
	Slightly Collapsed	SI	M	M
	Moderate	SI	M	M
	Slightly Overinflated	SI	M	M
	Overinflated	SI	M	M

PaO2 is HIGH		**Patient Condition**		
		Deteriorating	Static	Improving
Lung Condition	Collapsed	M	SD	BD
	Slightly Collapsed	M	SD	BD
	Moderate	M	SD	BD
	Slightly Overinflated	M	SD	BD
	Overinflated	M	SD	BD

Table 7.2: The fuzzy rule-bases for the advice on settings changes for PEEP (SI: Small Increase, BI: Big Increase, M: Maintain, SD: Small Decrease, BD: Big Decrease).

PaO2 is LOW		**Patient Condition**		
		Deteriorating	Static	Improving
Lung Condition	Collapsed	BI	BI	SI
	Slightly Collapsed	SI	SI	M
	Moderate	SI	SI	M
	Slightly Overinflated	SI	M	M
	Overinflated	M	SD	BD

PaO2 is NORMAL		**Patient Condition**		
		Deteriorating	Static	Improving
Lung Condition	Collapsed	BI	SI	SI
	Slightly Collapsed	SI	SI	M
	Moderate	SI	M	M
	Slightly Overinflated	SI	M	SD
	Overinflated	M	SD	BD

PaO2 is HIGH		**Patient Condition**		
		Deteriorating	Static	Improving
Lung Condition	Collapsed	BI	SI	SI
	Slightly Collapsed	SI	SI	M
	Moderate	SI	M	M
	Slightly Overinflated	SI	SD	SD
	Overinflated	SD	BD	BD

7.3.3.1 Control of FiO2/PEEP

To achieve the ideal level of PEEP which maximises gas exchange and minimises over-distension remains a challenge. In the work presented by Wang (2008), the proposed advisory system did not provide settings for PEEP because of the unproven SOPAVent model prediction performance on PEEP. In this current work, the rule-base for the PEEP/FiO2 sub-unit is developed with the aim of maintaining PaO2 within the acceptable normal range and also of minimising lung over-distension by incorporating the information about the regional lung function provided by the aEIT system and the information of oxygen level in the blood provided by the blood gasses variables.

To further analyse this control feature, the surface of the fuzzy rule-base for setting PEEP at various PaO2 levels, patient conditions and lung conditions was generated as shown in Figure 7.6. In this case, the PaO2 and patient condition (percentage change in hypoxemia index) are at normalised values, while the lung conditions are represented by the index ranges from (0 to 1). It can be seen that the action of big increase in the PEEP setting will be when the PaO2 is at the low level (0.2 to 0.4), the lung is in a collapse condition (0 to 0.1) and the patient condition is deteriorating (-0.2 to -1). When the lung is in a slightly overinflated region (0.6 to 0.9) and the patient condition is at deteriorating, the advisor will recommend to increase the PEEP slightly so that it will not further inflate the lung. The advice for the big decrease of the PEEP will take place whenever there is an overinflated lung (0.9 to 1), especially when PaO2 is at the high level (0.6 to 1) and the patient is improving (0.4 to 1). The above mentioned actions of the advisor shows that it was designed to be sensitive to the patient's lung condition, especially when the level of oxygen in the blood is certain to be sufficient to the patient and the patient is improving.

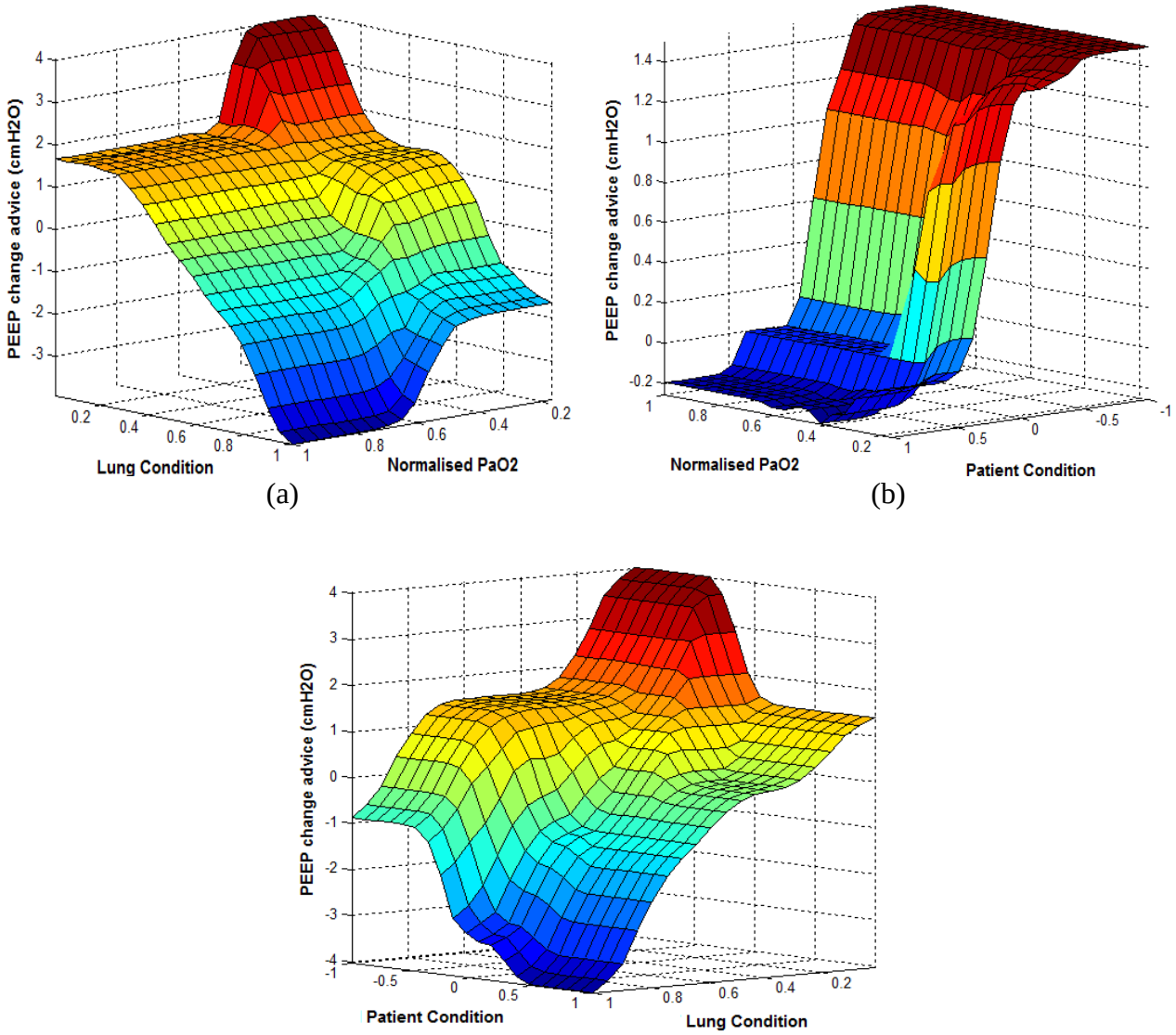

Figure 7.6: The output of the PEEP rule-base: (a) at various PaO2 levels and lung conditions, (b) at different patient conditions and PaO2 levels, and (c) at different lung conditions and patient conditions.

7.4 Development of Pinsp/RR sub-unit

7.4.1 Fuzzy partitions for the inputs and outputs

The main objectives of this sub-unit are to maintain the patient PaCO2 within the acceptable normal range and avoid excessive tidal volume (VT). Therefore, PaCO2 and VT are the two variables that need to be included as the inputs to this sub-unit. Apart from these two variables, information about the lung condition similar to the one described in the FiO2/PEEP sub-unit is also included. The structure of the fuzzy rule-bases in the Pinsp/RR sub-unit is shown in Figure 7.7. The nine (9) primary input variables to this subunit include the PaCO2, tidal volume (VT), MEEV, LLAD, RLAD, LLMD, RLMD, LLPD and RLPD.

The same fuzzy sets were used to represent IMRD, MEEV and lung condition. As for the PaCO2 and VT variables, three (3) fuzzy sets were applied respectively: LOW, NORMAL and HIGH. The ranges of LOW, NORMAL and HIGH for both PaCO2 and VT variables were determined based on the clinician's expert knowledge and shown in Table 7.3. Both PaCO2 and VT were normalised in the range [0 1]. For the consequent layer, five (5) sets were assigned which were also similar to the one used in FiO2/PEEP subunit: SLIGHT INCREASE (SI), BIG INCREASE (BI), MAINTAIN (M), SLIGHT DECREASE (SD) and BIG DECREASE (BD). These fuzzy sets correspond to the actions needed to be taken with respect to the Pinsp and RR settings. The output member with the maximum membership value was then chosen as the final output.

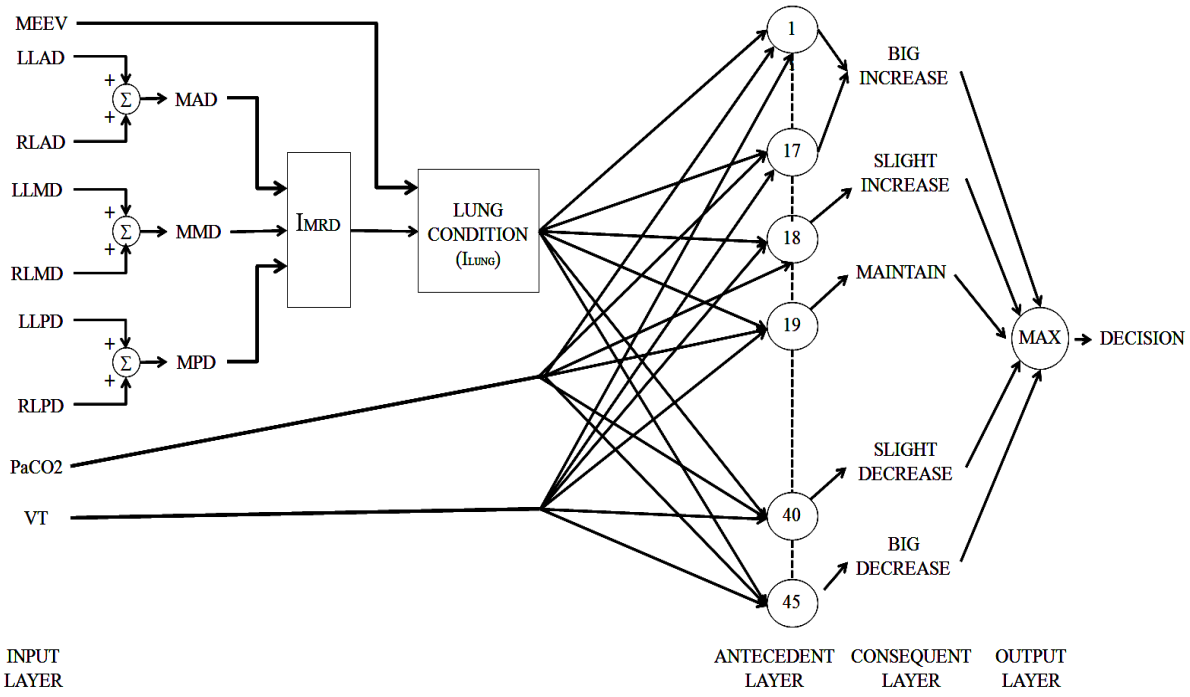

Figure 7.7: Structure of the fuzzy rule-base for Pinsp/RR subunit.

Table 7.3: Ranges of fuzzy set LOW, NORMAL and HIGH for PaCO2 and VT variables.

	RANGES	
	PaCO2 (kPa)	**VT (ml/kg)**
LOW	<4	<7
NORMAL	[4 8]	[7 9]
HIGH	>8	>9

7.4.2 Parameters for the fuzzy input membership functions

For Pinsp/RR sub-unit, the inputs which differ from the FiO2/PEEP sub-unit are the PaCO2 and VT. For these two variables, the fuzzy membership functions were derived from the knowledge given by the expert clinician. Sigmoidal membership functions were used for LOW and HIGH, whereas Gaussion membership functions was used for fuzzy set NORMAL as shown in Figures 7.8 and Figure 7.9.

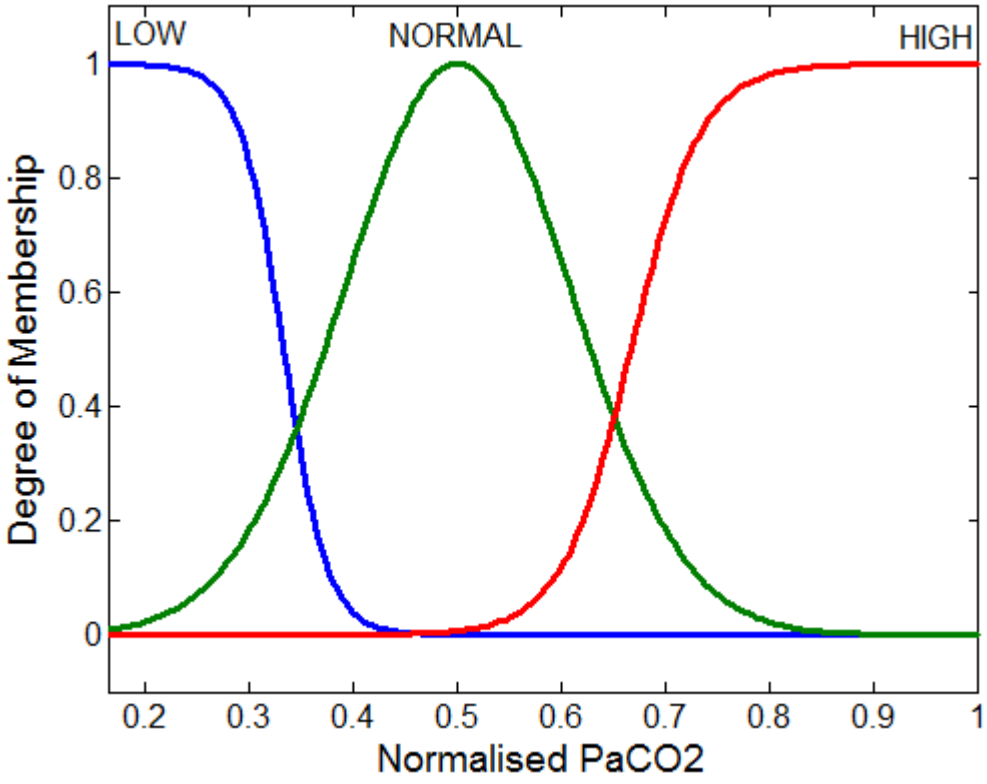

Figure 7.8: Fuzzy membership functions for the normalised PaCO2.

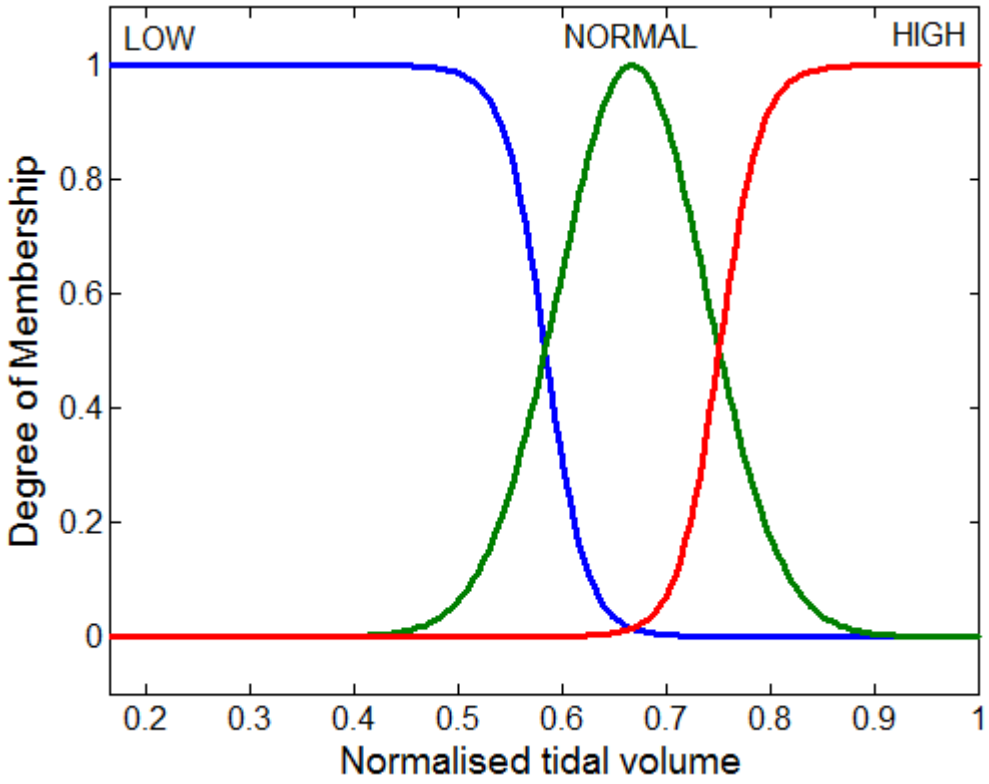

Figure 7.9: Fuzzy membership functions for the normalised tidal volume.

7.4.3 Pinsp/RR fuzzy rule-base derivation

The expert clinician's knowledge and experience in changing the Pinsp and RR are also exploited here to derive the fuzzy rule-base for this sub-unit. For this study, the expert clinician needs to consider information on the lung condition extracted from the aEIT system (MEEV and regional lung densities), the information of blood gas (PaCO2) and the tidal volume (VT) to make decisions on changing the Pinsp and RR. The expert clinician was given five settings to choose from: i) SMALL DECREASE (SD), ii) BIG DECREASE (BD), iii) MAINTAIN (M), iv) SMALL INCREASE (SI) and v) BIG INCREASE (BI). Following discussions with the clinician, membership functions for all the settings are drawn based on each setting range decided as shown in Figure 7.10.

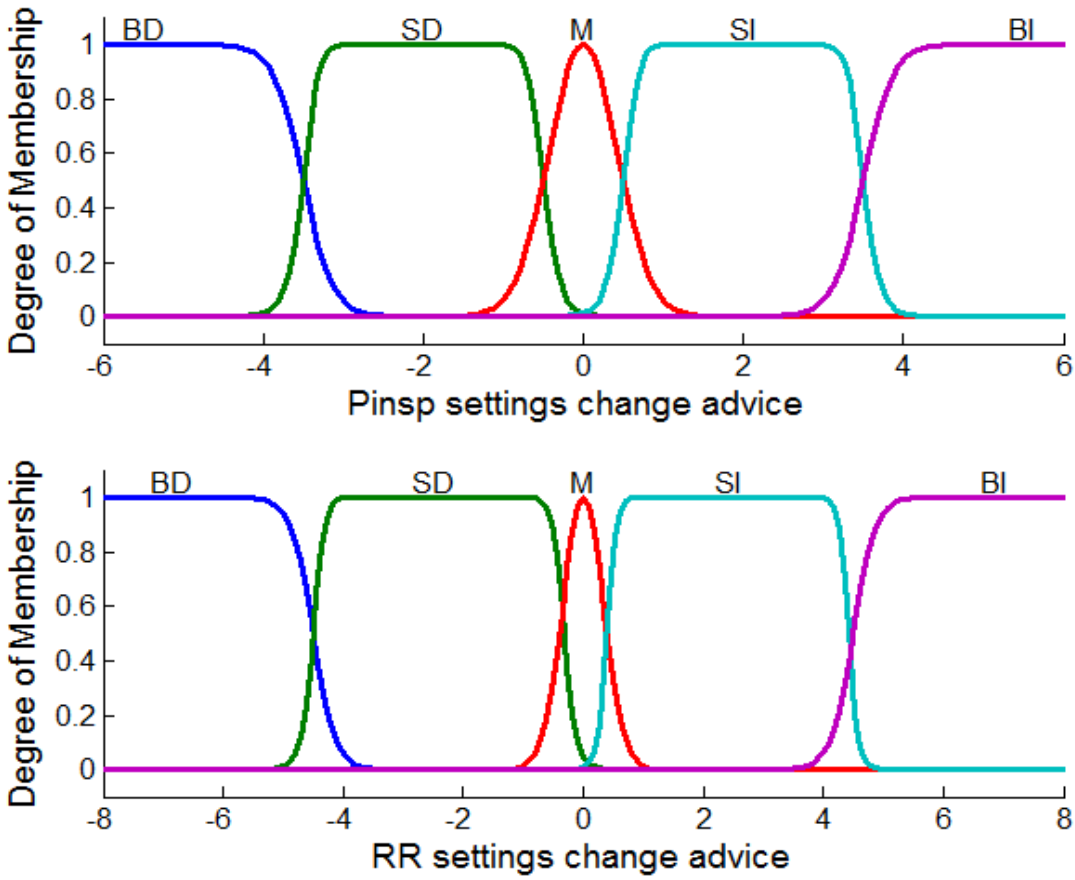

Figure 7.10: Membership functions for advice on changes in Pinsp and RR settings.

Table 7.4 and **Table 7.5** show the fuzzy rule-bases provided by the expert clinician for changing of Pinsp and RR respectively, encompassing possible AND combinations of the given input fuzzy values.

Table 7.4: The fuzzy rule-bases for advice on the settings changes for Pinsp (SI: Small Increase, BI: Big Increase, M: Maintain, SD: Small Decrease, BD: Big Decrease).

PaCO2 is LOW		Tidal Volume (VT)		
		Low	Normal	High
Lung Condition	Collapsed	SI	SI	M
	Slightly Collapsed	SI	M	M
	Moderate	SD	SD	SD
	Slightly Overinflated	SD	SD	BD
	Overinflated	SD	BD	BD

.

PaCO2 is NORMAL		Tidal Volume (VT)		
		Low	Normal	High
Lung Condition	Collapsed	BI	SI	M
	Slightly Collapsed	BI	SI	M
	Moderate	SI	M	SD
	Slightly Overinflated	M	M	SD
	Overinflated	M	SD	SD

PaCO2 is HIGH		Tidal Volume (VT)		
		Low	Normal	High
Lung Condition	Collapsed	BI	BI	SI
	Slightly Collapsed	BI	SI	SI
	Moderate	BI	SI	SI
	Slightly Overinflated	SI	SI	M
	Overinflated	SI	SI	M

Table 7.5: The fuzzy rule-base for the advice on settings changes for RR (SI: Small Increase, BI: Big Increase, M: Maintain, SD: Small Decrease, BD: Big Decrease).

PaCO2 is LOW		**Tidal Volume (VT)**		
		Low	Normal	High
Lung Condition	Collapsed	SI	M	M
	Slightly Collapsed	M	M	SD
	Moderate	SD	SD	SD
	Slightly Overinflated	SD	SD	BD
	Overinflated	SD	BD	BD

PaCO2 is NORMAL		**Tidal Volume (VT)**		
		Low	Normal	High
Lung Condition	Collapsed	M	M	SI
	Slightly Collapsed	M	M	SI
	Moderate	M	M	M
	Slightly Overinflated	M	M	SD
	Overinflated	M	SD	SD

PaCO2 is HIGH		**Tidal Volume (VT)**		
		Low	Normal	High
Lung Condition	Collapsed	SI	BI	BI
	Slightly Collapsed	SI	BI	BI
	Moderate	M	SI	SI
	Slightly Overinflated	M	M	SI
	Overinflated	SD	SD	M

7.4.3.1 Control of Pinsp/RR

In the Pinsp/RR sub-unit, the information of 'Lung Condition' seems to be the check and balance in arriving at the decision of changing the Pinsp and RR settings. The objectives of this sub-unit are to maintain the patient PaCO2 within the acceptable normal range and avoiding excessive VT. To further analyse this control feature, examples from the 3-D-surface of the fuzzy-rule base for control of Pinsp were generated. Figure 7.11 shows the outputs of the advice for setting Pinsp at various PaCO2 levels, VT and lung conditions. In this case, PaCO2 and VT are at normalised values, while lung conditions are represented by the index ranges from (0 to 1). .

It can be seen that when VT is at high level (>0.8), PaCO2 is between low and normal [0.2 0.65] and the lung condition is between slightly overinflated and overinflated [>0.6], the clinician will either decrease the Pinsp setting slightly or big to ensure that the VT is not too large. This is crucial because if the patient is experiencing an overinflated lung, a large VT may cause the patient's lung to have volutrauma (Neligan, 2002). Whereas the action of slightly or big increase of the Pinsp setting mostly takes place when the PaCO2 is at high level [>0.8], the lung is at a collapsed or at a slightly collapsed condition [<0.4] and VT is at a low level [<0.5]. This action avoids an excessive amount of CO2 in the patient's blood.

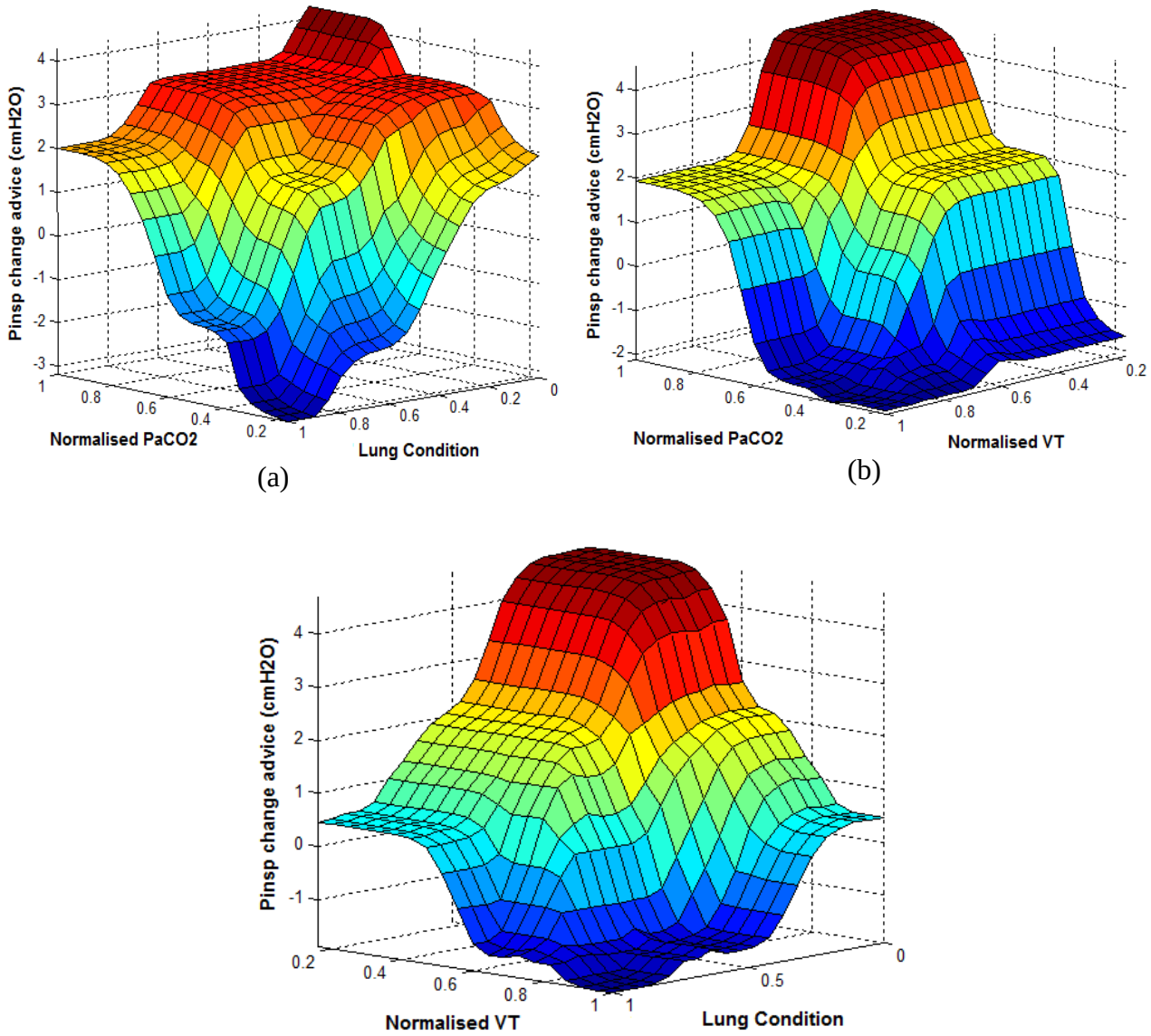

Figure 7.11: The outputs of the Pinsp rule-base: (a) at various PaCO2 levels and lung conditions, (b) at different PaCO2 levels and VT levels (c) at different VT levels and lung conditions.

7.5 Closed-loop validation of the decision support system via simulations of the hybrid aEIT-SOPAVent models

The aim of this closed-loop validation is to evaluate the EIT-based decision support system's ability to deal with different patient's scenarios that may occur in the actual clinical environment and to investigate whether the system can produce consistent performances on achieving the optimal compromise between the various competing goals. In this validation, the previously developed extended version of SOPAVent model (Goode, 2001; Wang, 2007) is employed to represent the simulated patient and predicts the values of blood gasses. Values for aEIT system variables (MEEV, MAD, MMD and MPD) were predicted using various ANFIS models which developed beforehand (see Chapter 6) to elicit the relationships between these variables with the ventilator parameters (PIP, PEEP, RR) and the blood gases parameter (PaO2/FiO2). The structure of the system's simulation is shown in Figure 7.12. All simulations run under the MATLAB environment.

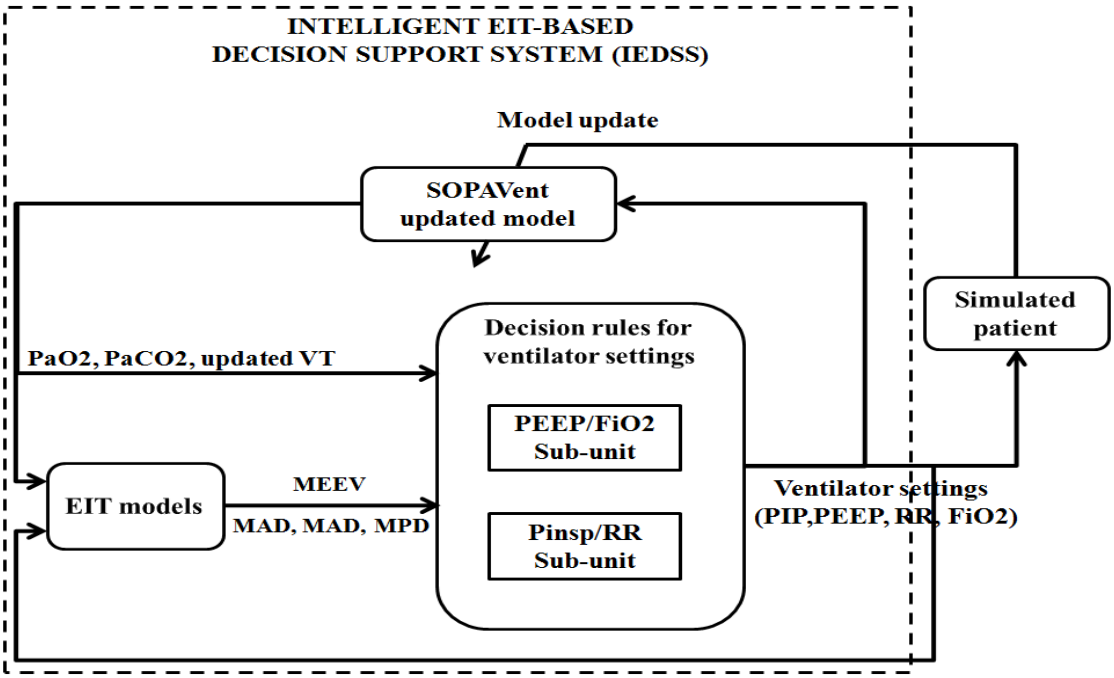

Figure 7.12: The general structure of the IEDSS.

7.5.1 Overview of SOPAVent model

SOPAVent (Simulation of Patients under Artificial Ventilation) was developed initially to provide simulated closed-loop validation of a prototype expert system (Goode, 2001). The model represents the exchange of O2 and CO2 in the lungs and tissues together with their transport through the circulatory system based on respiratory physiology and mass balance equations. The model uses a compartmental structure (Figure 7.13), where the circulatory system is represented by lumped arterial, tissue, venous and pulmonary compartments. The lung is sub-divided into three compartments:

a) An ideal alveolus compartment, where all gas exchanges take place with a perfusion-diffusion ratio of unity.
b) A dead space compartment representing lung areas that are ventilated but not perfused.
c) A shunt compartment that is a fraction of cardiac output, representing both anatomical shunts and lung areas that are perfused but not ventilated.

(The details of the model equations are described in the Appendix A of this thesis.)

SOPAVent is designed to provide steady-state blood gases predictions for totally ventilated and relatively stable patients. The inputs of the model are the ventilator settings (FiO_2, PEEP, PIP, RR, T_{insp}) and the outputs are the arterial pressures PaO2 and PaCO2. The dynamic relationship between the inputs and the outputs depends on the model parameters and constants. The model parameters are patient-specific and the model can therefore be matched to each patient provided the parameters are known. These parameters include patient's age, gender, weight and height, body temperature, haemoglobin level (Hb), arterial pH, bicarbonate concentration, respiratory quotient, tidal volume, cardiac output (CO), oxygen consumption (VO2), carbon dioxide production (VCO2), shunt and relative dead space (Kd).

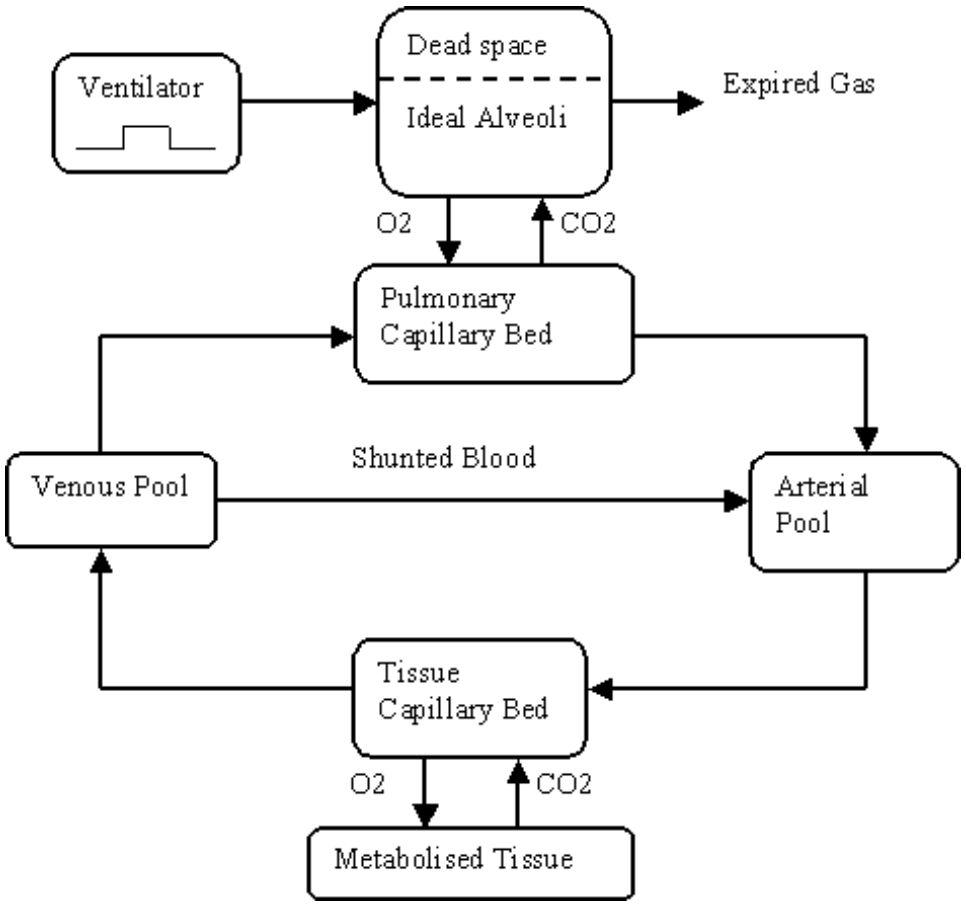

Figure 7.13: Schematic diagram of the SOPAVent model [Goode, 2001].

In the early development stages of SOPAVent, some of the parameters were readily available as part of routine clinical measurements and some parameters were not, namely the shunt, dead space, VCO2, VO2 and CO, hence leading to problems during model validation. Apart from this, invasive measurements were used to obtain some of the parameters such as VCO2, VO2 and CO, which had led to uncertain and inaccurate predictions of the blood gases (Goode, 2001). Therefore, in 2003 this original version of SOPAVent had been improved and these invasive parameters had been derived non-invasively using a mean population method and the shunt and dead space were derived by tuning the model. However, the tuning was found to be time-consuming and sometimes no results would be established due to the non-convergence of the optimisation algorithm (Kwok, 2003). Recently, significant

improvements have been made on the SOPAVent in order to increase the performance and use it as the core of an adaptive decision support system for mechanical ventilation management (Wang, 2008). New estimation methods for the following model parameters: relative dead space (Kd), Tidal Volume (VT), VCO2 as well as shunt have been made available within the model hence rendered the new SOPAVent a totally non-invasive model. This new version of SOPAVent is also able to represent the patient state accurately and will as a result lead to a good blood gasses prediction by continuously updating the five key model parameters (Shunt, Kd, VCO2, VO2 and airway resistance (Raw)) based on the continuous measurements from ICU. By defining different parameter data changing scenarios, the model can be exploited as a patient simulator which can be used for testing any newly designed decision support system (Wang *et al*., 2006; Wang *et al*., 2007).

7.5.2 Validation method

In the actual clinical environment, the patient's clinical condition may deteriorate or improve over time. Therefore, in this assessment, the performance of the intelligent EIT-based decision support system (IEDSS) was evaluated within different clinical scenarios under two (2) simulation conditions:

i) An acute increase in shunt and then returns to the baseline level after approximately 2 h.

ii) An acute increase in Kd and then returns to the baseline level after approximately 2 h.

In this simulation, the IEDSS generates ventilator settings advice for FiO2, PEEP, Pinsp and RR every thirty-minute (30 min). The simulated patient parameters were changed according to the designed scenario and at every thirty-minute (30 min) interval; the simulated patient data (PaO2, PaCO2, VT, ventilator settings) were input to the system to update the patient model and the EIT models. The derived ventilator

settings were then input to the simulated patient to simulate the patient states in the next thirty-minute (30 min). Each simulation lasted about four and a half (4.5) hours and started with a thirty-minute (30 min) period of stabilisation where the simulated patient's ventilator settings were maintained at the initial values.

A total of ten (10) ICU patient data sets were used to reproduce the initial patient state in the simulated scenario for successive validation of the IEDSS. The demographic information of the ten patients is summarised in Table 7.6.

Table 7.6: The demographic information of the ten ICU patients.

Patient	Gender	Age	Weight (kg)	Height (cm)
1	M	66	68	175
2	M	68	57	173
3	M	40	71	164
4	F	28	68	176
5	M	66	68	175
6	M	47	66	165
7	M	42	65	175
8	M	53	66	172
9	F	66	56	165
10	F	66	60	165

7.5.3 Validation results and discussions

One patient's results are shown in Figure 7.14 and Figure 7.15 (further patients' closed-loop simulation results are included in the Appendix B of this thesis). These results were obtained from a 66 year old female patient with a weight of 60 kg and a height of 165 cm. Figure 7.14 shows the results of the patient's state and the ventilator settings which were changed when the patient shunt is increased from 15% to 21% in a thirty (30)-minute period and returned to the baseline after approximately two (2) hours. The increase of shunt led to a reduction in PaO2 from 12kPa to 8kPa. Thereafter, the IEDSS responded correctly by increasing FiO2 from 0.5 to 0.63 and PEEP was increased from 7 cmH2O to 9 cmH2O. This, in turn, led to an increased PaO2 back to 11kPa which is within the normal range (10kPa to 14kPa). Increasing the shunt also triggered a slight increased in PaCO2 from 6kPa to 7kPa. During this condition, the Pinsp/RR sub-unit in the IEDSS responded by increasing the Pinsp from 14cmH2O to 15cmH2O and RR from 20breath/min to 22breath/min and as the result, PaCO2 was decreased to 6.2kPa after 30-minute.

As the shunt was reduced from 21% to 15% in the 30-minute period one and a half hour later, the patient PaO2 was increased from 11kPa to 23kPa and the PaCO2 was decreased from 6kPa to 5kPa. In detecting this change, the IEDSS responded correctly by reducing FiO2 from 0.63 to 0.47 and PEEP from 9cmH2O to 5cmH2O in order to restore PaO2 back to its normal range. To increase the PaCO2, the IEDSS has also reduced the Pinsp from 15cmH2O to 13cmH2O and RR from 22breath/min to 19breath/min.

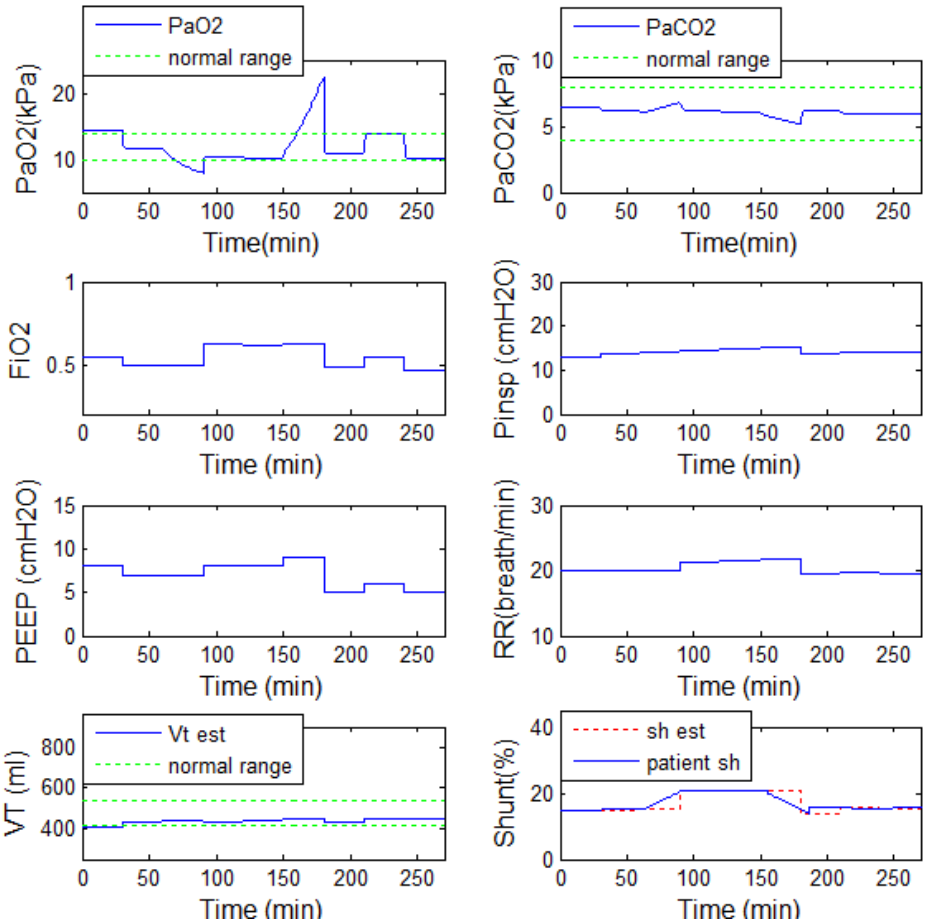

Figure 7.14: Simulation of an acute shunt changes.

Figure 7.15 shows the results corresponding to simulations of the patient with an acute change in the relative dead-space (Kd). In this simulation, Kd was increased from 0.32 to 0.47 in a thirty-minute (30 min) period and returned to the baseline after approximately two (2) hours. The increase in Kd has led to a rise in PaCO2 from 6.05kPa to 7.36kPa. Due to this increase, the IEDSS responded by increasing Pinsp from 14cmH2O to 16cmH2O and RR from 20breath/min to 22breath/min. Approximately one and a half hour later (1.5h), the Kd was reduced from 0.47 back to the baseline in the 30-minute period. The patient's PaCO2 was seen to drop from 6.79kPa to 5.45kPa, which was still within the normal range (4kPa to 8kPa). The IEDSS responded by reducing both Pinsp and RR gradually. The changes of Pinsp and RR made by the IEDSS were enough to keep the PaCO2 value within the normal range.

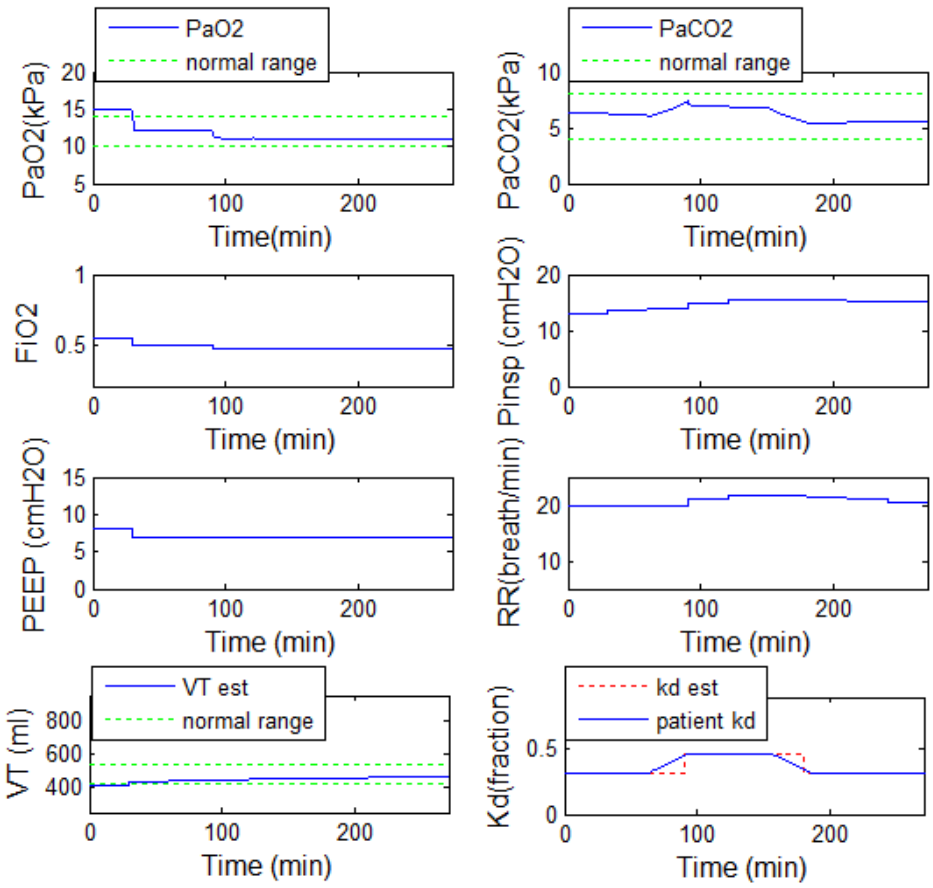

Figure 7.15: Simulation of an acute Kd changes.

Apart from the qualitative study to evaluate the system's performance, a quantitative approach has also been implemented to assess the ability of the IEDSS to keep the blood gasses within the acceptable limit. The percentage time of the simulated patients' PaO2, PaCO2 and VT that appeared to be out of the normal range during the acute change of shunt and Kd was chosen as the performance index. In this analysis, the first thirty (30) minutes of the simulation results are excluded because they were considered to be within patient stabilisation period. The ten (10) simulated patient results are summarises in Table 7.7 and Table 7.8.

Table 7.7: Performance index for the ten simulated patients with acute changes in the shunt**.**

Patient	% Time out of range		
	PaO2	**PaCO2**	**VT**
1	14.40	0	0
2	38.52	0	0
3	25.19	0	0
4	28.52	0	0
5	14.07	0	0
6	25.93	0	0
7	12.96	0	0
8	13.33	0	11.11
9	26.30	0	0
10	13.33	0	0

Table 7.8: Performance index for the ten simulated patients with acute changes in the Kd.

Patient	% Time out of range		
	PaO2	**PaCO2**	**VT**
1	0	0	0
2	0	14.4	0
3	0	0	0
4	0	0	0
5	0	0	0
6	0	19.3	0
7	0	0	0
8	0	2.96	11.11
9	0	0	0
10	0	0	0

It can be seen from the tables that the IEDSS is able to generate satisfactory ventilator settings advice to manage the patients with different clinical scenarios with the average percentage of PaO2 and PaCO2 being out of range being only about 21% and 2% respectively. According to the expert clinician, the most important aspect to consider in these simulations is the final value of PaO2, PaCO2 and VT (at the end of each simulation). These values need to be within their acceptable normal range at the end of each simulation as one of the performance indexes to show that the IEDSS is able to keep the blood gasses and the VT within the acceptable limit. Table 7.9 shows the ranges for normal PaO2, PaCO2 and VT and Table 7.10 and Table 7.11 show the values for PaO2, PaCO2 and VT at the end of each simulation in all ten (10) patients.

Table 7.9: Ranges for NORMAL PaO2, PaCO2 and VT variables.

	Ranges		
	PaO2 (kPa)	**PaCO2 (kPa)**	**VT (ml/kg)**
NORMAL	[10 14]	[4 8]	[7 9]

Table 7.10: Values of PaO2, PaCO2 and VT at the end of simulation of an acute shunt change.

Patient	**PaO2 (kPa)**	**PaCO2 (kPa)**	**VT (ml/kg)**
1	10.5	5.91	8.12
2	10.0	7.23	8.56
3	10.7	7.81	9.00
4	10.0	5.85	7.94
5	11.0	5.92	8.04
6	10.5	6.12	9.00
7	12.1	6.15	8.62
8	13.6	6.11	8.27
9	10.0	6.33	7.95
10	10.0	5.97	7.52
Average	**9.84**	**6.34**	**8.30**

Table 7.11: Values of PaO2, PaCO2 and VT at the end of simulation of an acute Kd change.

Patient	PaO2 (kPa)	PaCO2 (kPa)	VT (ml/kg)
1	11.7	5.64	8.13
2	10.0	7.66	9.0
3	11.0	6.90	9.0
4	11.9	6.56	7.90
5	11.1	5.75	8.12
6	13.5	7.43	7.26
7	12.0	5.49	8.54
8	12.5	5.81	8.27
9	11.2	6.50	8.61
10	11.0	5.59	7.70
Average	**10.3**	**6.33**	**8.25**

From these tables it can be seen that all PaO2, PaCO2 and VT values are within the normal range at the end of both simulations, which means that not only the IEDSS can generate good advice for the ventilator settings but it is also able to manage the patients to be within the desirable conditions.

Another important feature of this IEDSS that makes it different with other decision support systems hitherto reported in the literature is its ability to provide information about the regional lung functions. MEEV is one of the aEIT extracted parameters that is commonly affected by changes of PEEP (Michelete *et al*., 2005). Figure 7.16 shows the results from one of the simulated patients comparing the MEEV prediction which are based on the previous developed intelligent model-based decision support system (Wang, 2008) advice on the ventilator settings and the current IEDSS during simulation of an acute change in shunt.

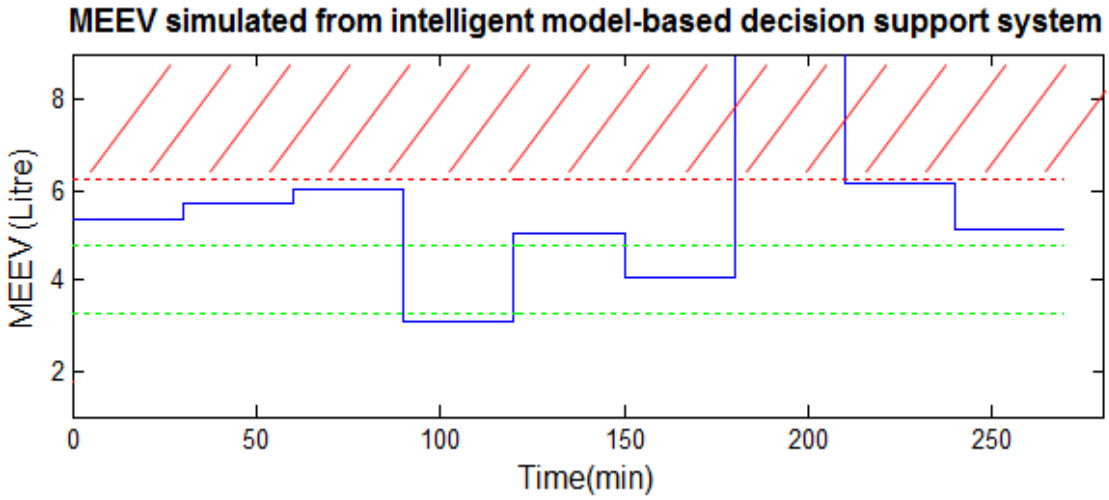

(a)

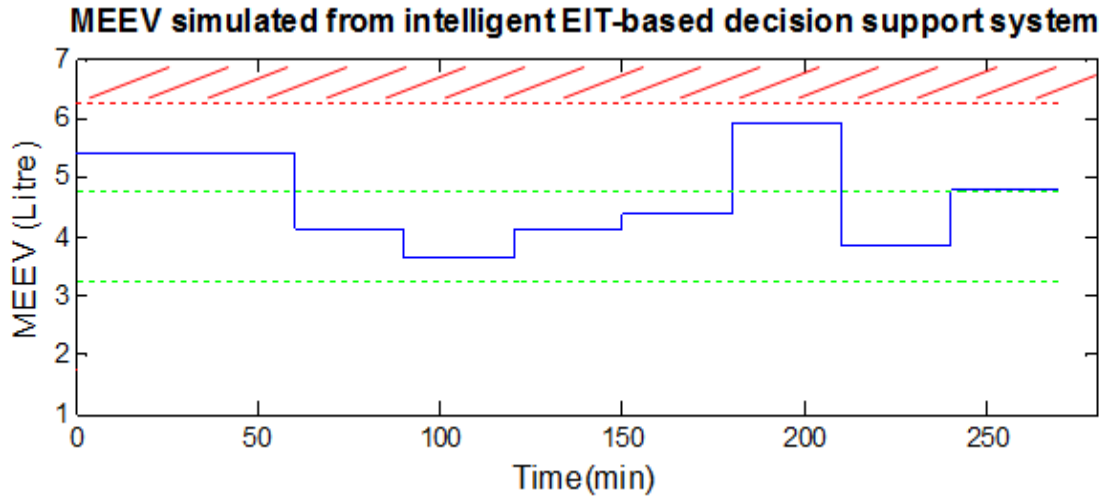

(b)

Figure 7.16: MEEV changes during an acute change of shunt (a) MEEV from the intelligent model-based decision support system (Wang, 2008) (b) MEEV from the IEDSS; The red stripes and dotted lines represent the overinflated region and the green dotted lines represent the normal region. The region between the green dotted and the red dotted lines represent the slightly overinflated region.

The ranges highlighted in the Caption of Figure 7.16 were first obtained from the study of EIT ventilated patients in the ICU. According to the expert clinician, these ranges are believed to be the common ranges found from the EIT ventilated patients.

The normal range values for this MEEV however were obtained from patients who were involved in a single lung ventilation using the aEIT system as described in detail in Chapter 5. Table 7.12 shows the ranges for MEEV represented by five regions: collapsed, slightly collapsed, normal, slightly overinflated and overinflated.

Table 7.12: MEEV ranges.

Regions	**MEEV ranges (litres)**
Collapsed	≤ 1.75
Slightly collapsed	$1.75 < MEEV < 3.25$
Normal	$3.25 \leq MEEV < 4.75$
Slightly overinflated	$4.75 \leq MEEV < 6.25$
Overinflated	≥ 6.25

In the clinical scenario, as shunt decreases, MEEV will increase resulting in an improvement in patient's oxygenation (Michelete *et al.*, 2005; El-Khatib and Jamaleddine, 2004). However, a very high MEEV is unfavourable in a real clinical situation because the lung will be overinflated and hence will increase the risks of lung injuries. As one can see from Figure 7.16 (a) and (b), MEEV tends to increase at the point when the shunt is decreased but with a different magnitude. Figure 7.16 (a) shows a higher MEEV value as compared to Figure 7.16 (b). To further support this result, a quantitative analysis has been conducted with the percentage time in the overinflated region being chosen as the performance index.

Table 7.13 shows the results of this analysis for the ten (10) simulated patients. It can be seen that with IEDSS, MEEV, which represents the lung of the patient, includes a profile that has a minimal time in the overinflated region with the average percentage time of 6.67%. However, the performance of the model-based advisory system that

does not include the knowledge of regional lung function in the decision making process, shows a higher percentage time of MEEV in the overinflated region, which is approximately 26%.

Table 7.13: The performance index for the ten simulated patients derived from the model-based advisory system and IEDSS during an acute change of the shunt.

Patient	**% Time that lungs in the overinflated region**	
	IEDSS	**Model-based**
1	0	11.11
2	0	33.33
3	11.11	33.33
4	11.11	33.33
5	0	0
6	22.22	33.33
7	11.11	55.55
8	0	33.33
9	11.11	11.11
10	0	11.11
Average	**6.67**	**25.55**

(Further patients' closed-loop simulation results are included in the Appendix B of this thesis.)

7.6 Summary

In this Chapter, a clinically significant intelligent EIT-based decision support system (IEDSS) which focuses the information of blood gases and regional lung functions derived from a respiratory physiology model of SOPAVent and ANFIS-based data-driven models has been designed to provide advice for ventilator settings, i.e. FiO2, PEEP, Pinsp and RR. The IEDSS incorporates expert knowledge with a fuzzy inference system in the analysis of physiological parameters and therapy determination. Based on the designed virtual patients, the IEDSS is validated via simulations of ramped increases and decreases in shunt and Kd. In all simulated scenarios, IEDSS has shown the ability to generate good advice for the ventilator settings and also to keep the patients' blood gases and other controlled parameters within the desired limits. Another important feature that makes IEDSS distinct from other current decision support systems is its ability to provide information about the regional lung functions. With IEDSS, MEEV, which represents the lung of the patient, leads to a profile that includes a minimal time in the overinflated region as compared to the previously developed model-based advisory system (Wang, 2008). All in all, IEDSS has shown that it can adapt to the patient state changes and respond correctly to achieve not only an overall optimal ventilatory therapy but to also minimise the risks of lung injuries in ICU patients.

CHAPTER 8

CONCLUSIONS AND FUTURE WORK

In the previous Chapters, research work on calibration and improvement of the aEIT system as well as development of the aEIT associated models and intelligent EIT-based decision support system (IEDSS) for critically-ill ventilated patients in ICU were presented. The hybrid aEIT-SOPAVent model had also been introduced to validate the IEDSS performance. In this Chapter, the achievements of this project will be reviewed first, which will be followed by discussions and recommendations of future work and directions for the research. Figure 8.1 depicts the overall summary of work done throughout the completion of this project.

8.1 Project achievements

8.1.1 Comparative study on healthy volunteers leads to calibration and improvement of aEIT system

EIT is a considerably new monitoring technique with the potential to becoming a valuable bedside tool for the assessment of lung regional ventilation distribution and the continuous guidance towards appropriate settings of mechanical ventilation for critical-ill patients in the ICU. Absolute measurements of lung resistivity and the resulting calculations of lung volumes are new developments in EIT research as most of the previous work has relied upon the assessment of impedance change relative to a baseline measurement.

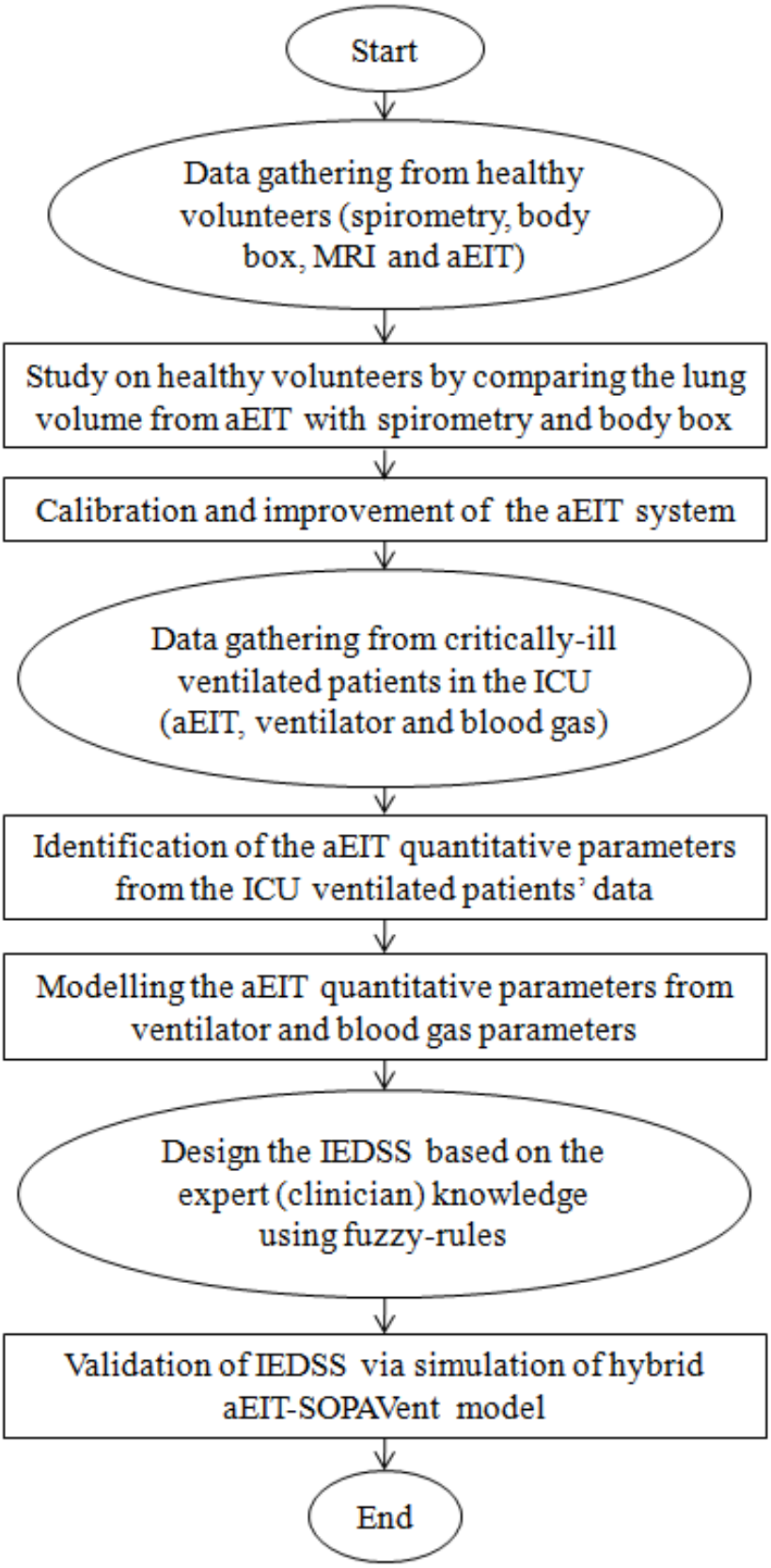

Figure 8.1: The overall structure of the research work.

The Sheffield Mk 3.5 absolute EIT system (aEIT) provides the potential to continuously monitor ventilation in or close to real-time on medium and long-term bases. The current system which uses 8 electrodes is easy to setup and is therefore an ideal candidate to gain acceptance in a clinical environment. Prior to its utilisation within the decision support system, a series of calibrations and improvements has been carried-out to enhance the accuracy and consistency of the estimated absolute lung volume and resistivity. In this thesis, a study involving, spirometry, body plethysmography (body box) measurements and MRI scans, was conducted on a population of healthy subjects to assess and redefine new zones of interest for the lungs, taking into account the individual body size, thoracic shape and gender.

The previous aEIT study on healthy volunteers included some limitations in terms of the small number of volunteers (only 8 males) involved and the only one position for the patients was considered (sitting) (Panoutsos *et al*., 2007). Therefore, a further study on healthy volunteers has been conducted in this thesis by considering more subjects (8 males and 4 females) with two different positions (sitting and supine). Based on the inputs from the expert clinician, these positions were considered because they are deemed to represent the most common positions adopted by patients in the ICUs. Results from the comparative study have shown that the previous version of the aEIT software (version 1.047) has the ability to measure lung volume of the healthy volunteers but with a range of errors especially when the subjects were in the supine position. In most of the measured lung volumes, aEIT tended to produce over-estimated values, which in this case were hypothesised as being triggered by the use of one fixed region of interest in the previous version of aEIT software (version 1.047) to estimate the absolute lung resistivity and volume. It is worth emphasising that this study had led to the new findings which demonstrate that the previous aEIT software (version 1.047) still needs to be further improved and validated in order for it to be used as a routine clinical tool.

The multiple region of interests (ROIs) were then developed based on the study of MRI scans of healthy subjects. The algorithm to choose a suitable ROI to be used in the calculations of absolute lung resistivity and volume was introduced together with the new sub-ROIs for estimation of regional lung ventilations. Indeed, the improved aEIT software (version 1.049) had shown a better accuracy in both spirometry and body box studies as compared to the old version of aEIT software. However, there is still room for improvements of the aEIT software, which will lead to new opportunities for research in the area of validating and improving the accuracy and consistency of the aEIT estimation of lung volume and as a result making the system suitable for clinical use.

8.1.2 aEIT clinical trials on critically-ill ventilated patients in the ICU

Another significant study performed in this thesis is the study of aEIT clinical trials on critically-ill ventilated patients in the ICU. From the current literature it transpired that the issue of PEEP settings remains a matter of great debate and there is still active research focusing on determining the 'ideal' PEEP settings for treatment of critically-ill ventilated patients. In the clinical trials from this study, the improved aEIT system (software version 1.049) was used to reflect the PEEP settings-induced changes on the aEIT quantitative parameters identified as being the mean end-expiratory lung volume (MEEV), mean tidal volume (MVT), mean arterior density (MAD), mean middle density (MMD) and mean posterior density (MPD). Relationship between aEIT quantitative parameters and ratio of arterial partial pressure of oxygen to fraction of inspired oxygen (PaO2/FiO2) were also studied. In this study, aEIT had shown the ability to quantitatively assess different conditions of the lung during mechanical ventilation in critically-ill patients induced by changes in PEEP settings. This is opposed to functional EIT (fEIT) that relies upon the assessment of impedance change relative to a baseline measurement and not the absolute value. Increasing PEEP has led to improved regional lung ventilation which was reflected in the values of aEIT

quantitative parameters, i.e. MEEV, MAD, MMD and MPD. The PaO2/FiO2 ratio however was found to provide only a global information about the patients' ventilation, while the regional densities given by MAD, MMD and MPD did have the potential to provide information about the regional lung ventilation distribution. Comparisons between tidal volume (VT) provided by the ventilator and VT calculated by the improved aEIT system revealed that the improved system is able to provide a good estimation of VT readings in ventilated patients. All in all, this study had shown that the improved aEIT system is capable of providing not only information on the overall lung volume but also on the regional lung ventilation distribution and when combined with PaO2/FiO2 ratio, it is foreseen that such information should be able to lead to a better understanding of the phenomena surrounding ventilated patients in order to assist clinicians in decision-making and consequently guide ventilator therapy.

8.1.3 Quantitative models for aEIT

The idea of modelling the aEIT quantitative parameters (i.e MEEV, MAD, MMD and MPD) from ventilator and blood gas parameters was introduced in this thesis with the intention to successfully replicate the behaviour of ventilated patients with EIT. This work is believed to be the first data-driven model developed to describe the behaviour of ventilator settings-induced changes in aEIT quantitative parameters for critically-ill ventilated patients. Despite using a limited amount of data to elicit such models, they were nevertheless able to show a very good agreement between the real data and the model predictions. In this work, PEEP, PIP and PaO2/FiO2 ratio were used as the inputs for MEEV model, while PEEP, PaO2/FiO2 ratio and RR were chosen as the inputs for MAD, MMD and MPD models. All the inputs were chosen based on discussions with the expert clinician and the correlation analyses performed.

8.1.4 Development and assessment of the intelligent EIT-based decision support system (IEDSS)

The developed ANFIS-based aEIT quantitative models in combination with a totally non-invasive and continuously updated blood gas model of ventilated patients (SOPAVent), has provided information on regional lung functions and blood gases respectively to form the basis for both design and evaluation of the intelligent EIT-based decision support system (IEDSS) for critically-ill ventilated patients in ICU. The main objectives of this decision support system were to maximise gas exchange and minimise over-distension of the lung by optimising the ventilator settings based on the patients' blood gases information, measured or set ventilator parameters and information on lung conditions provided by aEIT. In realising this, two sub-units were considered: i) PEEP/FiO2 and ii) Pinsp/RR, which affect patients' oxygenation and PaCO2 levels respectively. The IEDSS had incorporates the expert knowledge (clinician) with a fuzzy inference system in the analysis of physiological parameters and therapy determination. Based on the designed virtual patients and simulated scenarios, IEDSS had shown the ability to generate good advice for the ventilator settings and keeping the patients' blood gases and other controlled parameters within the desired clinical limits. From the results, the developed IEDSS had achieved not only an overall optimal ventilatory therapy but has the potential to minimise the risks of lung injuries in the patient.

8.2 Recommendations for future work

Indeed, the work involved in this project includes some limitations that need to be addressed and improve in the near future. In the study of healthy volunteers, the population number studied has to be increased, especially for female subjects, in order for the aEIT system to cope better with a wider range of subject sizes and shapes. Similarly for the study on the ICU ventilated patients, where more data are needed to verify the findings that have been outlined previously in this research. It would also

be beneficial to include more patients that have the CT scan images in the study so that a comparison between the aEIT recorded data (i.e. the regional lung densities) and the CT scan images can be carried-out to determine how well the aEIT detects the regional lung collapse or over distension. More ventilated patients' data are also required in order to increase the range of the training and testing data and hence further validate the ANFIS-based models elicited during the course of this project.

There also exist some issues about the time duration for EIT data recordings during the clinical trials on the critically-ill ventilated patients. The durations of EIT data recordings were not long enough for it to be able to display more changes in absolute lung volume and densities as the result of changing the ventilator settings, especially PEEP. In this case, it is foreseen that a better methods in organising the time for EIT recordings need to be established. It would also be beneficial to prolong the EIT data recordings, especially for patients with a long stay in ICU as more observations can be invaluable in supporting the studies. The use of more advance EIT hardware such as an electrode belt or wireless electrodes also need to be considered to help increase the patients' comfort and better electrode positioning during the clinical trials.

The MEEV acquired from the aEIT system for ventilated patients in the ICU have not yet been verified with any established method due to some ethical issues. Therefore, in future it is recommended that established methods such as nitrogen wash-out (Wanger *et al.*, 2005) can be included in patients' study to measure the lung volume (in this case FRC values) and compare them with the values of the MEEV provided by the aEIT system.

The current aEIT system's software can also be further improved, particularly in the area of lung volume estimation accuracy. An example of such attempt has been initiated by the Sheffield Group recently, where the first data-driven model was

developed to describe the behaviour of the lung Resistivity-Volume in the aEIT system (Mohamad Samuri *et al.*, 2011). This model was developed with the aim to bypass the non-linear equations used in the aEIT system's software to infer absolute lung volumes from resistivity data, where most of these equations are empirical/theoretical and introduce uncertainties and inaccuracies in the final estimations of lung volumes. Research in this area is still ongoing to identify more parameters (that are easily measured) to be included in the modelling structure which may lead to a truly 'generic' model that is able to account for inter and intra-individual parameter variability.

Although the current decision support system has shown the ability to generate an overall optimal ventilatory therapy and minimise the chances of lung injuries in the patient, the system should be further tested. This is because, as stated before, the aEIT quantitative models used to estimate the MEEV, MAD, MMD and MPD values of the simulated patients lack data for adequate training and generalisation, which may cause some inaccuracies in the values estimated during the validation process of the decision support system. Therefore, it is essential that after further improvement and validation being made to these models, the performance of the decision support system be re-tested via a series of simulated patients data and followed by validation using real clinical data and designed clinical trials in the ICU environment.

REFERENCES

Adler, A., *et al*. (1996). "Impedance imaging of lung ventilation: do we need to account for chest expansion." IEEE Trans. Biom. Eng. **43**: 414-420.

Albert, R. K and Hubmayr, R. D. (2000). "The prone position eliminates compression of the lungs by the heart." Am. J. Respir. Crit. Care. Med **161**: 1660-1665.

Allerod, C., Rees, S.E., Rasmussen, B.S., Karbing, D.S., Kjaergaard, S., Thorgaard, P., Andreassen, S. (2008). "A decision support system for suggesting ventilator settings: Retrospective evaluation in cardiac surgery patients ventilated in the ICU." Computer Methods and Programs in Biomedicine **92**: 205-212.

Artigas, A., Bernard, G. R., Carlet, J., Falke, K., Hudson, L., Lamy, M., Marini, J. J., Matthay, M. A., Pinsky, M. R., *et al*. (1998). "The American-European Concensus Conference on ARDS, part 2: ventilator, pharmacologic, supportive therapy, study design strategies and issues related to recovery and remodeling." Am. J. Respir. Crit. Care. Med **157**: 1332-1347.

Barber, D. C. (1995). "Electrical impedance tomography." The Biomedical Engineering Handbook **2**: 1151-1164.

Barber, D. C., Borsic, A. (2005). "Electrical Impedance Tomography: Methods, History and Application." Series in Medical Physics and Biomedical Engineering 348-371.

Barber, D. C., Brown, B. H. (1984). "Applied potential tomography." J. Phys. E: Sci. Instrum **17**: 723-733.

Barber, D. C., Brown, B. H. (1985). "Recent developments in applied potential tomography – APT." Information Processing in Medical Imaging 106-121.

Barber, D. C., Brown, B. H., *et al*. (1989). "Applied potential tomography." Journal of the British Interplanetary Society **42**(7): 391-3.

Barber, D. C., Seagar, A. D. (1987). "Fast reconstruction of resistance images." Clinical Physics & Physiological Measurement **8(**Supplement A): 47-54.

Behr, J., Furst, D. E. (2008). "Pulmonary function tests." Rheumatology **47**: 65-67.

Bernard, G. R., Artigas, A., Brigham, K. L., Carlet, J., Falke, K., Hudson, L., Lamy, M., Legall, J. R., Morris, A., Spragg, R. (1994). "The American-European Concensus Conference on ARDS. Definitions, mechanisims, relevant outcomes and clinical trial coordination." Am. J. Respir. Crit. Care. Med **149**: 818-824.

Bikker, I. G., Leonhardt, S., Miranda, D. R., Bakker, J., Gommers, D. (2010). "Bedside measurement of changes in lung impedance to monitor alveolar ventilation in dependent and non-dependent parts by electrical impedance tomography during a positive end-expiratory pressure trial in mechanically ventilated intensive care unit patients." Critical Care **14**:R100.

Brown, B. H, Barber, D. C. (1987). "Electrical impedance tomography; the construction and application to physiological measurement of electrical impedance images." Medical Progress through Technology **13**: 69-75.

Brown, B. H. (2001). "Medical impedance tomography and process impedance tomography: a brief review." Meas. Sci. Technol, **12**: 991-996.

Brown, B. H. (2003). "Electrical impedance tomography (EIT): a review." Journal of Medical Engineering Technology **27**: 97-108.

Brown, B. H., Barber D. C., Leathard A. D., Lu, L., Wang, W., Smallwood, R.H., Wilson, A. J. (1994). "High frequency EIT data collection and parametric imaging." Innovation Technol. Biol. Med. **15**: 1-8.

Brown, B. H., Barber D. C., Seagar, A. D. (1985). "Applied potential tomography: possible clinical applications." Clin. Phys. Physiol. Meas. **6**: 109-121.

Brown, B. H., Barber, D. C. (1987). "Electrical impedance tomography; the construction and application to physiological measurement of electrical impedance images." Medical Progress through Technology **13**: 69-75.

Brown, B. H., Barber, D. C. (1988). "Possibilities and problems of real-time imaging of tissue resistivity." Clin. Phys. Physiol. Meas. **9**:121-125.

Brown, B. H., Barber, D. C., Wang, W., Lu, L., Leathard, A. D., Smallwood, S. H., Hampshire, A. R., Mackay, R., Hatzigalanis, K. (1994). "Multi-frequency imaging and modelling of respiratory related electrical impedance changes." Physiological Measurement, **15**: A1-A12.

Brown, B. H., Leathard, A. D., *et al*. (1995). "Measured and expected Cole parameters from electrical impedance tomographic spectroscopy images of the human thorax." Physiological Measurement **16**(3 Suppl A): A57-67.

Brown, B. H., Mills, G. H. (2006). "Indirect measurement of lung density and air volume from Electrical Impedance Tomography EIT data." World Congress on Medical Physics and Biomedical Engineering, Seoul, Korea.

Brown, B. H., Primhak, R. A., Smallwood, R. H., Milnes, P., Narracott, A. J., Jackson, M. J. (2002). "Neonatal lungs--can absolute lung resistivity be determined non-invasively?" Medical & Biological Engineering & Computing **40**: 388-394.

Butcher, R. and Boyle, M. (1997). Mechanical Ventilation: Learning Package pp: 1-71.

Carlo, W. A., Pacifico, L., Chatburn, R. L., Fanaroff, A. A. (1986). "Efficacy of computer-assisted management of respiratory failure in neonates." Pediatrics **78**:139-43.

Cole, K. S., Cole, R. H. (1941). "Dispersion and absorption in dielectrics: I. Alternating current characteristics." J Chemical Physics **9**:331-351.

Coulombe, N., Gagnon, H., Marquis, F., Skrobik, Y., Guardo, R. (2005). "A parametric model of the relationship between EIT and total lung volume." Physiological Measurement **26**: 401-411.

Denai, M., Mahfouf, M., Mohamad-Samuri, S., Panoutsos, G., Brown, B. H., Mills, G. H. (2010). "Absolute Electrical Impedance Tomography (aEIT) Guided Ventilation Therapy in Critical Care Patients: Simulations and Future Trends." IEEE Transactions on Information Technology in Biomedicine **14**: 641-649.

Dojat, M., Pachet, F., Guessoum, Z., Touchard, D., Harf, A., Brochard, L. (1997). "NeoGanesh: A working system for the automated control of assisted ventilation in ICUs." Artificial Intelligence in Medicine **11**: 97-117.

Duck, F. A. (1990). "Physical properties of tissue." Academic press, London, ISBN 0-12-222800-6.

East, T.D., Wallace, C.J., Moris, A.H., *et al*. (1995). "Computers in critical care." Critical Care Nursing Clinics of North America **7**: 203-217.

El-Khatib, M. F., and Jamaleddine, G. W. (2004). "A new Oxygenation Index for Reflecting Intrapulmonary Shunting in Patients undergoing Open-Heart Surgery." Chest **125**: 592-596.

Erlandsson, K., Odenstedt, H., Lundin, S., Stenqvist, O. (2006). "Positive end-expiratory pressure optimisation using electrical impedance tomography in morbidly obese patients during laparoscopic gastric bypass surgery." Acta Anaesthesiol Scand. **50**: 833-839.

Ferguson, G.T. (2006). "Why Does the Lung Hyperinflate." Proc. Am. Thorac. Soc **3**: 176-179.

Frank, J. A., Matthay, M. A. (2003), "Science Review: Mechanisms of ventilator-induced lung injury." Critical Care **7**: 233-241.

Frerichs,I., Schmitz, G., Pulletz, S., Schadler, D., Zick, G., Scholz, J., Weiler, N. (2007). "Reproducibility of regional lung ventilation distribution determined by electrical impedance tomography during mechanical ventilation." Physiol. Meas. **28**, pp: 261-267.

Geselowitz, D.D. (1971). “An application of electrocardiographic lead theory to impedance plethysmography.” IEEE Trans. Biomed. Eng. **18**:38-41.

Gisser, D. G., Isaacson, D., Newell J. C. (1988). “Theory and performance of an adaptive current tomography system.” Clin. Phys. Physiol. Meas. **9**(Suppl.): A : 35-41.

Goode, K. M. (2001). Model-based development of a fuzzy logic advisor for artificially ventilated patients. PhD thesis. The University of Sheffield.

Grandmaison, G. L. (2001). "Organ weight in 684 adult autopsies: new tables for Caucasoid population." Forensic Science International **119**: 149-154.

Griffiths,H., Leung, H. T., Williams, R. J. (1992). “Imaging the complex impedance of the thorax.” Clin. Phys. Physiol. Meas. **13**: 77-81.

Hahn, G., Just, A., Dudykevych, T., Frerich, I., Hinz, J., Quintel, M., Hellige, G. (2006). “Imaging pathologic pulmonary air and fluid accumulation by functional and absolute EIT.” Physiol. Meas. **27**: 187-198.

Hanson III, C. W., Marshall, B. E. (2001). “Artificial intelligence applications in the intensive care unit: A review.” Crit. Care Med, **29**: 427–435.

Harris, N. D., Suggett, A. J., Barber, D. C., Brown, B. H. (1987). “Applications of applied potential tomography APT in respiratory medicine.” Clin. Phys. Physiol. Meas. **8**: 155-165.

Harris, R. (2005). “Pressure-Volume Curves of the Respiratory System.” Respiratory Care **50**:78-98.

Heinze, H., Sedemund-Adib, B., Heringlake, M., Meier, T., Eichler, W. (2010). “Relationship Between Functional residual Capacity, respiratory Compliance and Oxygentaion in Patients Ventilated After Cardiac Surgery.” Respiratory Care **55**: 589-594.

Henderson, R. P. and J. G. Webster (1978). "An impedance camera for spatially specific measurements of the thorax." IEEE Transactions on Biomedical Engineering **25**: 250-254.

Hinz, J., Hahn, G., Neumann, P., Sydow, M., Mohrenweiser, P., Hellige, G., Burchardi, H. (2003). “End-expiratory lung impedance change enable bedside monitoring of end-expiratory lung volume change.” Intensive Care Med. **29**: 37-43.

Hinz, J., Moerer, O., Neumann, P., Dudykevych, T., Frerichs, I., Hellige, G., Quintel, M. (2006). “Regional pulmonary pressure volume curves in mechanically ventilated patients with acute respiratory failure measured by electrical impedance tomography.” Acta. Anaesthesiol. Scand. **50**:331-339.

Hinz, J., Neumann, P., Dudykevych, T., *et al*. (2003), "Regional Ventilation by Electrical Impedance Tomography: A comparison with ventilation Scintigraphy in pigs." CHEST, **124**: 314-322.

Jang, J. (1993). "ANFIS: Adaptive-network-based fuzzy inference system." IEEE Transactions on System, Man, and Cybernetics **23:** 665-685.

Karbing, D. S., Kjaergaard, S., Smith, B. W., Espersen, K., Allerod, C., Andreassen, S., Rees, S. E. (2007). "Variation in the PaO2/FiO2 ratio with FiO2: mathematical and experimental description, and clinical relevance." Critical Care **11**: R118.

Kilic, Y.A., Kilic, I. (2010). "A Novel Fuzzy Logic Inference Ssystem for Decision Support in Weaning from Mechanical Ventilation." J. Med. Syst **34**:1089-1095.

Korzhenevskii, A. V., Kornienko, V. N., Yu. Kultiasov, M., Cherepenin, V. A. (1997). "Electrical impedance computerized tomography for medical applications." Instruments and Experimental Techniques **40**: 415-421.

Kunst, P.W., Bohm, S. H., de Vazquez, A., Amato, M.B., Lachmann, B., Postmus, P.E. *et al*. (2000). "Regional pressure volume curves by electrical impedance tomography in a model of acute lung injury." Crit. Care. Med **28**: 178-83.

Kwok, H. F. (2003). SIVA: an intelligent advisory system for intensive care ventilators. PhD thesis. The University of Sheffield.

Kwok, H.F., Linkens, D.A., Mahfouf, M., and Mills, G.H. (2004). "SIVA: A Hybrid Knowledge-and-Model-Based Advisory System for Intensive Care Ventilators." IEEE trasactions on information technology in biomedicine **8**: 161-172.

Kwok, H.F., Linkens, D.A., Mahfouf, M., Mills, G.H. (2003). "Rule-base derivation for intensive care ventilator control using ANFIS." Artificial Intelligence in Medicine, **29**: 185-201.

Lehr, J.A. (1972). "A vector derivation useful in impedance plethysmograpic fields calculations." IEEE Trans. Eng. **19**: 156-157.

Lu, Q., Rouby, J-J. (2000). "Measurement of pressure-volume curves inpatients on mechanical ventilation: methods and significance." Critical Care **4**:91-100.

Mamdani, E. H. (1974). "Application of fuzzy algorithms for control of simple dynamic plant." In: Proceedings IEEE. 1585-1588.

Mason, D.G., Edwards, N.D., Linkens, D.A., Reilly, C.S. (1996). "Performance assessment of a fuzzy logic controller for atracurium-induced neuromuscular block." British Journal of Anaesthesia **76**: 396-400.

Meier, T., Luepschen, H., Karsten, J., Leibecke, T., Grobherr, M., Gehring, H., Leonhardt, S. (2008). "Assessment of regional lung recruitment and derecruitment during a PEEP trial based on electrical impedance tomography." Intensive Care Med. **34**: 543-550.

Mentzelopoulos, S. D., Roussos, C., Zakynthinos, S. G. (2005). "Prone position reduces lung stress and strain in severe acute respiratory distress syndrome." Eur. Respir. J. **25**: 534-544.

Mentzelopoulos, S. D., Zakynthinos, S. G., Roussos, C., Tzoufi, M. J., Michalopoulos, A. S. (2003). "Prone Position Improves Lung mechanical Behaviour and Enhances Gas Exchange Efficiency in Mechanically Ventilated Chronic Obstructive Pulmonary Disease Patients." Anesth. Analg **96**: 1756-67.

Michelet, P., Roch, A., Brousse, D., D'Journo, X. –B., F.Bregeon, D. Lambert, G. Perrin, L. Papazian, P. Thomas, J-p. Carpentier and Auffray, J-P. (2005). "Effect of PEEP on oxygenation and respiratory mechanics during one-lung ventilation." British Journal of Anaesthesia **95**(2): 267-73.

Miller, P. (1985). "Goal-directed critiquing by computer: ventilator management." Computer and Biomedical Research **18**: 422-38.

Mohamad-Samuri, S., Panoutsos, G., Mahfouf, M., Mills, G. H., Brown, B. H. (2011). "Neural-Fuzzy Modelling of Lung Volume using Absolute Electrical Impedance Tomography." In BIOSIGNALS 43-50.

Moloney E. D., Griffiths, M. J. (2004). "Protective ventilation of patients with acute respiratory distress syndrome." British Journal of Anaesthesia **92**:261–270.

Nebuya, S. *et al*. (2006). "Study of the optimum level of electrode placement for the evaluation of absolute lung resistivity with the Mk3.5 EIT system." Physiol. Meas. **27**: S129-S137.

Nebuya, S., Koike, T., Imai, H., Noshiro, M., Brown, B. H., Soma, K. (2010). "Measurement of lung function using Electrical Impedance Tomography (EIT) during mechanical ventilation." Journal of Physics, Conference Series **224**: 012029.

Neligan, P. (2002). "Critical Care Medicine Tutorials." The University of Pennsylvania. http://www.ccmtutorials.com/.

Nemoto, T., Hatzakis, G.E., Thorpe, C.W., Olivenstein, R., Dial, S., Bates, J.H.T. (1999). "Automatic Control of pressure support mechanical ventilation using fuzzy logic." AM J Respir. Crit. Care Med **160**:550-6.

Noble, T. J., Harris, N. D., *et al*. (2000). "Diuretic induced change in lung water assessed by electrical impedance tomography." Physiological Measurement **21**(1): 155-63.

Nopp, P., Harris, N. D., *et al*. (1997). "Model for the dielectric properties of human lung tissue against frequency and air content." Medical & Biological Engineering & Computing **35**(6): 695-702.

Norman G. G. Hepper, Ward S. Fowlwer, H. Frederic Helmholz, JR (1960). "Relationship of Height to Lung Volume in Healthy Men." Journal of the Americam College of Chest Physicians **37**: 314-320.

Osheroff, J.A., Pifer, E.A *et al*., (2004). "Clinical decision support implementers' workbook." Chicago: HIMSS. www.hims.org/edsworkbook.

Panoutsos, G., Mills, G. H., Wang, A., Mahfouf. M., Brown, B. H. (2007). "Initial comparisons of absolute electrical impdedance tomography (EIT) lung volume estimates with Spirometry." British Journal of Anaesthesia **98**: 294P.

Panoutsos, G., Tunney, D. R., Mills, G. H., Al-Jabary, T., Mahfouf, M., Brown, B. H. (2008). "An improved algorithm for accurate absolute EIT lung volume estimation and localisation." International conference of the American Thoracic Society, Toronto, Canada.

Pullets, S., Elke, G., Zick, G., Schadler, D., Scholz, J., Weiler, N., Frerichs, I. (2008). "Performance of electrical impedance tomography in detecting regional tidal volumes during one-lung ventilation." Acta Anaesthesiol Scand. **52**: 1131-1139.

Rees, S.E., Allerod, C., Murley, D., Zhao, Y., Smith, B.W., Kaegaard, S., Thorgaard, P., Andreassen, S. (2006). "Using Physiological Models and Decision Theory for Selecting Appropriate Ventilator Settings." Journal of Clinical Monitoring and Computing **20**: 421-429.

Ross, J.J., Mason, D.G., Linkens, D.A., Edwards, N.D. (1997). "Self-learning fuzzy logic control of neuromuscular block." British Journal of Anaesthesia **78**: 412-415.

Scaublin, J., Derighetti, M., Feigenwinter, P., Petersen-Felix, S., Zbinden, A.M. (1996). "Fuzzy logic control of mechanical ventilation during anaesthesia." British Journal of Anaesthesia **77**: 636-641.

Shahsavar, N., Gill., Ludwigs, A., Carstensen, H., Larsson, O., Wigertz and Matell, G. (1994). "VentEx: an on-line knowledge-based system to support ventilator management." Technology and Health Care **1**: 233-243.

Shahsavar, N., Ludwigs, U., Blomqvist, H., Grill, H., Wigertz, O., Matell, G. (1995). "Evaluation of a knowledge-based decision-support system for ventilator therapy management." Artificial Intelligence in Medicine **7**: 37-52.

Sim, I., Gorman, P., *et al*. (2001). "Clinical decision support systems for the practice of evidence-based medicine." J. Am Med Inform Assoc **8:** 527-534.

Sitting, D. F., Pace, N. L., Gardner, R. M., Beck, E., Morris, A. H. (1989). "Implementation of a computerised patient advice system using the HELP clinical information system." Computers and Biomedical Research **22**: 474-87.

Smallwood, R. H., Hampshire, A.R.., *et al*. (1999). "A comparison of neonatal and adult lung impedances derived from EIT images." Physiological Measurement **20**(4): 401-13.

Smith, R. W., Freeston, I. L., Brown, B. H. (1995). "A real-time electrical impedance tomography system for clinical use--design and preliminary results." IEEE Transactions on Biomedical Engineering **42**: 133-140.

Spencer, R. P. (2003). "Male/Female weight of internal organs: Examination across multiple populations." Americal Journal of Human Biology **15**: 643-646.

Sugeno, M., Kang, G.T. (1988). "Structure Identification of Fuzzy Model", Fuzzy Sets and systems **28**:15-33.

Sun, Y., Kohane, I., Stark, A.R. (1994). "Fuzzy Logic Assisted Control of Inspired Oxygen in Ventilated Newborn Infants." AMIA 757: 761.

Sundaresan, A., GeoffreyChase, J. (2011). "Positive end expiratory pressure in patients with acute respiratory distress syndrome – The past, present and future." Biomed. Signal Process. Control **7**: 93-103.

Takagi, T., Sugeno, M. (1985). "Fuzzy identification of systems and its applications to modelling and control." IEEE Trans. Systems, Man., and Cybernatics **15**:166-132.

Tehrani, F.T., Roum, J.H. (2008). "FLEX: A New Computerised System for Mechanical Ventilation." Journal of Clinical Monitoring and Computing **22**: 121-130.

Tremblay, L.N., Slutsky, A. S. (2006). "Ventilator-induced lung injury: from the bench to the bedside." Intensive Care Med **32**: 24-33.

Tunney, D. R. (2007). "Electrical Impedance Tomography: an evaluation of it's ability to detect changes in lung volume and expansion." B. Med Sci. Dissertation. The University of Sheffield.

Tunney, D. R., Panoutsos, G., Al-Jabary, T., Mahfouf, M., Brown, B. H., Mills, G. H. (2008) "Electrical Impedance Tomography: an evaluation of its ability to detect changes in lung volume and expansion during single lung ventilation" British Journal of Anaesthesia **100**: 584P.

Victorino, J. A. *et al*. (2003), "Imbalances in Regional Lung Ventilation: A validation study on electrical impedance tomography." Am J Respir. Crit. Care Med **169**: 791-800.

Wang, A. (2008). Hybrid Modelling and Decision Support for Ventilator Management in Intensive Care Units. PhD thesis. The University of Sheffield.

Wang, A., Mahfouf, M., and Mills, G. H. (2006). "A continuously updated hybrid blood gas model for ventilated patients." 6th IFAC Symposium on Modeling and Control in Biomedical Systems Reims.

Wang, A., Mahfouf, M., Mills, G.H., Panoutsos, G., Linkens, D.A., Goode, K., Kwok, H.F and Denai, M. (2010). "Intelligent model-based advisory system for the management of ventilated intensive care patients. Part II: Advisory system design and evaluation." Journal of Computer Methods and Programs in Biomedicine **99**: 208-217.

Wang, A., Panoutsos, G., Mahfouf, M., Mills, G. H. (2007). "An improved blood gas intelligent hybrid model for mechanically ventilated patients in the Intensive Care Unit." Proceedings of the 5th IASTED International Conference on Biomedical Engineering Innsbruck, Austria pp. 73-78.

Wanger,J., Clausen,J.L., Coates,A., Pedersen, O.F., *et al*. (2005). "Standardisation of the measurement of lung volumes." European Respiratory Journal. **26**: 511-522.

Wilson, A. J., Milnes, P., Waterworth, A. R., Smallwood, R. H., Brown, B. H. (2001). "Mk3.5: A Modular, Multifrequency Successor to the Mk3a EIS/EIT System." Physiol. Meas. **22**: 49-54.

Wilson, A. J., P. Milnes, *et al*. (2001). "Mk3.5: a modular, multi-frequency successor to the Mk3a EIS/EIT system." Physiological Measurement **22**: 49-54.

Zbinden, A.M., Feigenwinter, P., Petersen-Felix, S., Hacisalihzade, S. (1995). "Arterial pressure control with isoflourine using fuzzy logic." British Journal of Anaesthesia **74**: 66-72.

Zhang, J. and Patterson, R.P. (2005). "EIT images of ventilation: what contributes to the resistivity changes." Physiol. Meas **26**: S81-S92.

Zubal, IG., Harrell, C. R., Smith, E. O., Rattner, Z., Gindi, G., Hoffer P. B. (1994). "Computerized three-dimensional segmented human anatomy." Medical Physics **21**:299-302.

APPENDIX A

SOPAVENT MODEL PARAMETERS

1) Oxygen transport and exchange equations:

$$\frac{dCaO_2}{dt} \cdot V_a = \dot{Q}_t[X \cdot CvCO_2 + (1-X) \cdot CpO_2 - CaO_2] \quad (A.1)$$

$$\frac{dCtO_2}{dt} \cdot V_t = \dot{Q}_t[CaO_2 - CtO_2] - \dot{V}_{O_2} \quad (A.2)$$

$$\frac{dCvO_2}{dt} \cdot V_v = \dot{Q}_t[CtO_2 - CvO_2] \quad (A.3)$$

$$\frac{dCpO_2}{dt} \cdot V_p = \dot{Q}_t(1-X)[CvO_2 - CpO_2 + O_2Diff] \quad (A.4)$$

$$\frac{dCAO_2}{dt} \cdot V_A = RR \cdot (V_T - V_D) \cdot \left(FiO_2 - \frac{CAO_2}{1000}\right) - \dot{Q}_t(1-X) \cdot O_2Diff \quad (A.5)$$

$$O_2Diff = B_{O_2}\left[P_{mean}\left(\frac{CAO_2}{1000}\right) - P_PO_2\right] \quad (A.6)$$

$$P_PO_2 = f_{inv}(CpO_2) \quad (A.7)$$

V_x x = *A* (Alveolar), *a* (arterial), *t* (tissue), *v* (venous), *p* (pulmonary) are the compartmental volumes in *litres*.

$\dot{Q}_t$ Cardiac output in *litres/min*.

X Fraction of blood shunted passed the lungs.

$\dot{V}_{O_2}$ Oxygen consumption by tissues in *ml of O_2/min (BTPS).*

V_D Alveolar deadspace volume in *ml (BTPS).*

V_T Ventilatory tidal volume in *ml (BTPS).*

RR Respiratory rate in *breath / min.*

CAO_2 Alveolar O_2 content in *ml of O_2/ litre of alveolar gas.*

CxO_2 x = a (arterial), t (tissue), v (venous), p (pulmonary) : O_2 concentration in *ml of O_2 /litre of blood*.

B_{O_2} O_2 diffusion constant in *ml of O_2/kPa/litre of blood.*

P_{mean} Mean airway pressure (kPa)

FiO_2 Inspired fraction of O_2

P_PO_2 Pulmonary partial pressure of O_2 in *kPa*.

f_{inv} Inverse of the O_2 dissociation function

2) Carbon dioxide transport and exchange equations

$$\frac{dCaCO_2}{dt} \cdot V_a = \dot{Q}_t[X \cdot CvCO_2 + (1 - X) \cdot CpCO_2 - CaCO_2] \quad (A.8)$$

$$\frac{dCtCO_2}{dt} \cdot V_t = \dot{Q}_t[CaCO_2 - CtCO_2] - \dot{V}_{CO_2} \quad (A.9)$$

$$\frac{dCvCO_2}{dt} \cdot V_v = \dot{Q}_t[CtCO_2 - CvCO_2] \quad (A.10)$$

$$\frac{dCpCO_2}{dt} \cdot V_p = \dot{Q}_t(1 - X)[CvCO_2 - CpCO_2 + CO_2Diff] \quad (A.11)$$

$$\frac{dCACO_2}{dt} \cdot V_A = RR \cdot (V_T - V_D) \cdot \left(FiCO_2 - \frac{CACO_2}{1000}\right) - \dot{Q}_t(1 - X) \cdot CO_2Diff \quad (A.12)$$

$$CO_2Diff = B_{CO_2}\left[Pmean\left(\frac{CACO_2}{1000}\right) - P_PCO_2\right] \quad (A.13)$$

$$P_PCO_2 = f_{inv}(CpCO_2) \quad (A.14)$$

$\dot{V}_{CO_2}$ Carbon dioxide consumption by tissues in *ml of CO_2/min (BTPS).*

$CACO_2$ Alveolar CO_2 content in *ml of CO_2/ litre of alveolar gas.*

$CxCO_2$ x = a (arterial), t (tissue), v (venous), p (pulmonary) : CO_2 concentration in *ml of CO_2 /litre of blood*.

B_{CO_2} CO_2 diffusion constant in *ml of CO_2/kPa/litre of blood.*

$FiCO_2$ Inspired fraction of CO_2

P_PCO_2 Pulmonary partial pressure of CO_2 in *kPa*.

f_{inv} Inverse of the CO_2 dissociation function

3) Gas Dissociation Functions (GDF)

Oxygen

$$C(O_2) = \beta_h \cdot Hb \cdot SO_2 + \alpha_b \cdot PO_2 \qquad (A.15)$$

Hb Haemoglobin concentration.

SO2 O_2 saturation fraction.

β_h Haemoglobin O_2 combining capacity.

α_b O_2 carrying capacity of blood plasma.

Carbon Dioxide

$$[\ CO_2]_{blood} = 22.2 \cdot [CO_2]_{plasma} \cdot \{d \cdot pcv + (1 - pcv)\}$$
$(A.16)$

pcv Packed cell volume fraction (or haematocrit).

A pH modelling and an airway modelling component were also developed and included into SOPAVent. Hence, the model provided PIP and pH predictions as well. The detailed descriptions of the model can be found in Goode, 2001.

APPENDIX B

Further patients' closed-loop simulation results

PATIENT 1

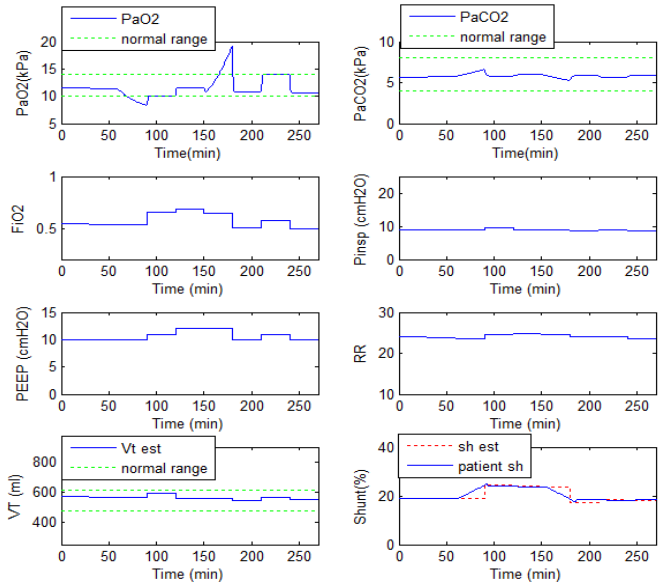

Simulation of an acute shunt changes.

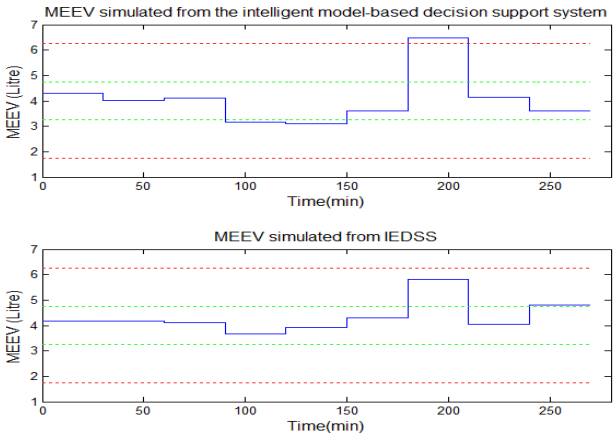

Comparison of MEEV changes produced by the intelligent model-based decision support system (Wang, 2008) and MEEV from the IEDSS during an acute change of shunt.

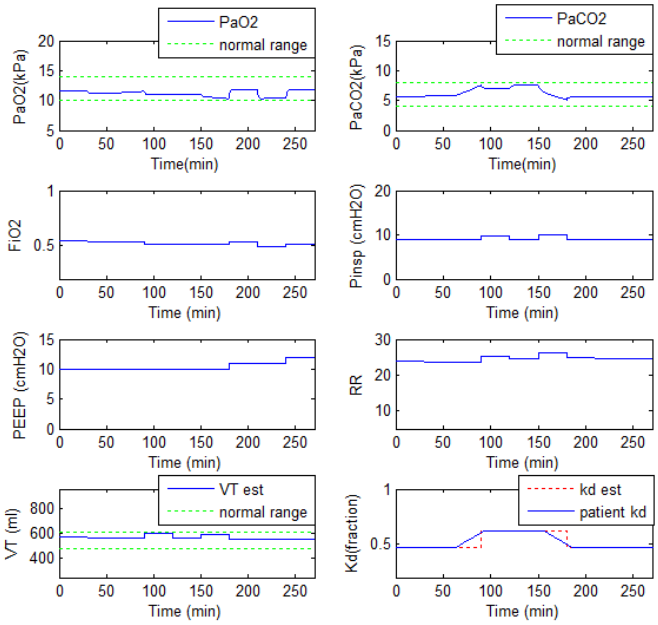

Simulation of an acute Kd changes.

PATIENT 2

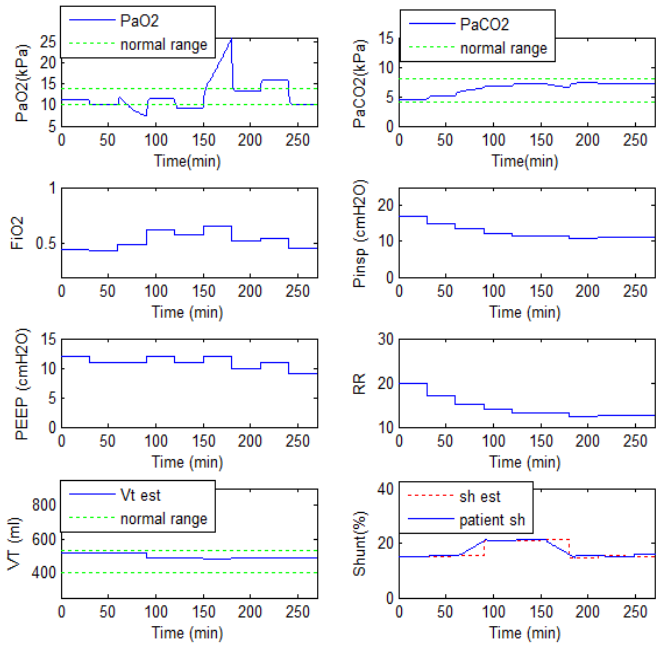

Simulation of an acute shunt changes.

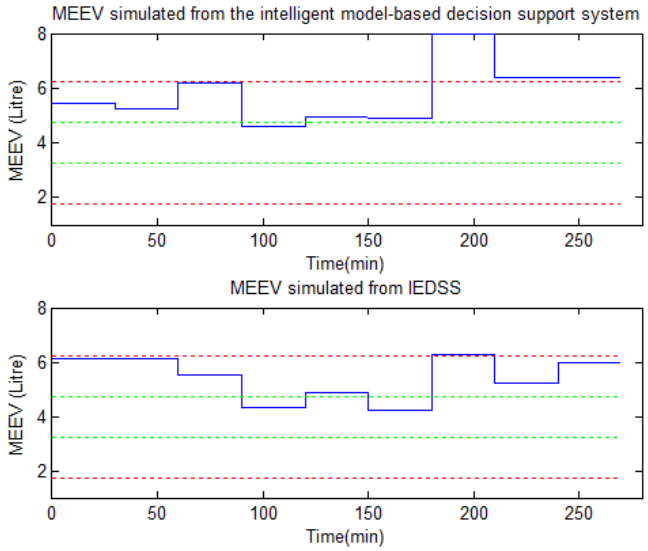

Comparison of MEEV changes produced by the intelligent model-based decision support system (Wang, 2008) and MEEV from the IEDSS during an acute change of shunt.

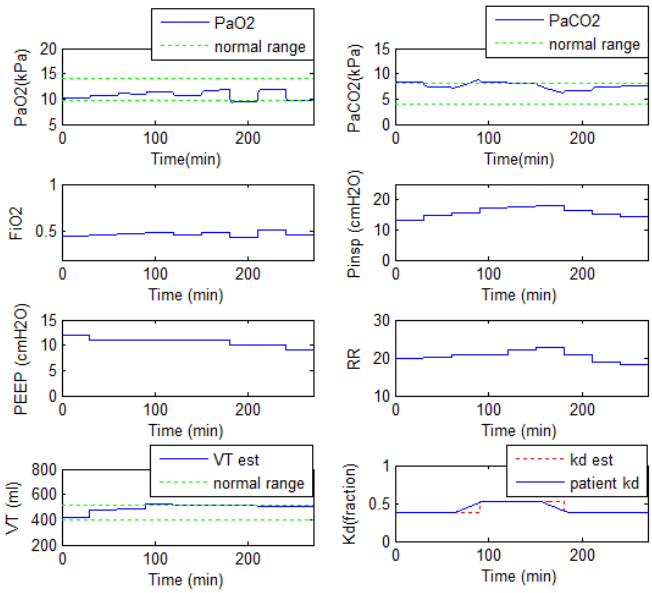

Simulation of an acute Kd changes.

PATIENT 3

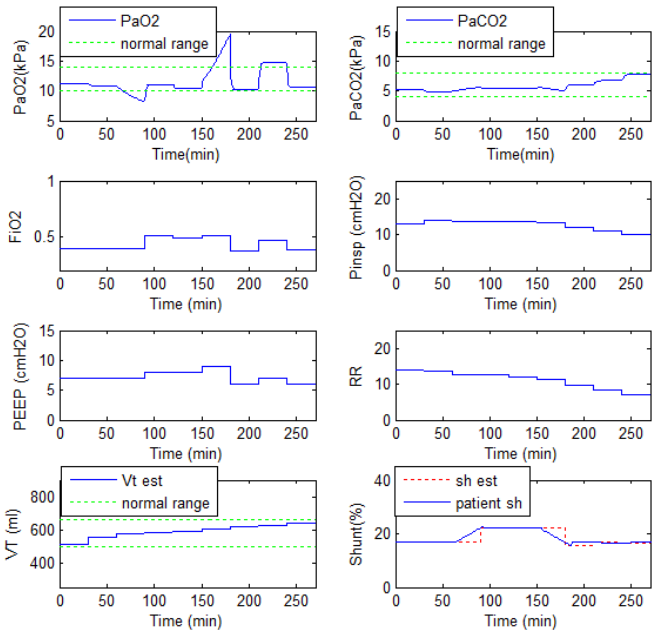

Simulation of an acute shunt changes.

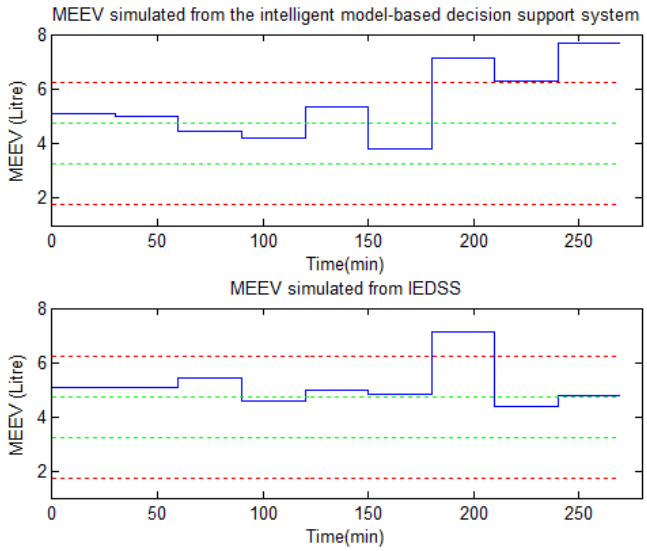

Comparison of MEEV changes produced by the intelligent model-based decision support system (Wang, 2008) and MEEV from the IEDSS during an acute change of shunt.

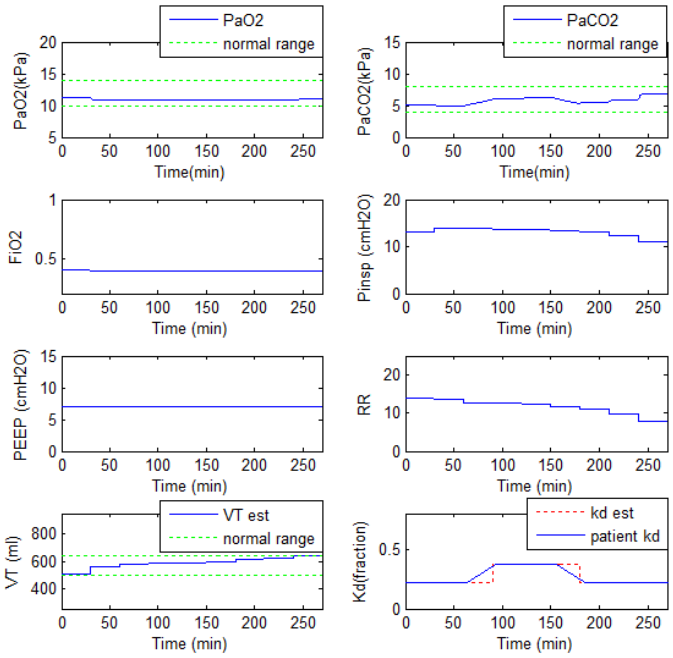

Simulation of an acute Kd changes.

PATIENT 4

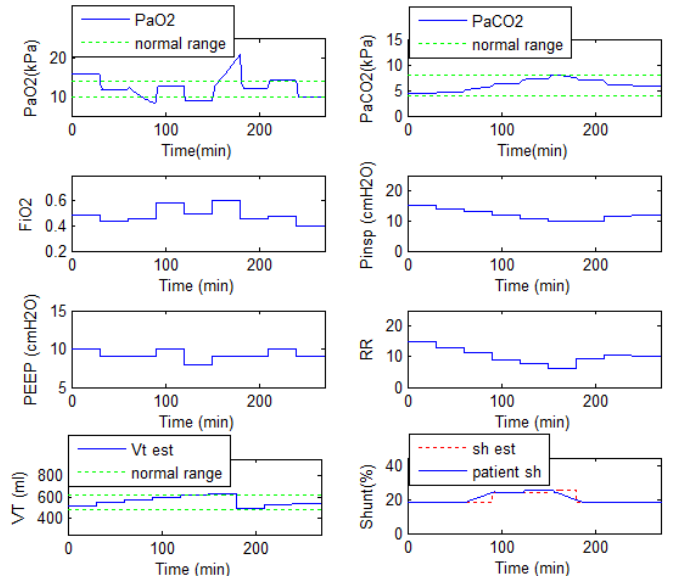

Simulation of an acute shunt changes.

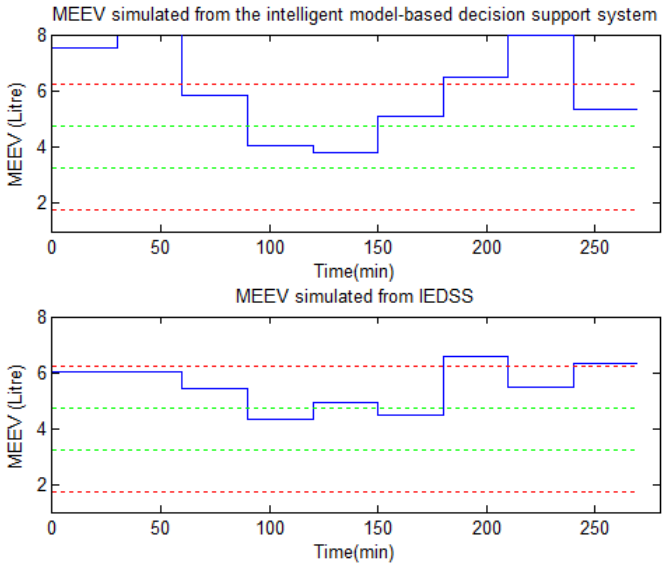

Comparison of MEEV changes produced by the intelligent model-based decision support system (Wang, 2008) and MEEV from the IEDSS during an acute change of shunt.

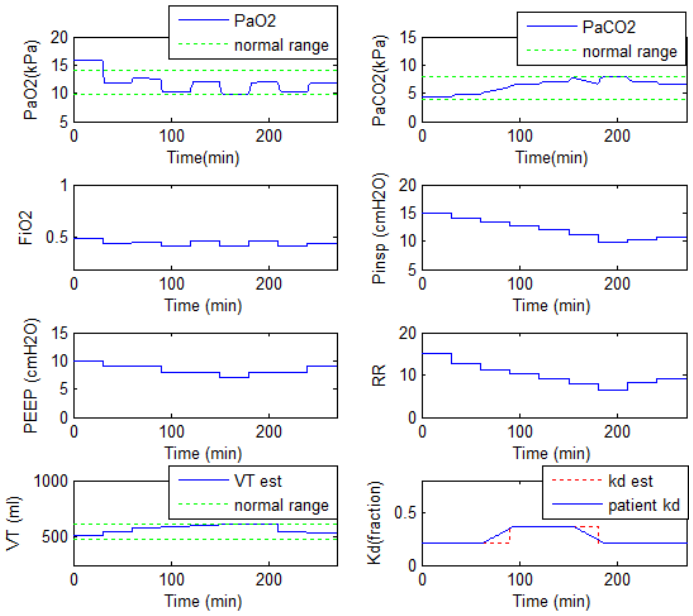

Simulation of an acute Kd changes.

PATIENT 5

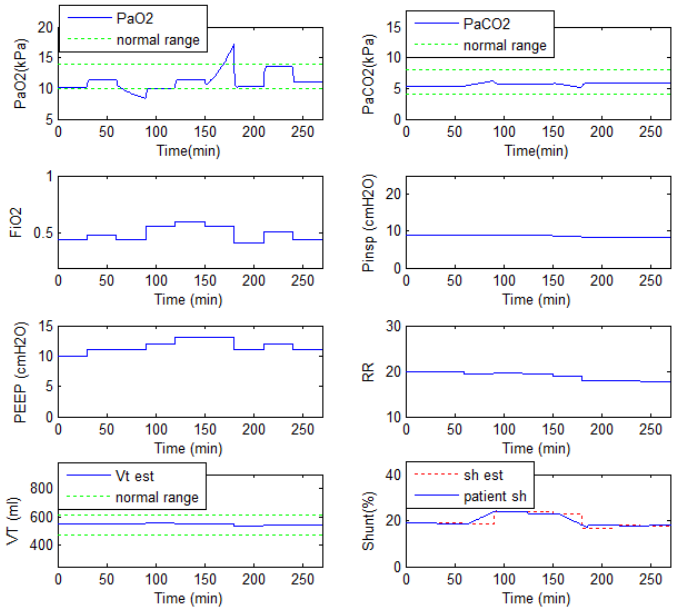

Simulation of an acute shunt changes.

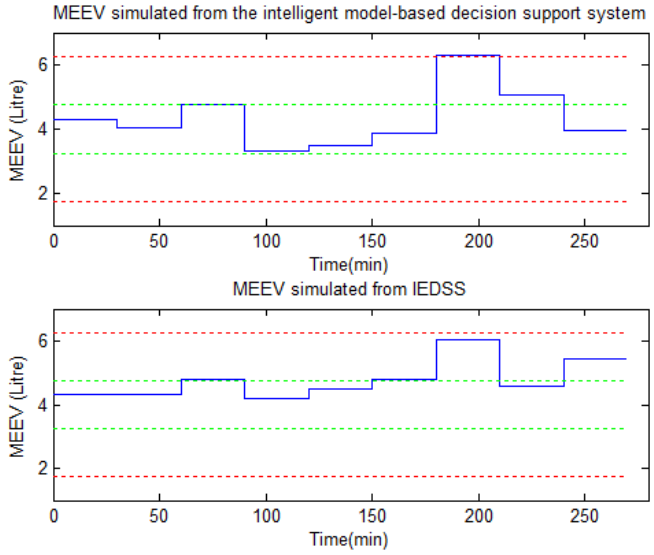

Comparison of MEEV changes produced by the intelligent model-based decision support system (Wang, 2008) and MEEV from the IEDSS during an acute change of shunt.

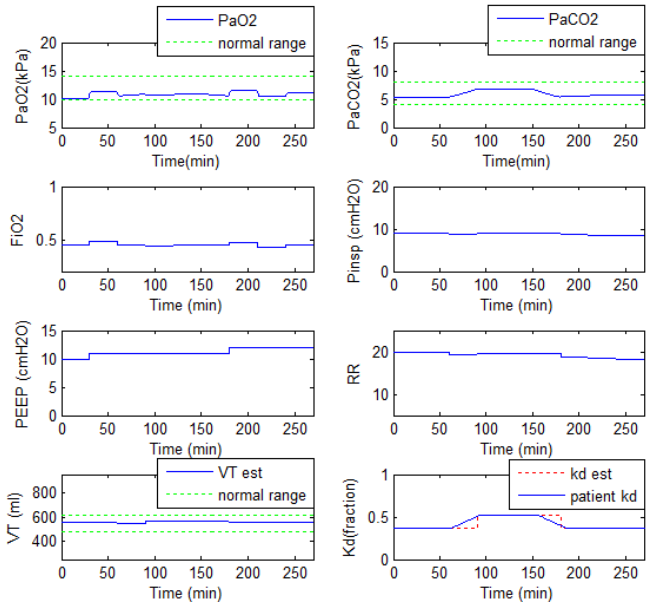

Simulation of an acute Kd changes.

PATIENT 6

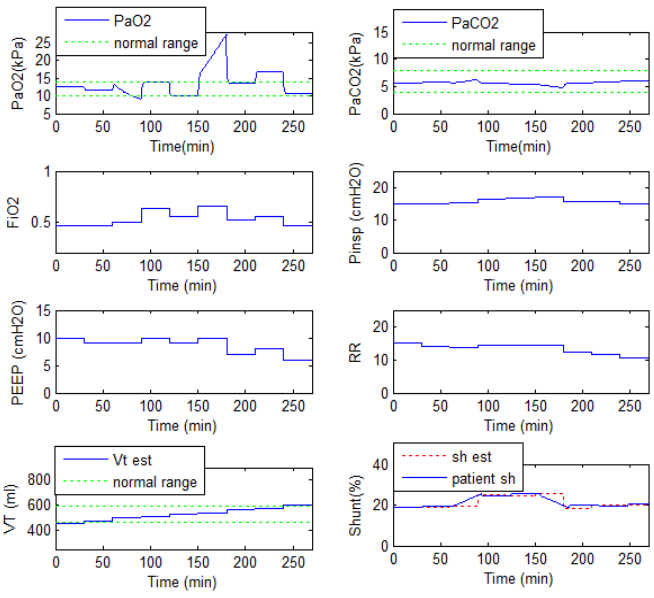

Simulation of an acute shunt changes.

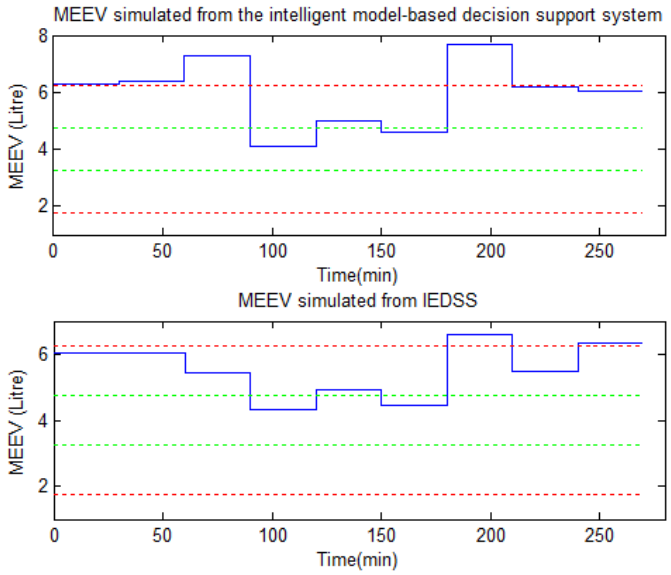

Comparison of MEEV changes produced by the intelligent model-based decision support system (Wang, 2008) and MEEV from the IEDSS during an acute change of shunt.

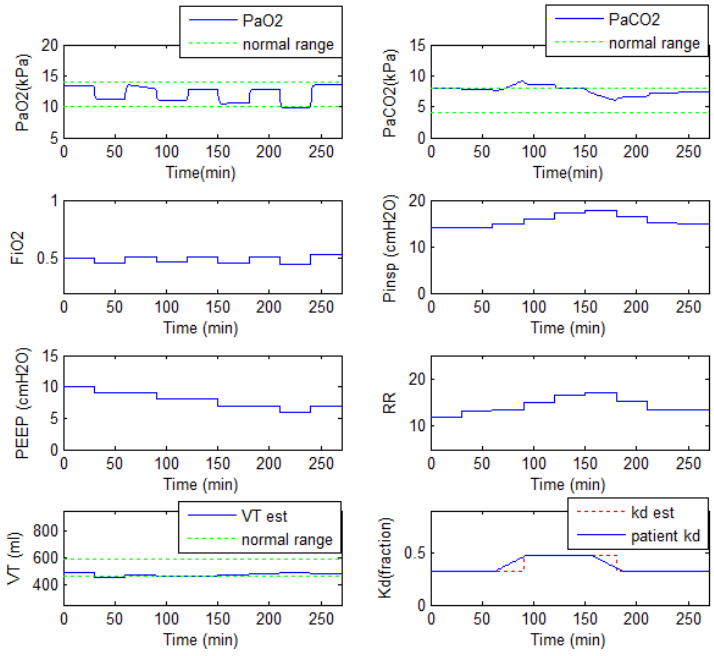

Simulation of an acute Kd changes.

PATIENT 7

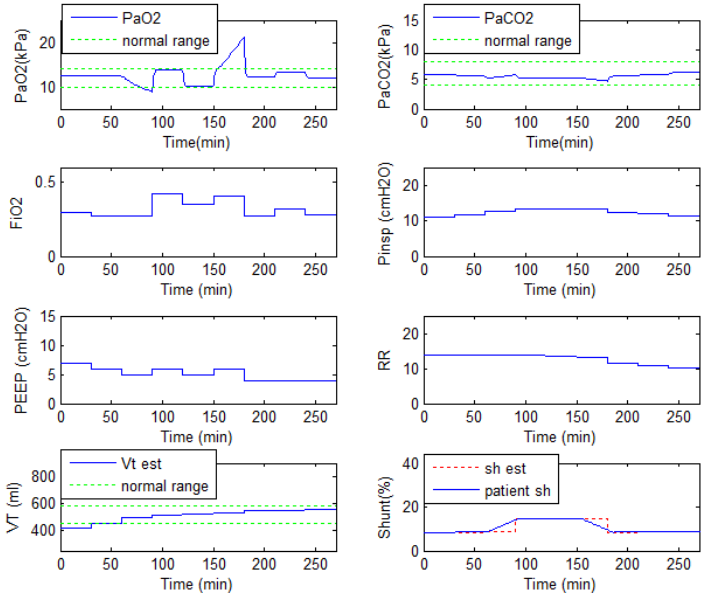

Simulation of an acute shunt changes.

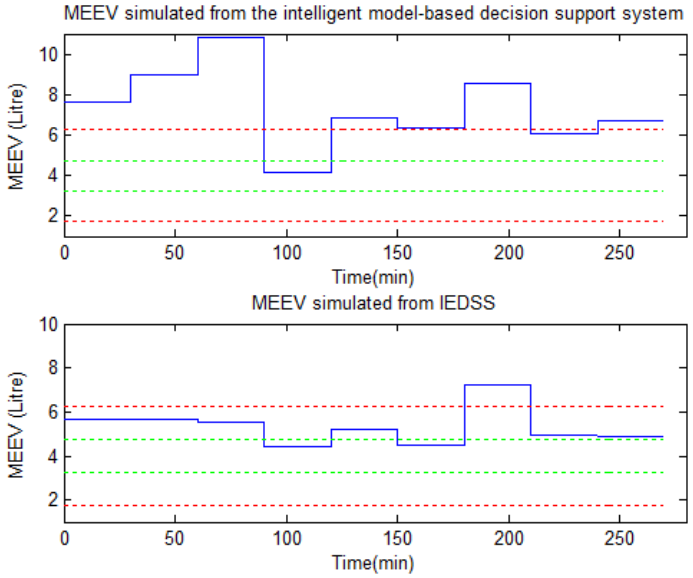

Comparison of MEEV changes produced by the intelligent model-based decision support system (Wang, 2008) and MEEV from the IEDSS during an acute change of shunt.

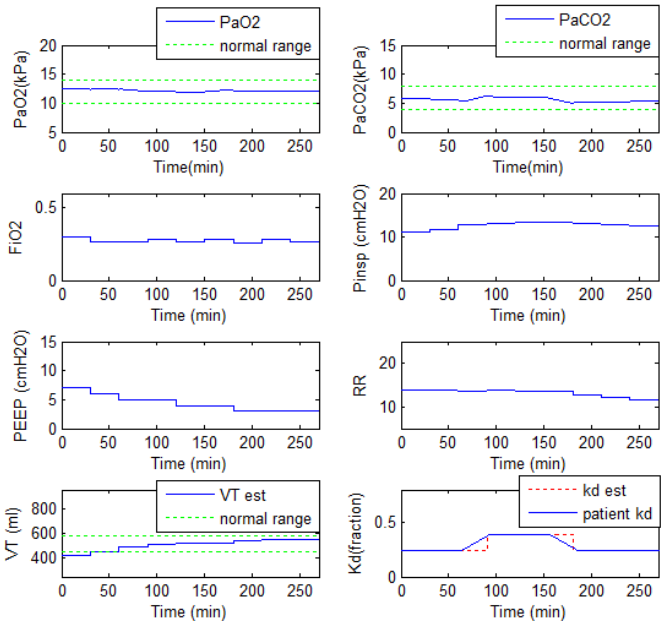

Simulation of an acute Kd changes.

PATIENT 8

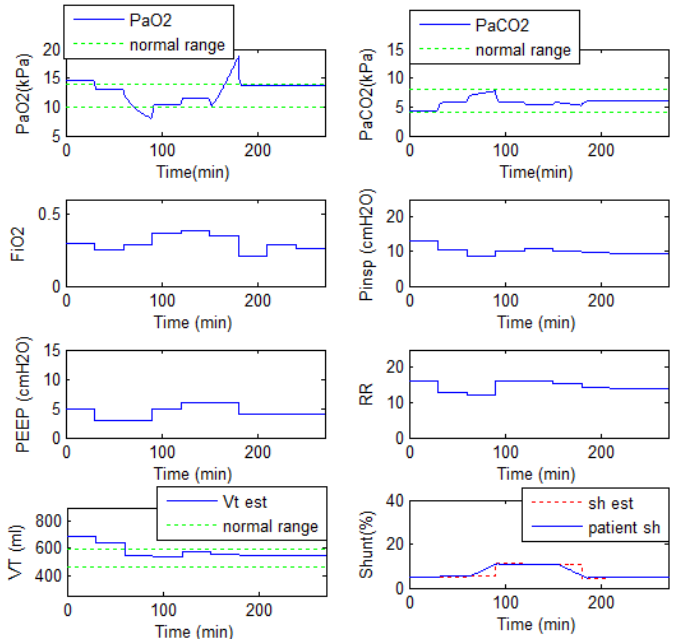

Simulation of an acute shunt changes.

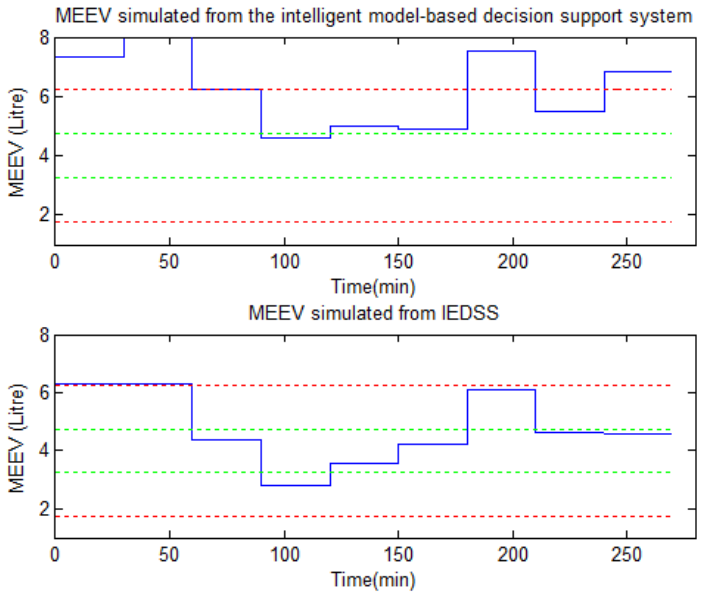

Comparison of MEEV changes produced by the intelligent model-based decision support system (Wang, 2008) and MEEV from the IEDSS during an acute change of shunt.

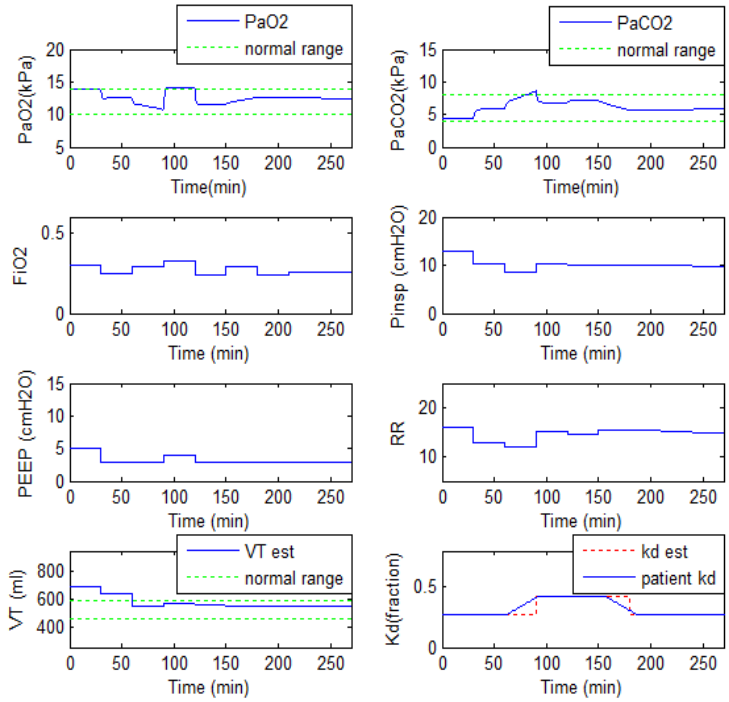

Simulation of an acute Kd changes.

PATIENT 9

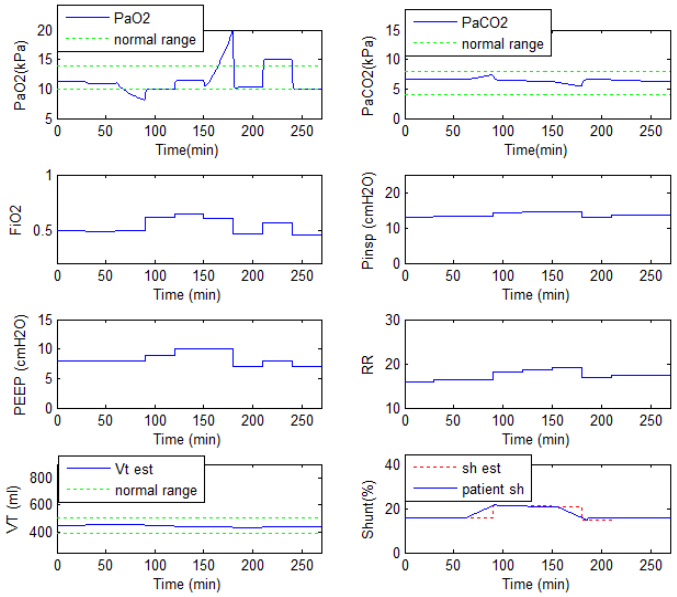

Simulation of an acute shunt changes.

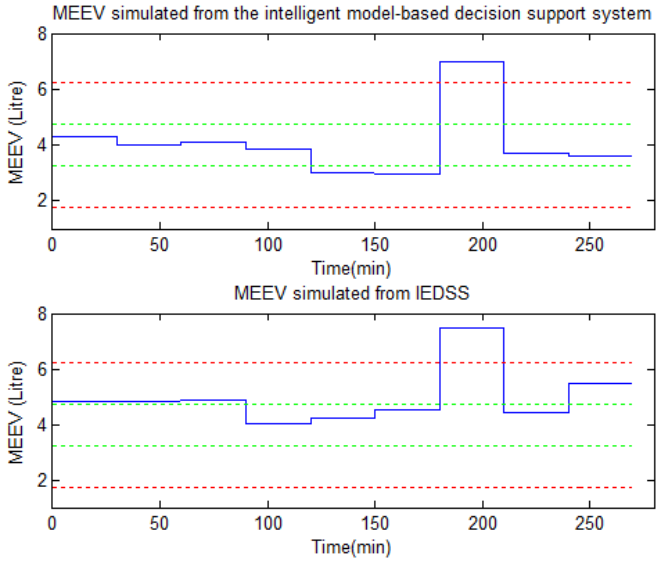

Comparison of MEEV changes produced by the intelligent model-based decision support system (Wang, 2008) and MEEV from the IEDSS during an acute change of shunt.

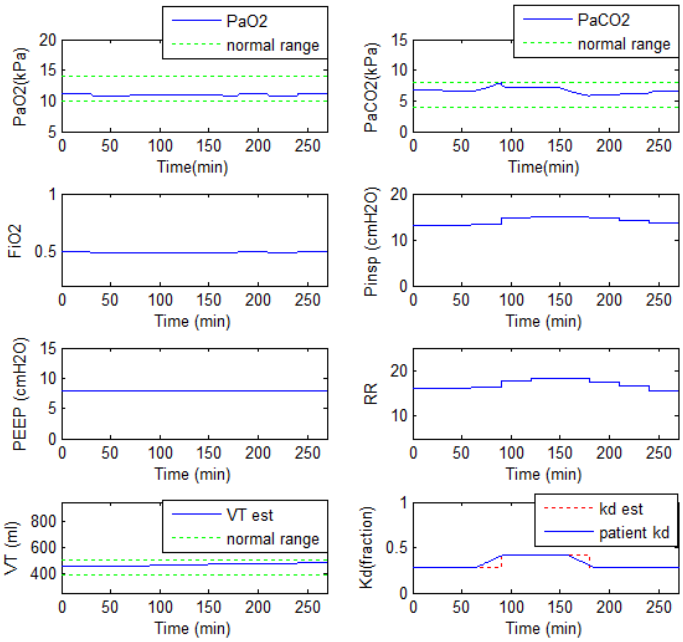

Simulation of an acute Kd changes.